THE UNIVERSITY OF CALGARY

DETECTION OF CRACKS AND CORRODED MEMBERS IN STRUCTURES FROM DYNAMIC RESPONSE

BY

KRZYSZTOF PALKA

A THESIS

SUBMITTED TO THE FACULTY OF GRADUATE STUDIES

IN PARTIAL FULFILLMENT OF THE REQUIREMENTS

FOR THE DEGREE OF MASTER OF SCIENCE

DEPARTMENT OF MECHANICAL ENGINEERING

CALGARY, ALBERTA

APRIL, 1996

THE UNIVERSITY OF CALGARY

FACULTY OF GRADUATE STUDIES

The undersigned certify that they have read, and recommend to the Faculty of Graduate Studies for acceptance, a thesis entitled "Detection of Cracks and Corroded Members in Structures from Dynamic Response", submitted by Krzysztof Palka in partial fulfillment of the requirements for the degree of Master of Science in Mechanical Engineering.

Dr. S.A. Lukasiewicz (Supervisor)
Department of Mechanical Engineering

Dr. O. Vinogradov
Department of Mechanical Engineering

Dr. R.E. Loov
Department of Civil Engineering

Abstract

This thesis presents an identification method to detect cracks and corroded members in vibrating structures. The method utilises measured dynamic response of a structure, and the mathematical identification procedure based on the least square technique. The application of Finite Element Method for the representation of all constraints and modal equations makes it possible to present the identification process in a simple and very efficient mathematical form. Propagation of cracks and other failures of the members changes the bending and axial stiffness of the members. The crack is detected by observing the change of the bending stiffness caused by the closing and opening of the crack in two different configurations. The proposed identification method allows a very high precision of the calculated results which is necessary to find even small changes in the bending stiffness of the members resulting from cracks and corrosion. The method was tested using simulated experimental data.

Acknowledgments

The author wishes to express his sincere gratitude and appreciation to his supervisor, Dr. S.A, Lukasiewicz, for his guidance, support and encouragement through the course of this work.

Thanks are also due to the fellow students of the Department of Mechanical Engineering, Reza Babaei and Mehrdad Farid, for their advice and cooperation. The financial assistance provided by Dr. S.A. Lukasiewicz as well as by the Department of Mechanical Engineering of the University of Calgary, are appreciated and acknowledged.

To my children

Table of Contents

Approval Page ii

Abstract iii

Acknowledgments iv

Dedication v

Table of Contents vi

List of Tables viii

List of Figures ix

Nomenclature xiv

Chapter 1 Introduction 1

1.1 General Background 1

1.2 Literature Review 5

1.2.1 The Analysis of Dynamic Behavior and Detection of Cracks in a Cracked Elastic Beam 5

1.2.2 The Analysis of Dynamic Behavior and Detection of Local Flexibilities in Truss and Frame Structures 13

1.2.3 The Methods of Identification of Dynamic System From Free Response 18

1.3 Objectives 20

1.4 Assumptions 21

Chapter 2 Formulation of Identification Technique 22

2.1 Stiffness Changes in Structures Due to Cracks and Corrosion 22

2.2 Dynamic Response of a Structure With Cracked and Corroded Members 28

2.3 Identification Technique 32

Chapter 3 Numerical Solutions and Techniques 36

3.1 Numerical Formulation of Identification Technique 36

3.1.1 General Solution and Matrix Formulation 36

3.1.2 Numerical Solution for System Identification 43

3.2 Data Generation Techniques 48

Chapter 4 Numerical Results and Analysis 57

4.1 Beam structure 57

4.2 Frame structure 75

4.3 Truss structure 83

Chapter 5 Concluding Remarks and Summary 94

5.1 Summary and Limitations 94

5.2 Concluding Remarks 97

References 98

List of Tables

Table 3.1 Key to determine cracked and corroded members from System Identification output data 45

Table 4.1 Results of identification procedure for twelve-element frame 79

List of Figures

Figure 1.1 Vibration response of point-loaded beam with and without crack 6

Figure 1.2 Cracked Bernoulli-Euler beam: experimental beam and comparison of frequency ratio 7

Figure 1.3 Analysis of a cantilever beam with two open cracks [30] 12

Figure 1.4 Kabe's example problem 15

Figure 1.5 Space Station Truss Structure analyzed by stiffness matrix adjustment method 16

Figure 1.6 Space Station Truss Structure analyzed by hybrid approach 17

Figure 2.1 Finite element model of beam with transverse crack 23

Figure 2.2 Loss of bending stiffness of beam due to transverse crack from FEM 25

Figure 2.3 Finite element model of truss with transverse cracks 26

Figure 2.4 Loss of axial stiffness due to transverse cracks 27

Figure 2.5 Stiffness changes due to corrosion 29

Figure 2.6 Stiffness changes due to cracks 31

Figure 3.1 Example of measured data 38

Figure 3.2 Flow chart of System Identification 46

List of Figures (cont'd)

Figure 3.3 Definition of influence coefficients (a) - nonlinear viscous damping c_{ij} (b) - nonlinear stiffness k_{ij} 50

Figure 3.4 Linear acceleration assumption in the extended time interval 51

Figure 4.1 Vibrating beam, different geometric configurations and stiffness coefficient table 58

Figure 4.2 Damped vibration of ten-element beam in first mode of vibration 60

Figure 4.3 Error versus time-step size and number of time-steps 61

Figure 4.4 Convergence history for data without measurement error, two different values of initial stiffness coefficients - '2' and '50' 62

Figure 4.5 Damped vibration of ten-element beam in first mode of vibration, displacement data with ±2.0% error of measurement 64

Figure 4.6 Convergence history for data with measurement error ±0.5% and ±1.0% .. 65

Figure 4.7 Convergence history for data with measurement error ±1.5% and ±2.0% .. 66

Figure 4.8 Convergence history for data with measurement error ±1.0 and ±3.0% for modified Newton-Raphson method 68

Figure 4.9 Convergence history for data with measurement error ±5.0 and ±13.0% for modified Newton-Raphson method 69

List of Figures (cont'd)

Figure 4.10 Accuracy of convergence for data with measurement errors processed with straight Newton-Raphson method (top) and modified Newton-Raphson method (bottom) 70

Figure 4.11 Strain energy and accuracy of convergence for elements with high changes in strain energy 71

Figure 4.12 Convergence history for few DOF, without measurement error (top), with ±1.0% measurement error (bottom) 73

Figure 4.13 Convergence history for few DOF with ±4.0% measurement error (top), accuracy of convergence (bottom) 74

Figure 4.14 Two dimensional model of twelve-element frame 76

Figure 4.15 Analysed vibration mode in two different configurations 77

Figure 4.16 Convergence history for data without measurement error for frame structure 78

Figure 4.17 Convergence history for data with ±5.0% measurement error for frame structure 80

Figure 4.18 Convergence history for data without measurement error for frame structure using only linear accelerations 81

List of Figures (cont'd)

Figure 4.19 Convergence history for data with ±1.0% measurement error for frame structure using only linear accelerations 82

Figure 4.20 Two dimensional model of eleven-element truss structure 84

Figure 4.21 Strain energy changes in elements of truss structure for first and second modes of vibration 85

Figure 4.22 Strain energy changes in elements of truss structure for third and fourth mode of vibration 86

Figure 4.23 Convergence history for data without measurement error, truss structure in third mode of vibration 87

Figure 4.24 Damped vibration of eleven-element truss in third mode of vibration . 88

Figure 4.25 Convergence history for data without measurement error, 10 (top) and 8 (bottom) DOF were considered for identification purposes 89

Figure 4.26 Convergence history for data without measurement error, 6 (top) and 4 (bottom) DOF were considered for identification purposes 90

Figure 4.27 Convergence history for data with ±5.0% measurement error, all (top) and 10 (bottom) DOF were considered for identification purposes ... 92

Figure 4.28 Convergence history for data with ±5.0% measurement error, 9 (top) and 8 (bottom) DOF were considered for identification purposes 93

Nomenclature

A	area of cross section of the truss element
A_e	area of cross section of the cracked truss element
a	vector of accelerations predicted by finite element model
a^*	vector of measured accelerations
a_1, a_2, a_3, a_4	constants in Wilson-θ method
B	matrix operator that chooses specific degrees of freedom from all degrees of freedom of vibrating structure
C	damping matrix
CD	expanded damping matrix for system identification
c_{ij}	damping coefficient as described in Wilson-θ method
D_0	matrix operator that limits the number of degrees of freedom for system identification
D_1	first order differential operator in matrix notation
D_2	second order differential operator in matrix notation
$\overline{D}$	matrix operator for equation of motion
$\tilde{D}$	matrix operator for equation of motion with constraints
DOF	degrees of freedom
E	modulus of elasticity
F	force vector
G	gradient vector
H	Hessian matrix
h	depth of beam/truss element
I	moment of inertia of cross-sectional area
K	stiffness matrix
KD	expanded stiffness matrix for system identification

Nomenclature (cont'd)

Ki_g	element 'i' stiffness matrix in global coordinate system
k_e	equivalent stiffness of cracked or corroded element
k_i	element 'i' coefficient matrix in global coordinate system
kd_i	expanded element 'i' coefficient matrix in global coordinate system
L	element length
l_e	length of cracked section of an element
M	mass matrix, applied moment
MD	expanded mass matrix for system identification
m	number of time-steps
N	number of variables
n	number of DOF
p_{ij}	unknown coefficient in system identification
R	objective function for system identification
S	matrix of constraints for finite element model of structure
T	denotes transposed matrix
t	time-step value
u	vector of displacements predicted by finite element model
x_i	variable
y	displacement in Wilson-θ method
$\dot{y}$	velocity in Wilson-θ method
$\ddot{y}$	acceleration in Wilson-θ method
Δ	change of a designated variable
δ	denotes finite correction of a variable
θ	angle
λ	vector of Lagrangian multipliers

Nomenclature (cont'd)

τ	modified time-step in Wilson-θ method
ω	natural frequency

CHAPTER I
Introduction

1.1 General Background

The dynamic response of structures can be used as a base for the detection and identification of structural faults. Faults, such as cracks or corrosion, introduce local flexibilities, which can change the dynamic behavior of a structure. In recent years considerable effort has been devoted to investigation of the relationship between crack location, crack size and the corresponding changes in modal shapes and eigenfrequencies. The studies in this area have been mostly limited to beam elements with local cracks. Since the theoretical analysis is complicated, there has been little research done to establish an effective, general method to analyze complex structures such as trusses or frames and to detect damage from monitoring of vibration.

Cracks found in structural elements have various causes. For instance fatigue cracks take place under service conditions as a result of limited fatigue strength. Cracks may also be due to mechanical defects, as in the case of turbine blades of jet engines. There are also cracks in mechanical components created as a result of manufacturing processes.

A crack that occurs in a structural element causes local loss of stiffness. Similarly, corrosion of the component of a structure also causes local loss of stiffness. However, the manner in which corrosion affects the dynamics of the whole structure is different from the way that cracks do. Corrosion, if present, changes the stiffness of the member, and the change does not depend on the geometry of the member during its motion. In contrast, the crack changes the stiffness of the element only when it is open. When the crack is closed the changes in the stresses introduced by the closed crack are small enough to assume that there is no significant change in the stiffness of the element as compared to an element without a crack. The situation becomes more complicated for beam elements when double-sided cracks occur. This can happen in the case of cycling loading. In this case the double crack affects the stiffness of the beam element of a structure similarly as does corrosion. The difference can be noticed by identifying the stiffness, and also at the same time by identifying the mass of the member which changes only in the case of the corrosion.

Until now investigations have concentrated on the analysis of the effect of a crack, or cracks on simple structures, such as beams, shafts or very simple truss and

frame structures. For truss and frame structures, the works done always tried to relate data from the analysis of an undamaged structure and data from a damaged structure, by analyzing the modal shapes and modal frequencies. As recently proven [46], identification based on measurement of natural frequencies and modal analysis does not always give unique results.

This thesis attempts to solve the problem of detection of cracks and corroded areas of beams, and members of truss and frame structures, by using the measured dynamic response and the mathematical identification technique based on the least square method. The data obtained from experimental examination of the vibrating structure, where the accelerations and displacements of certain points of the structure are measured, are compared with the corresponding data computed from the ideal model. The dynamic response (accelerations and displacements as a function of time) are used as a source of information. In contrast to all previous work done in this area, it is not necessary to identify the modal shapes or natural frequencies of a structure. Instead, a very straight-forward approach to determine the stiffness property of each element of the structure is used, based on the least square method. The method can be used to determine the other parameters of a vibrating structure, such as damping properties and the mass of each element. The application of Finite Element Method for the representation of the model and all constraints makes it possible to present the identification process in a very simple and efficient mathematical form. Analyzing the vibrating structure, a vibration mode and time period can be selected in which the members of a structure have

the same geometrical configuration. This means that for beam elements each element has the same positive or negative curvature, and the truss element is stretched or compressed continuously during the analyzed time period. This observation is used to determine the stiffness of each element in a different geometrical mode if the loss of stiffness is due to the crack. The stiffness decreases only when the crack is open. In the case due to corrosion the loss of stiffness does not change with time. In this work, one-sided cracks, caused by fluctuating loading, are considered for beam elements and double-sided cracks for the truss elements. Because the finite element model of structure can introduce some imperfections to system identification, the same identification method is used to find initial stiffness, damping properties and masses by analyzing data from vibration of an undamaged structure. This data obtained from the analysis of an undamaged structure, can be used later as initial data for the system identification analysis of the damaged structure.

In the present study a simple beam, a two-dimensional truss structure and a two-dimensional frame structure are analyzed. The method is verified using data obtained from the finite element program written by the author. This program uses the Wilson-θ Method to calculate the dynamic response of the structure. Then using accelerations and displacements as input data, and roughly assumed stiffness of the elements of the structure, real flexural properties of the structure are found. By analyzing geometrical modes of elements, cracks and corroded areas are located.

1.2 Literature Review

1.2.1 Analysis of dynamic behavior and detection of cracks in a cracked elastic beam

The first analysis of the behavior of a beam with cracks, known to the author, was done fifty years ago in the USA. In 1944 P.G. Kirmser [16] discussed the effect of the crack on the natural frequencies of a vibrating beam. He had found that for the flexural problem, the natural frequencies of a beam with a slot at mid-span agreed with the experimental values when an equivalent slot width of 5 times the actual width was used. In his work he introduced equivalent moment for bending, force for tension and torque for torsion acting at the position of the slot to represent its influence on the bar element he examined. This simple concept was an idealization, since much of the material adjacent to the slot is ineffective in carrying the load. The equivalent slot dimensions which vary with the width and depth of the cut must be established by experimentation.

Later W.T. Thomson [43] investigated the possibility of detecting cracks in slender bars. Although he only attempted to theoretically determine the effect of flexible discontinuities on flexural, longitudinal, and torsional vibration of slender bars, he expressed his belief in the possibility to determine the position and depth of a crack by carrying out experiments. Using ideas from Kirmser's research, he approached the problem using the operational method based on Laplace transformation. He was able to

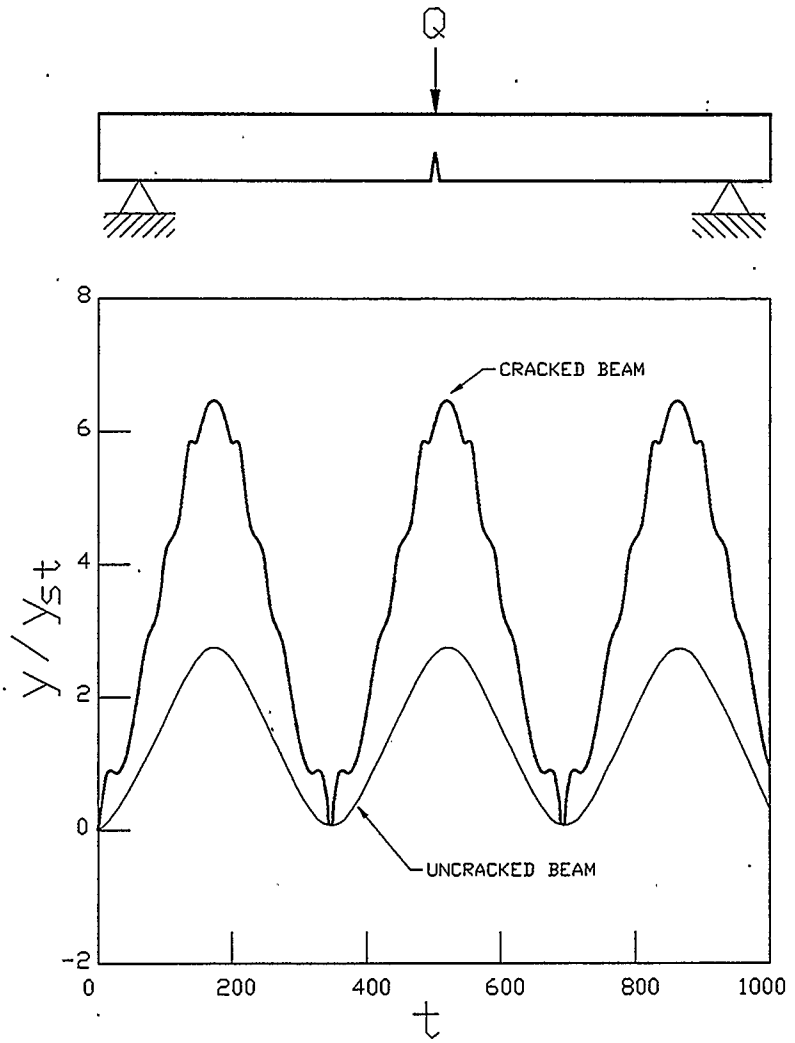

Figure 1.1 Vibration response of point-loaded beam with and without crack

determine the influence of a slot on the natural frequency of a beam and found that for very small cracks the influence on the natural frequency is negligible, however for deeper slots the changes increase quite rapidly.

In 1981 H.J. Petroski [32], using the same approach as Hetenyi, Kimser and Thomson [43, 10, 16], represented the deflection of a beam in his analysis using Fourier series. He related Stress Intensity Factor K to the deflection of a beam for static and dynamic cases. He demonstrated that the crack increases the overall vibration amplitude of the beam (Fig. 1.1).

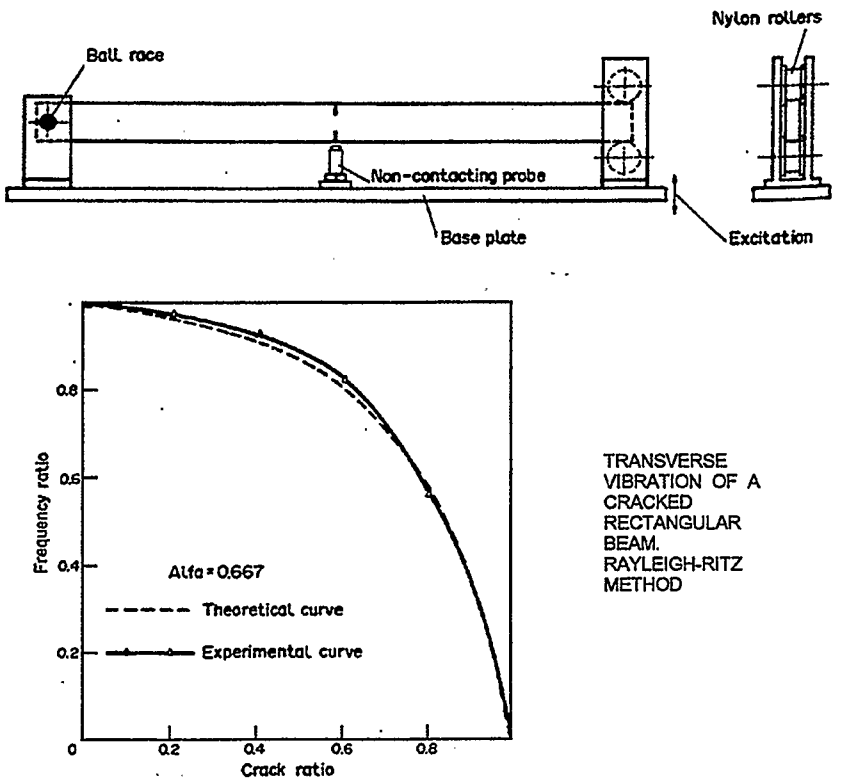

Figure 1.2 Cracked Bernoulli-Euler beam: experimental beam and comparison of frequency ratio

Interest in the problem of cracked beams has increased in recent years since failure analysis and prediction have become an issue in engineering practice. Researchers have become interested in the problems related to eigenfrequency changes in structures due to cracks. R.D. Adams and P. Cawley [1] used a method based on sensitivity analysis to deduce the location of damage and the Finite Element Method to represent the model of the structure. The method was applied to the case of a flat plate with the assumption that the modulus of elasticity in the damaged area was equal to zero. The sensitivity of the change in the eigenvalue was evaluated for each element in the model. The results of the analysis agreed well with the experimental findings. The drawback of this method was the use of huge computing resources and the long time required to predict the location of the damage.

S. Christides and A.S. Barr [3] introduced a crack in their mathematical model of a beam by means of stress and strain changes in the vicinity of the cracked section. In particular, the perturbation in the stress induced by the crack was incorporated through a local function which assumes an exponential decay with distance from the crack and which includes a parameter which can be evaluated by experimental testing (Fig. 1.2). Data from experimental tests, exactly matched the changes in the first natural frequency, with the crack depth calculated from the theoretical model.

A year later, in 1985, M.M.F. Yuen [45] presented results from his research in which he wanted to find the relationship between damage location, damage size and the changes in the eigenvalues and eigenvectors of a cantilever subjected to damage. At the

beginning of his article he emphasized the importance of detecting damage in the structures before failure. A finite element model of a uniform cross sectioned cantilever was chosen to provide data for the analysis. The changes in the eigenvalues and eigenvectors were shown to follow a definite trend in relation to the location and the extent of damage. There was no experimental work done to support this theory, and the small differences in the eigenvalues and eigenvectors obtained by a 50% reduction in the modulus of elasticity, makes the usefulness of his method questionable.

In 1990, G.-L. Qian, S.-N. Gu and J.-S. Jiang [33], published the results of the investigation of the dynamic behavior and crack detection of a beam with a crack. The authors derived an element stiffness matrix of a beam with a crack from an integration of stress intensity factors using strain energy of an element without a crack and additional strain due to the crack. Using the principle of virtual work, the stiffness matrix of the cracked element was derived. From the equation of motion the eigenfrequencies have been determined for different crack lengths and positions. Calculated values were compared with the experimental data from work of P. Gudmundson. Since the calculated results agree quite well with the experimental data, the presented method looks feasible for crack detection in engineering practice.

The article presented by P.F. Rizos, N. Aspragathos and A.D. Dimarogonas [35] on identification of crack location and magnitude in a cantilever beam from the vibration modes, has shown how to determine the location and depth of the crack from the modal shapes after introducing a crack as a local loss of stiffness represented by a spring. The

experiment performed by these authors showed good agreement of experimental data and with the data calculated from the theoretical approach. But overall, the presented method lacks accuracy for very small cracks and cannot distinguish location of symmetrically located cracks. As all previously presented methods, this one also neglects damping. At the end the authors admitted that for more complex structures accuracy will be progressively smaller.

Combining ideas from the last two papers, W.M. Ostachowicz and M. Krawczuk [30] presented in 1991, an analysis of the effect of two open cracks upon the frequencies of the natural flexural vibrations in a cantilever beam. A crack was represented as an equivalent stiffness element derived using the stress intensity factor (Fig. 1.3). FEM was used to model the beam, and the equation of motion was solved numerically to analyze the dynamic behavior of the beam. The results of the calculation indicated the relationship between the position and magnitude of the crack, and the first frequencies of the cantilever beam natural vibration. The only thing which was questionable was the equivalent stiffness of the crack, which changes very rapidly with crack depth after the initial stage of crack development. For example, for a crack depth of 15% of beam height, stiffness was about 50% of that of a beam without a crack, for a depth of 50% it was around 'zero'. This is totally different from the equivalent stiffness obtained by the author of this thesis and presented in Fig. 2.2.

A different method, utilizing the relation between the changes in the eigenfrequencies, the local stiffness losses and the mode shape functions of the

undamaged system, was presented in 1993 by U. Pabst and P. Hagedorn [31]. Rayleigh's Quotient was used as a base for the crack detection procedure. This method uses information on the stiffness distribution of the structure only for normalizing the modal shapes. All other data used in that procedure are modal data and were obtained from measurement. Experiments conducted to find cracks of depth 37.5% of the height of a beam have shown the good accuracy (error of the order of 1-5%) of this method for finding crack location. On the other hand, this method was unable to deal with the problem of opening and closing of the cracks or cracks exceeding the region of validity of Hooke's law at the tip.

Being aware of the limitations of the previously presented methods, A. Morassi [29] used a perturbation method to evaluate the first order perturbation of the eigenfrequencies. The local flexibility, introduced by the crack, is represented in his work by a massless rotational spring whose stiffness depends on the severity of the crack. A graphical method is used to find the position and severity of the crack. There is no experimental work to support the results obtained by computer modeling and since very accurate measurement of eigenfrequencies is necessary for this procedure, one can suspect that this method is very sensitive to measurement errors. Two years later, in 1995, W.M. Hasan [8] extended this work to the case of a beam on an elastic foundation and was able to find the position and severity of a crack using the same approach as A. Morassi.

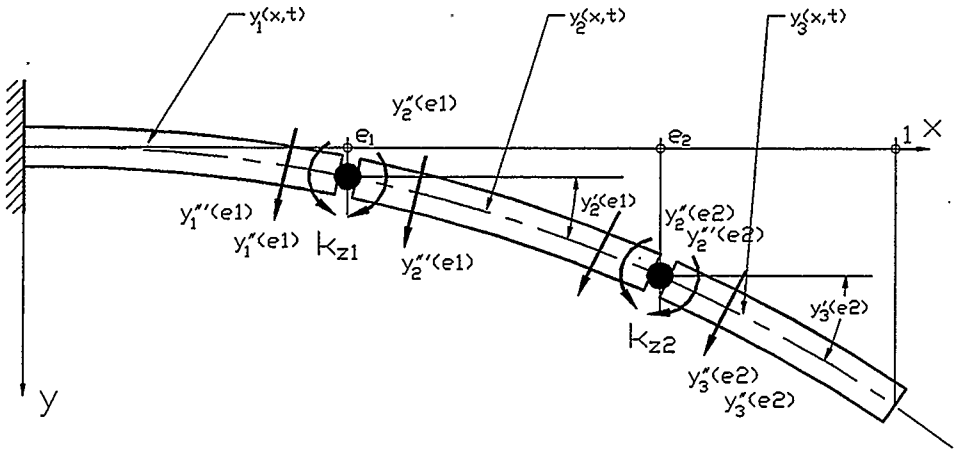

Clamped beam with two cracks

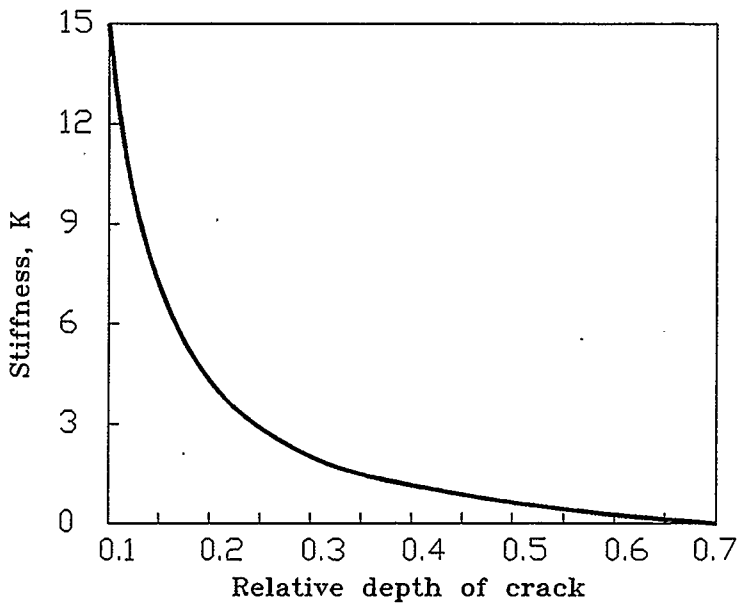

Relation between K and depth of a crack

Figure 1.3 Analysis of a cantilever beam with two open cracks [30]

1.2.2 Analysis of dynamic behavior and detection of local flexibilities in truss and frame structures

The ability to locate and assess damage in flexible truss and frame structures has progressed considerably in the last five years. Many local (measurement) approaches have been developed and evaluated previously, including X-ray, optical, infrared, and ultrasonic methods. Global methods (mathematical approaches), currently under development, use vibration response and system identification techniques to detect damage in flexible structures. Almost all approaches are based on eigenvalue and eigenvector derivatives. Hendrix et.al. [9] presented an eigenvalue sensitivity identification procedure and performed a numerical simulation to obtain clustered and low-frequency vibration modes, characteristic for large flexible structures. Mass, damping and stiffness matrices were constructed in terms of small sets of physical property parameters. Estimation and correction of initial parameters was determined by using first-order eigenvalue derivatives and the difference between the measured and predicted frequencies. Since using the eigenvalue sensitivity method, less information about the system is needed than for the eigenvector sensitivity method, the second method is expected to be more efficient. Flanigan [5] applied an eigenvector sensitivity approach for model refinement of a truss structure. The illustration of this method was presented by Ricles and Kosmatka [34]. First, residual modal force vectors were used to locate the damage, second, a weighted eigenvector sensitivity analysis was carried out to

estimate the extent of the damage. Smith and Beattie [39] incorporated the incomplete measurement procedure for damage assessment, but not for damage location (Fig. 1.4).

An advantage of sensitivity identification is that the damage can be assessed with incomplete measurements. Also, areas in a property matrix far from damaged areas remain unaffected by using a localized set of physical parameters. A disadvantage is that an inclusive set of physical parameters must be defined before sensitivity analysis can be successful. Experiments show that algorithms are often not robust with respect to errors in the modal data, and lead to numerical difficulties with near-singular sets of equations. Lin [17] proposed an improved method that employs analytical and experimental data, both eigenvalues and eigenvectors, to calculate sensitivity coefficients. Numerical experiments with a truss structure indicate that this method overcomes difficulties associated with previous procedures, such as small convergence, and ability to handle small damage.

Recently, multiple-constraints matrix adjustment identification methods have shown promise in determining damage location and assessment in flexible structures. S.W. Smith and S.L. Hendrix [37] presented a detailed review of these methods. Through the solution of the constrained optimization problem, formulated with the matrix Forbenious norm, this approach produces adjusted FEM property matrices that more closely match the structural properties determined from tests of the structure. Stiffness loss in the FEM model is established to determine damage severity and location. Comparing the two stiffness matrices for a structure, one from an undamaged model and

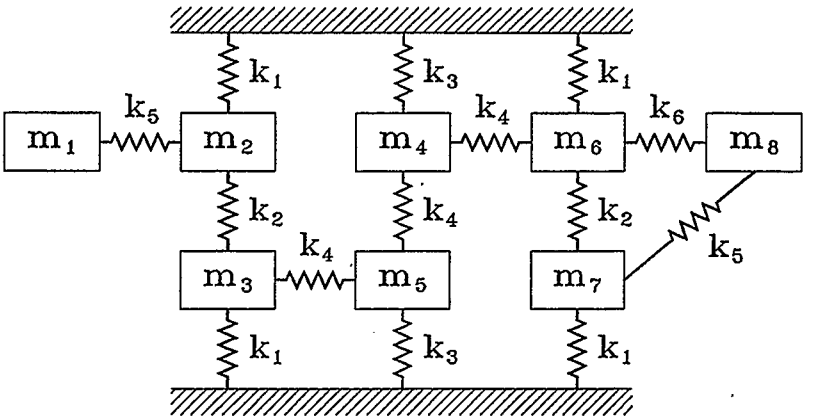

$k_1 = 1000$	$k_4 = 100$	$m_1 = 0.001$
$k_2 = 10$	$k_5 = 1.5$	$m_{2-7} = 1.0$
$k_3 = 900$	$k_6 = 2.0$	$m_8 = 0.002$

Figure 1.4 Kabe's example problem

another obtained from limited measurement of the dynamic response of the damaged structure, allowed damaged members to be identified. Since this method updates all matrix elements, sometimes it is difficult to interpret the results as physical changes associated with each element (Fig. 1.5).

For better detection of damage in a flexible structure, the hybrid approach [4], that combined the advantages of both eigensensitivity and matrix adjustment techniques, was investigated by C. Li and S.W. Smith (Fig. 1.6). First multiple-constraint stiffness matrix adjustment algorithms were used to formulate the general form of the objective function to minimize the Frobenius norm of the matrix of residual force vectors. Only an

undamped system was taken into consideration. Later physical parameter sensitivities were introduced through a first-order expansion of the stiffness matrix. As a result, the least square problem was solved to identify the set of physical property parameters. From acceleration obtained as input data for all DOF, eigenfrequencies and modal shapes were computed as input data for system identification. The experiment conducted with the truss structure with 96 DOF confirms the ability of the method to identify the damage location in the structure.

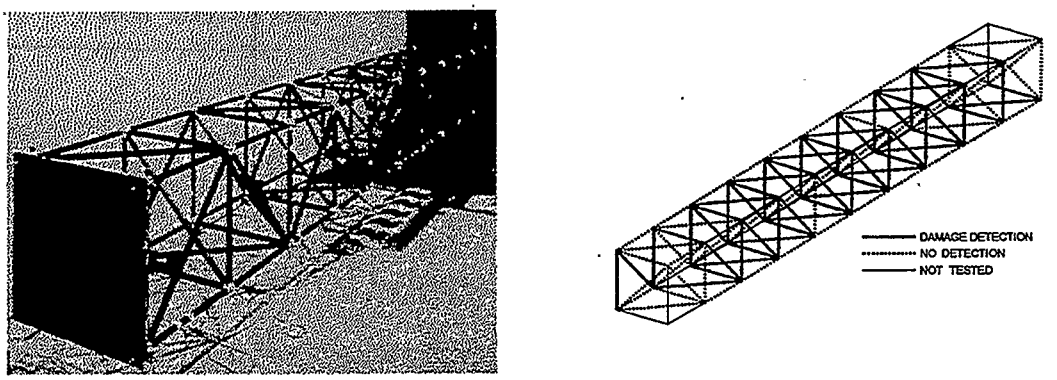

Figure 1.5 Space Station Truss Structure analyzed by stiffness matrix adjustment method

Eight-bay damage case definitions

Damage case	Element label	Element type	Bay
1 (a)[a]	46	Longeron	1
2 (h)	35	Longeron	3
3 (l)	22	Longeron	5
4 (e)	36	X-batten	3
5 (o)	35 and 99	Longeron and diagonal	3

[a]Labeling in parentheses from Kashangaki's designations

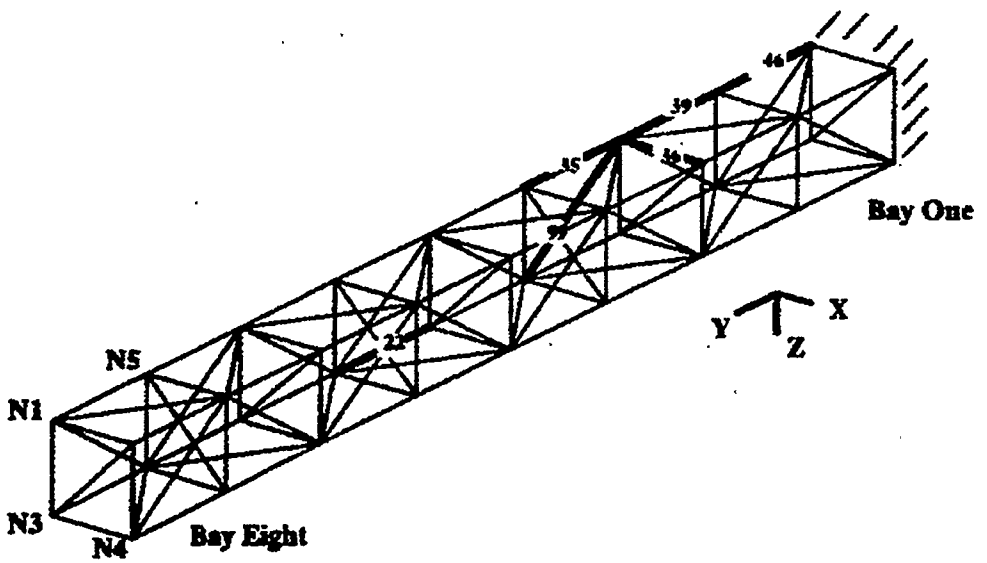

Figure 1.6 Space Station Truss Structure analyzed by hybrid approach

1.2.3 Methods of identification of the dynamic system from free response

The experimental measurement of the dynamic system is usually pursued through determination of the natural frequencies and modes of a structure and comparison with the analytical system response data. Many test procedures have been proposed [11] to determine eigenfrequencies and modal shapes of a structure from experimental measurement. They vary in the manner in which the structure is excited, the quantities which are measured, and the manner in which the experimental data are analyzed. Most modal vibration methods are based on the assumption, that there is no mode coupling. Although some methods have been introduced to deal with modal interference and they require advance determination that mode coupling will occur, their yield accuracy is not much greater than that of the other methods. It is obvious that when using data which is not very accurate it will be hard to identify a vibrating system correctly. Since to obtain modal data one is not required to measure response of the structure at all DOF, the aforementioned methods received most attention in the past. The direct use of dynamic response measurements from all degrees of freedom was also examined. This approach allows determination of the modal characteristic of structure more accurately.

Then different methods were applied to identify the dynamic system. Statistical parameter estimation [18], matrix perturbation theory [5], matrix adjustment procedure [14], simultaneous expansion and orthogonalization of measured modes [39] or hybrid

approach [4] are just a few presented in the past. There is no obvious choice since all of them have some limitations.

Two years ago a simple and efficient method was presented by S.A Lukasiewicz and R. Babaei, based on the least square technique, and minimization of the global error functional [22, 23]. Using directly measured data from all DOF, a dynamic system was identified and it was also shown that the method was able to deal with noisy data and provide accurate results. Further development of this method looks like a natural way to obtain an identification technique to deal with local loss of stiffness in flexible structures.

1.3 Objectives

The purpose of this thesis is to develop and evaluate an identification method for the detection of local changes in flexibilities of a structure from its dynamic behavior. All known previous works used changes in natural frequencies and/or modal shapes of locally damaged structures and did not always give unique results. However, a few works [22, 23] have been done to utilize the least square technique for identification of vibrating systems. The results were so promising, that it appeares appropriate to explore the possibilities of its use for damage detection. Therefore, a new method based on the least square technique and minimization of the global error functional, is developed and utilized. To evaluate the identification method three different structures will be analyzed. The influence of artificially generated measurement error on the accuracy of the solution will be investigated, to ensure that the method is able to handle real problems.

1.4 Assumptions

Throughout the formulation and evaluation process, it is assumed that:

(1) Accelerations and displacements are the measured quantities representing dynamic response of a structure.

(2) The only changes associated with occurrence of cracked and corroded members are changes in stiffness of a structure. Changes in mass or damping properties are not considered.

(3) The structure will vibrate freely during the analyzing period after being excited.

CHAPTER II
Formulation of Identification Technique

2.1 Stiffness changes in structures due to cracks and corrosion

The loss of the axial and bending stiffness of a beam due to a transverse crack can be examined using Finite Element Method. In this work ANSYS 5.2 was used to perform the evaluation. A member of rectangular cross-section with a crack was modelled using a large number of elements and a singular element in the tip of the crack (Fig. 2.1 and Fig. 2.3). The equivalent stiffness for the member was obtained. The results of that analysis for the bending stiffness changes are presented in Fig. 2.2. The area surrounding the crack was analysed using Finite Element Method. The length of the section modelled by FEM was assumed l_e=10h. This length is satisfactory to eliminate the effect of the boundary condition on the stiffness of the cracked area.

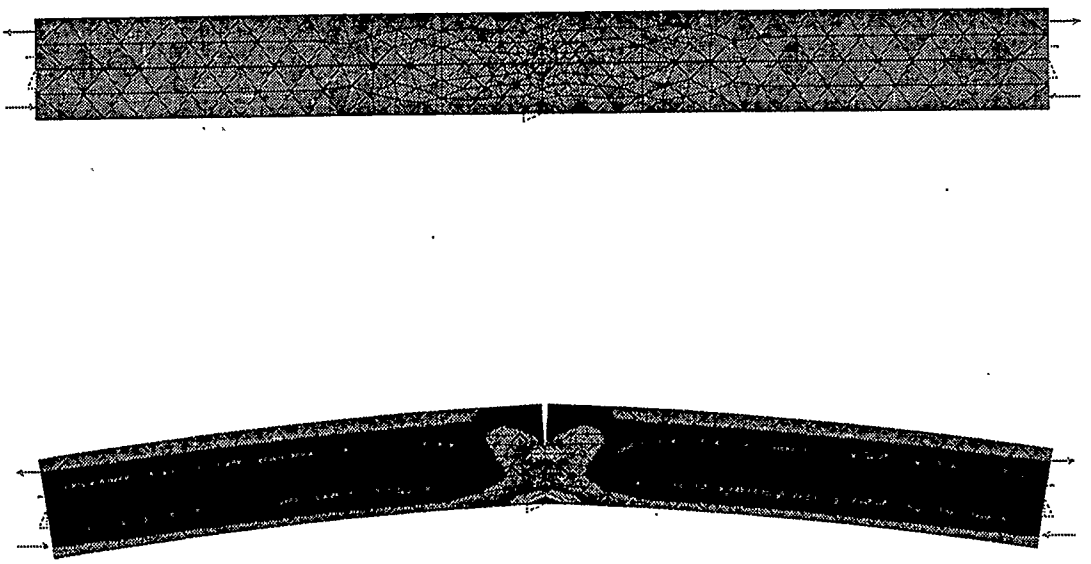

Figure 2.1 Finite element model of beam with transverse crack

The equivalent bending stiffness for the member with dimensions $h \times 1 \times L$ shown in Fig. 2.2 is derived in the following way.

Rotation caused by applied moment M is:

$$\varphi = \frac{ML}{EI}. \tag{2.1}$$

Stiffness of the cracked section of the length l_e can be represented as:

$$EI_e = k_e EI_o, \tag{2.2}$$

where EI_o describes sections without a crack and l_e is the length modelled by FEM.

Since $L = 2\,l_o + l_e$, we can represent φ as:

$$\varphi = \frac{2Ml_o}{EI_o} + \frac{Ml_e}{EI_e}. \tag{2.3}$$

Substituting (2.2) in (2.3) gives:

$$\varphi = \frac{M}{EI_o}\left[2l_o + \frac{l_e}{k_e}\right]. \tag{2.4}$$

Meanwhile, Eq. (2.4) can be rewritten as:

$$\frac{\varphi}{ML} = \frac{1}{EI_o}\left[\frac{2l_o}{L} + \frac{l_e}{k_e L}\right] =$$

$$= \frac{1}{EI_o}\left[1 - \frac{l_e}{L} + \frac{l_e}{k_e L}\right] =$$

$$= \frac{1}{EI_o}\left[1 - \frac{l_e}{L}\left(1 - \frac{1}{k_e}\right)\right]. \tag{2.5}$$

Equations (2.1) and (2.5) yield:

$$\frac{\varphi}{ML} = \frac{1}{EI_E} = \frac{1}{EI_o}\left[1 - \frac{l_e}{L}\left(1 - \frac{1}{k_e}\right)\right]. \tag{2.6}$$

Since $l_e = 10h$,

$$\frac{1}{EI_E} = \frac{1}{EI_o}\left[1 - \frac{10h}{L}\left(1 - \frac{1}{k_e}\right)\right]. \tag{2.7}$$

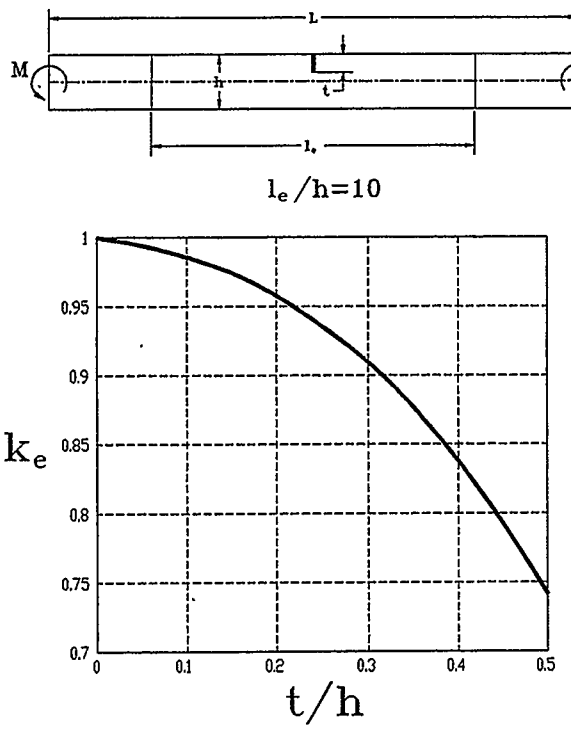

Figure 2.2 Loss of bending stiffness of beam due to transverse crack from FEM

The above equation can be rearranged as:

$$\frac{EI_E}{EI_o} = \frac{1}{1-\frac{10h}{L}\left(1-\frac{1}{k_e}\right)}, \tag{2.8}$$

where k_e is a stiffness coefficient presented in Fig. 2.2. Figure 2.2 and Eq. (2.8) can be used to find the crack length in the analysed member if the actual stiffness is known.

Similar analysis was performed to estimate the axial stiffness changes and the results are presented in Fig. 2.4. The equivalent axial stiffness for the member with dimensions $h \times 1 \times L$ and $l_e = 10 \times h$ shown in Fig. 2.3 is derived in a similar way as the equivalent bending stiffness.

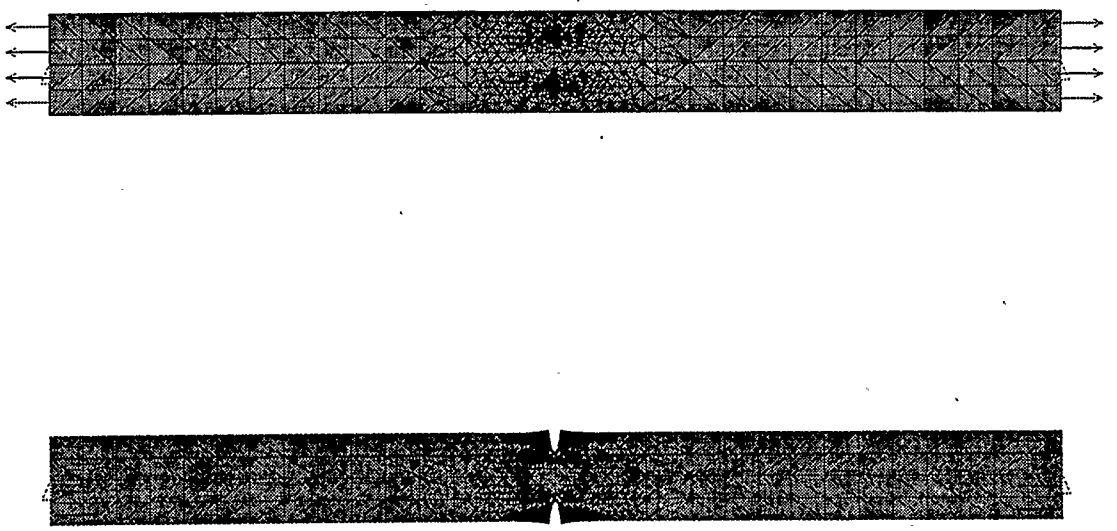

Figure 2.3 Finite element model of truss with transverse cracks

Finally, we can obtain the expression:

$$\frac{EA_E}{EA_o} = \frac{1}{1 - \frac{10h}{L}\left(1 - \frac{1}{k_e}\right)} . \tag{2.9}$$

On the other hand, corrosion changes the bending and axial stiffness of a member of a structure in a simpler way. By changing the cross-sectional area, stiffness is changed directly, and there is no need to derive any special expression.

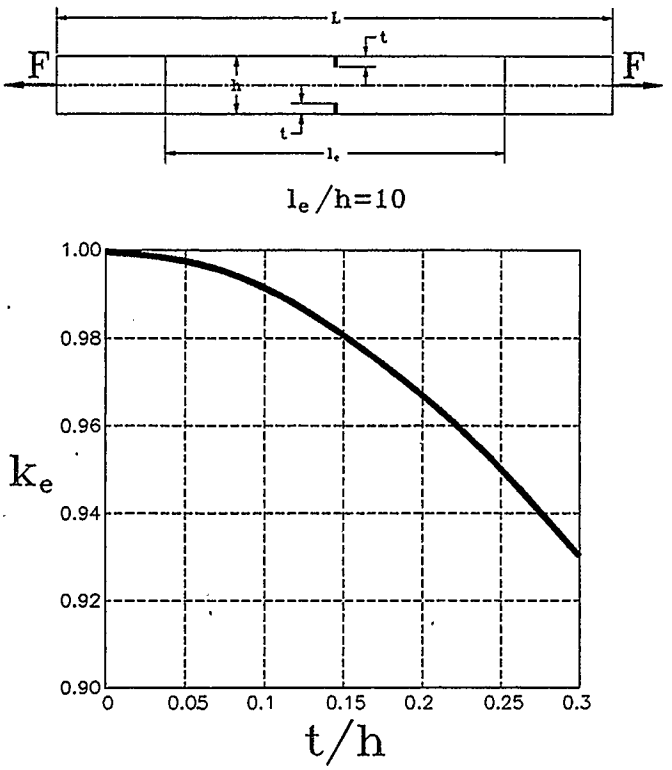

Figure 2.4 Loss of axial stiffness due to transverse cracks

2.2 Dynamic response of a structure with cracked and corroded members

Dynamic behavior of structures (designated as beams or trusses) carrying the loads and producing lateral and/or axial displacements depends on a number of properties. These properties, such as mass, stiffness and damping characteristics can be significantly affected by changes in the structure due to corrosion or cracks. It is important to properly identify these changes, since they alter the behavior of the elements of the structure in a different way.

When dealing with changes caused by corrosion, the effect of the cross-section area decrease is predictable. A smaller cross-section area gives smaller flexural and axial stiffness of the element (Fig. 2.5). Also the mass of the affected elements changes, since less material has a smaller mass. Damping properties are likely to be affected, but the actual influence is not exactly known, and only experimental works could provide an answer to this problem. Since for the loaded structure, the effect of stiffness changes is most significant, mass and damping changes of the beam and truss elements are not taken into consideration in this thesis.

When cracks are present in vibrating structures, their influence on the behavior of the structure is more complex. As presented in Fig. 2.6, the loss of the stiffness can only occur for the Open Crack Mode. It is assumed that in the Closed Crack Mode there is no stiffness changes of the element. This is an accurate enough approximation of the real

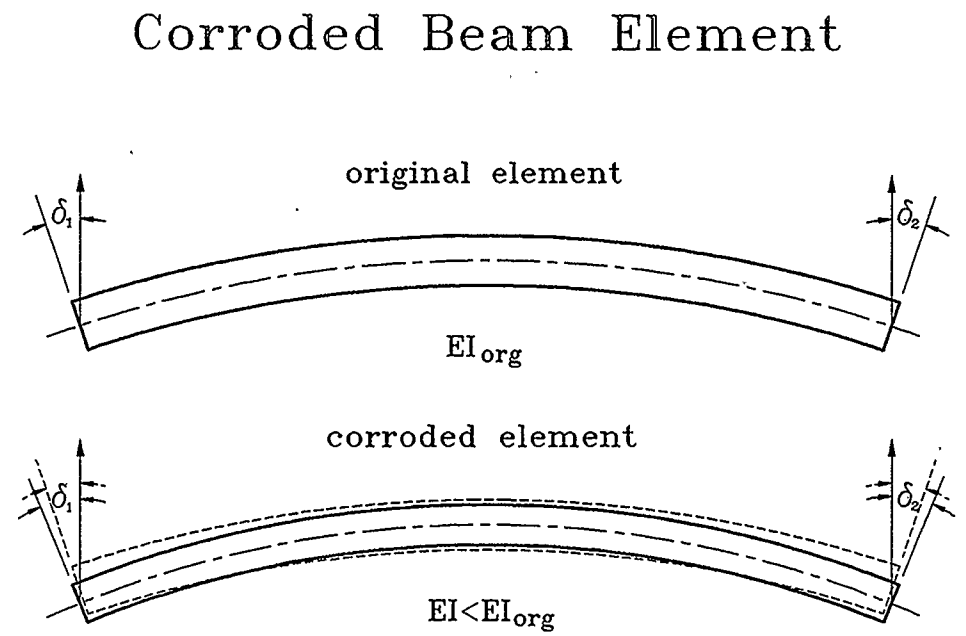

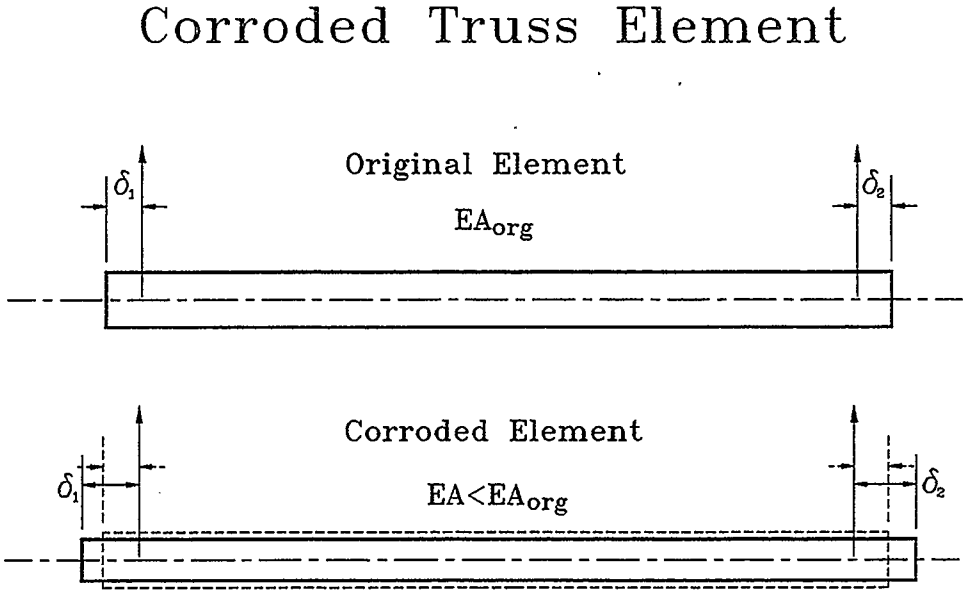

Figure 2.5 Stiffness changes due to corrosion

behavior of very fine cracks, since stress changes induced by contact of closed surfaces of a crack, are very local and relatively small. The stiffness of the element can only decrease due to crack opening. The curvature of the member can be established by knowing the angular displacement of the member at both ends.

This procedure is appropriate only if the element is vibrating in its first mode. If the structure is excited in a controllable way, this requirement can be simply satisfied. If not, the structure must be divided into more elements to satisfy the condition that each member is in the first mode of vibration. A truss member behaves in a similar fashion. The decrease in the stiffness appears when cracks are open, and this mode could be recognized by analyzing the axial displacement of the ends of the truss element.

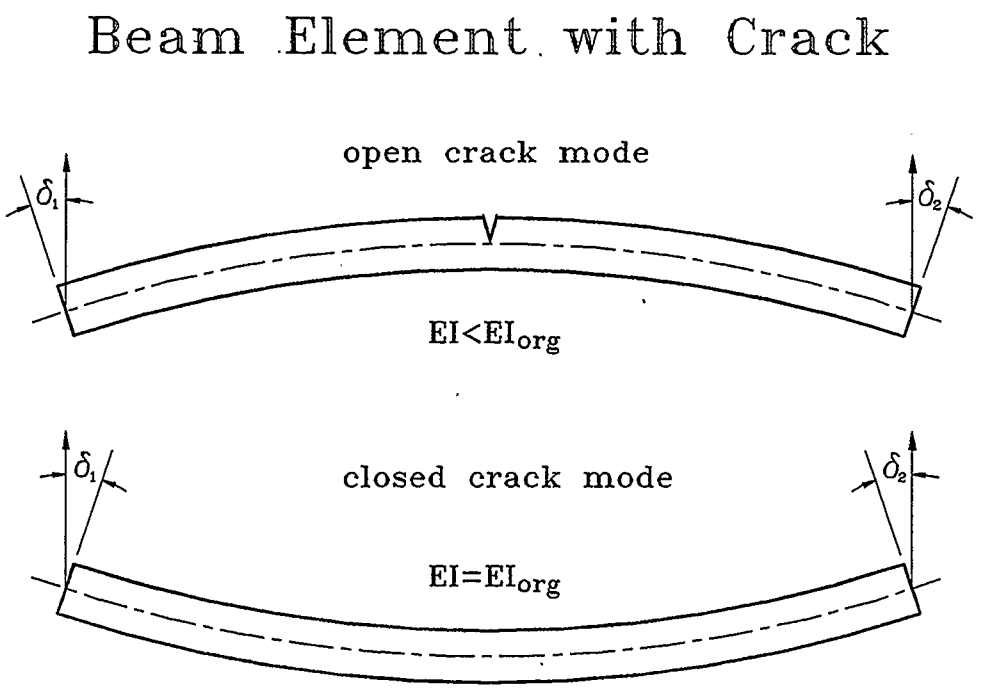

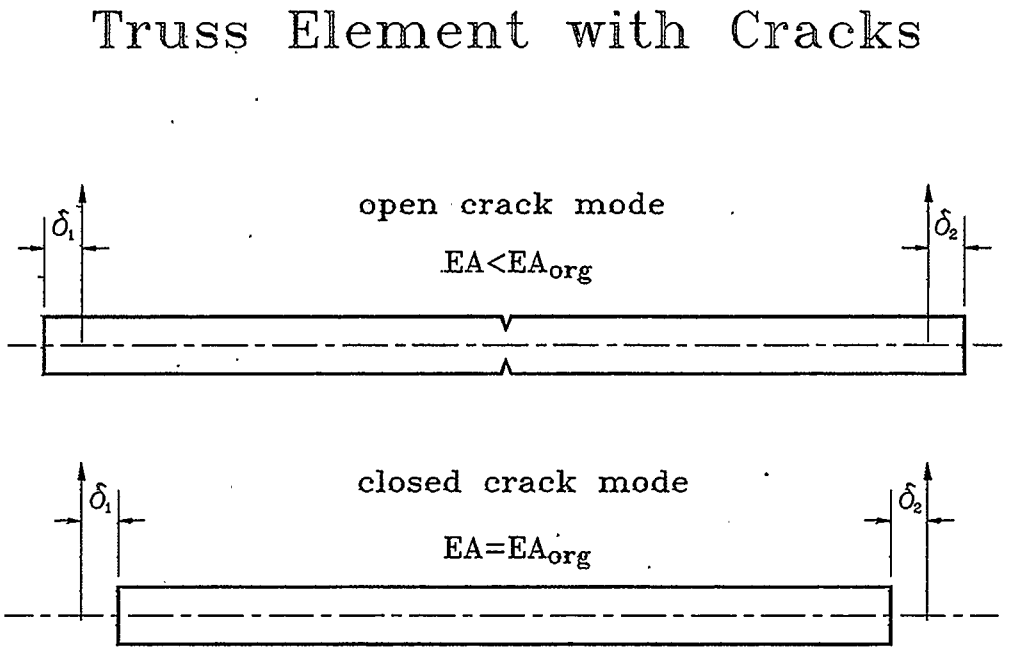

Figure 2.6 Stiffness changes due to cracks

2.3 Identification technique

The method of least squares is used to identify the vibrating system. The model system equations are considered as constraint equations for an optimisation problem where the differences between the measured values and the values predicted by the model are minimised.

A general dynamic system is presented by a matrix equation

$$M\ddot{u} + C\dot{u} + Ku - F = 0, \tag{2.10}$$

where M is the mass matrix, C - the damping matrix, K - the stiffness matrix and F - the vector of external forces. In this case F is equal to zero since only free vibration is considered. The matrices M, C, and K are of the range n x n, where n is the number of degrees of freedom of the system. The operator $\overline{D}$ can be introduced in the form:

$$\overline{D}u \equiv \left[MD_2 + CD_1 + KD_0\right]u, \tag{2.11}$$

where D_2, D_1 and D_0 are the matrices of differential operators of the second, first and zero order. Let us assume that the acceleration vector a^* is measured and m values for each n (DOF) are obtained. Two vectors of accelerations a_{nm} are created:

A vector of accelerations predicted by the model:

$$a^T = \left[a_{11}, a_{12} \ldots a_{1m}, a_{21}, a_{22} \ldots a_{2m}, \ldots, a_{n1} \ldots a_{nm}\right]^T = D_2 u^T, \tag{2.12}$$

where

$$u^T = \left[u_{11}, u_{12} \ldots u_{1m}, u_{21}, u_{22} \ldots u_{2m}, \ldots, u_{n1} \ldots u_{nm}\right]^T \tag{2.13}$$

is the vector of nodal displacements.

The vector of measured accelerations is:

$$a^{*T} = \left[a^*_{11}, a^*_{12} \ldots a^*_{1m}, a^*_{21}, a^*_{22} \ldots a^*_{2m}, \ldots, a^*_{n1} \ldots a^*_{nm}\right]^T, \tag{2.14}$$

where m is the number of samples for each acceleration a_n.

The values a^{*T} are affected by noise and other experimental errors. The matrices M, C and K are also unknown and should be found from the analysis of the experimental data. To find u, M, C and K, the method of least squares can be applied. Let us define the global error of measurement R, in the time interval T, as follows:

$$R = \frac{1}{2}\left[D_2 u - D_0 a^*\right]^T \left[D_2 u - D_0 a^*\right] + \left[\overline{D} u\right]^T [\lambda] + [Su]^T [\lambda], \tag{2.15}$$

where λ is the vector of the Lagrangian multiplier,

$$[\lambda]^T = [\lambda_{12}, \lambda_{13} \ldots \lambda_{1,m-1}, \lambda_{22}, \lambda_{23} \ldots \lambda_{2,m-1}, \ldots, \lambda_{n2} \ldots \lambda_{n,m-1}]^T, \tag{2.16}$$

and $[\overline{D}u]^T$ and $[Su]^T$ are the matrices of constraint equations for model (2.8); S(u) presents a set of k additional constraint equations such as boundary conditions, initial conditions and other constraints which can be imposed on the parameters of the system. All these constraint equations are written only at the internal points of the interval T to be able to calculate the first and second derivatives in equation (2.8) by means of the finite difference approximation. The matrices $\overline{D}$ and S can be combined into one matrix $\widetilde{D} = \overline{D} + S$. Parameters p_{ij} are related to the stiffness K, damping C and mass M matrices. Minimising the error R with respect to u_{ij}, λ_{ij} and p_{ij}, the following set of equations can be obtained:

$$\frac{\partial R}{\partial u} = D_2^T \left(D_2 u - D_0 a^* \right) + \widetilde{D}^T \lambda = 0, \tag{2.17a}$$

$$\frac{\partial R}{\partial \lambda} = \widetilde{D} u = 0, \tag{2.17b}$$

$$\frac{\partial R}{\partial p_{ij}} = \left(\frac{\partial \widetilde{D}}{\partial p_{ij}} u \right)^T \lambda = 0. \tag{2.17c}$$

The above set of non-linear equations can be solved by means of any iterative technique suitable for the solution of the non-linear algebraic equations.

If instead of an acceleration for all degrees of freedom, measurement for a limited number of DOF is performed, the objective function can by modified in the following way:

$$R = \frac{1}{2} \left[B D_2 u - a^* \right]^T \left[B D_2 u - a^* \right] + \left[\overline{D} u \right]^T [\lambda] + [Su]^T [\lambda], \tag{2.18}$$

where B matrix is an operator to the measured degrees of freedom from the finite element model. Minimising the error R with respect to u_{ij}, λ_{ij} and p_{ij}, the following set of equations can be obtained:

$$\frac{\partial R}{\partial u} = D_2^T B^T \left(B D_2 u - a^* \right) + \tilde{D}^T \lambda = 0, \tag{2.19a}$$

$$\frac{\partial R}{\partial \lambda} = \tilde{D} u = 0, \tag{2.19b}$$

$$\frac{\partial R}{\partial p_{ij}} = \left(\frac{\partial \tilde{D}}{\partial p_{ij}} u \right)^T \lambda = 0. \tag{2.19c}$$

By solving the above set of a non-linear equations, p_{ij} values are obtained, which give us all the parameters of the vibrating structure.

CHAPTER III
Numerical Solutions and Techniques

3.1 Numerical Formulation of Identification Technique

3.1.1 General Solution and Matrix Formulation

As stated in the previous chapter, to identify a vibrating system a set of nonlinear equations must be solved. The results can be obtained by means of any iterative technique suitable for the solution of the set of nonlinear algebraic equations. The Newton-Raphson method will be used in this work to obtain the solutions. A typical problem gives N gradient relations to be zeroed, involving variables $x_i, i = 1,2,\ldots,N$:

$$\frac{\partial F(x_i)}{\partial x_i} = 0 \qquad i = 1,2,\ldots,N \tag{3.1}$$

Let $\frac{\partial F}{\partial x_i}$ denote the entire vector of $\frac{\partial F(x_i)}{\partial x_i}$. In the neighborhood of x_i, each component of the gradient $\frac{\partial F}{\partial x_i}$ can be expanded in Taylor series:

$$\frac{\partial F}{\partial x_i}(x_i + \delta x_i) = \frac{\partial F}{\partial x_i} + \sum_{j=1}^{N} \frac{\partial^2 F}{\partial x_i \partial x_j} \delta x_j + O(\delta x_i^2). \tag{3.2}$$

The vector of partial derivatives appearing in equation (3.2) is the Gradient vector **G** and the matrix of partial derivatives is the Hessian matrix **H**:

$$G_i = \frac{\partial F}{\partial x_i} \qquad H_{ij} = \frac{\partial^2 F}{\partial x_i \partial x_j}. \tag{3.3}$$

In matrix notation equation (3.2) is:

$$\frac{\partial F}{\partial x_i}(x_i + \delta x_i) = G_i + H_{ij} \delta x_j + O(\delta x_i^2). \tag{3.4}$$

By neglecting terms of order δx_i and higher and by setting $\frac{\partial F}{\partial x_i}(x_i + \delta x_i) = 0$, we obtain a set of linear equations for the correction δx_j that move each gradient of $\frac{\partial F}{\partial x_i}$ closer to zero simultaneously. Namely

$$\delta x_j = -[H_{ij}]^{-1} G_i. \tag{3.5}$$

Matrix equation (3.5) is solved, the corrections are added to the solution vector,

$$x_{new} = x_{old} + \delta x_i \tag{3.6}$$

and the process is iterated to convergence.

The above method, very efficient and elegant from a mathematical point of view, is inconvenient if we have to assemble a gradient vector and Hessian matrix manually. Even for a very simple problem it is time consuming and prone to mistakes [21, 22]. Fortunately, after analyzing the pattern of the gradient vector and Hessian matrix, it is feasible to find a matrix notation which makes it possible to simply write any differential equation using differentiating operators, and to assemble a gradient vector and Hessian matrix automatically.

To explain how all the vectors and matrices are arranged in our problem, let us assume that the data for accelerations from a three degrees of freedom system were obtained. A four time-step interval was used as presented in Figure 3.1. The number of degrees of freedom is denoted as n and the number of time-steps as m. In this case n = 3, and m = 4 respectively. The vector of measured acceleration is:

$$a^{*T} = \left[a_{11}^{*}, a_{12}^{*}, a_{13}^{*}, a_{14}^{*}, a_{21}^{*}, a_{22}^{*}, a_{23}^{*}, a_{24}^{*}, a_{31}^{*}, a_{32}^{*}, a_{33}^{*}, a_{34}^{*}\right]^{T}. \tag{3.7}$$

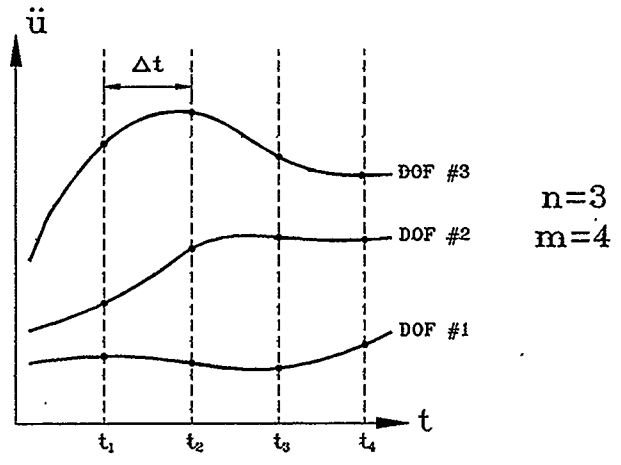

Figure 3.1 Example of measured data

The vector of accelerations predicted by the model is:

$$a^T = \left[a_{11}, a_{12}, a_{13}, a_{14}, a_{21}, a_{22}, a_{23}, a_{24}, a_{31}, a_{32}, a_{33}, a_{34}\right]^T = D_2 u^T, \qquad (3.8)$$

where

$$u^T = \left[u_{11}, u_{12}, u_{13}, u_{14}, u_{21}, u_{22}, u_{23}, u_{24}, u_{31}, u_{32}, u_{33}, u_{34}\right]^T. \qquad (3.9)$$

By representing the derivatives of u by the central finite difference, we have:

$$\ddot{u}_{ij} = \frac{u_{i(j-1)} - 2u_{ij} + u_{i(j+1)}}{(\Delta t)^2}, \qquad (3.10)$$

and

$$\dot{u}_{ij} = \frac{u_{i(j-1)} - u_{i(j+1)}}{(2\Delta t)}. \qquad (3.11)$$

The differential operators D_1 and D_2 can be defined such as:

$$\ddot{u}^T_{n(m-2)} = D_2 u^T_{nm} \qquad \dot{u}^T_{n(m-2)} = D_1 u^T_{nm}. \qquad (3.12)$$

Because the finite difference derivatives are used, the final vectors of the computed accelerations and velocities have the size of $n \times (m-2)$. Differential operators D_2 and D_1 have the dimensions of $n \times (m-2), n \times m$. In this case ($n = 3$ and $m = 4$), D_2 has 6 rows and 12 columns:

$$D_2 = \frac{1}{(\Delta t)^2}\left[\begin{array}{cccc|cccc|cccc} 1 & -2 & 1 & 0 & 0 & 0 & 0 & 0 & 0 & 0 & 0 & 0 \\ 0 & 1 & -2 & 1 & 0 & 0 & 0 & 0 & 0 & 0 & 0 & 0 \\ \hline 0 & 0 & 0 & 0 & 1 & -2 & 1 & 0 & 0 & 0 & 0 & 0 \\ 0 & 0 & 0 & 0 & 0 & 1 & -2 & 1 & 0 & 0 & 0 & 0 \\ \hline 0 & 0 & 0 & 0 & 0 & 0 & 0 & 0 & 1 & -2 & 1 & 0 \\ 0 & 0 & 0 & 0 & 0 & 0 & 0 & 0 & 0 & 1 & -2 & 1 \end{array}\right]. \qquad (3.13)$$

Similarly D_1 is:

$$D_1 = \frac{1}{(2\Delta t)}\left[\begin{array}{cccc|cccc|cccc} -1 & 0 & 1 & 0 & 0 & 0 & 0 & 0 & 0 & 0 & 0 & 0 \\ 0 & -1 & 0 & 1 & 0 & 0 & 0 & 0 & 0 & 0 & 0 & 0 \\ \hline 0 & 0 & 0 & 0 & -1 & 0 & 1 & 0 & 0 & 0 & 0 & 0 \\ 0 & 0 & 0 & 0 & 0 & -1 & 0 & 1 & 0 & 0 & 0 & 0 \\ \hline 0 & 0 & 0 & 0 & 0 & 0 & 0 & 0 & -1 & 0 & 1 & 0 \\ 0 & 0 & 0 & 0 & 0 & 0 & 0 & 0 & 0 & -1 & 0 & 1 \end{array}\right]. \quad (3.14)$$

To build the equation of motion (2.10), proper assembly of M, C and K matrices is required. Since the vectors of acceleration and displacement have the dimensions $n \times (m-2)$, another operator with the same number of elements as the solution of the equation of motion must be established. Let us denote this operator D_0:

$$D_0 = \left[\begin{array}{cccc|cccc|cccc} 0 & 1 & 0 & 0 & 0 & 0 & 0 & 0 & 0 & 0 & 0 & 0 \\ 0 & 0 & 1 & 0 & 0 & 0 & 0 & 0 & 0 & 0 & 0 & 0 \\ \hline 0 & 0 & 0 & 0 & 0 & 1 & 0 & 0 & 0 & 0 & 0 & 0 \\ 0 & 0 & 0 & 0 & 0 & 0 & 1 & 0 & 0 & 0 & 0 & 0 \\ \hline 0 & 0 & 0 & 0 & 0 & 0 & 0 & 0 & 0 & 1 & 0 & 0 \\ 0 & 0 & 0 & 0 & 0 & 0 & 0 & 0 & 0 & 0 & 1 & 0 \end{array}\right]. \quad (3.15)$$

The original matrices M, C and K of size n,n are:

$$M = \begin{bmatrix} M_{11} & M_{12} & M_{13} \\ M_{21} & M_{22} & M_{23} \\ M_{31} & M_{32} & M_{33} \end{bmatrix} \quad C = \begin{bmatrix} C_{11} & C_{12} & C_{13} \\ C_{21} & C_{22} & C_{23} \\ C_{31} & C_{32} & C_{33} \end{bmatrix} \quad K = \begin{bmatrix} K_{11} & K_{12} & K_{13} \\ K_{21} & K_{22} & K_{23} \\ K_{31} & K_{32} & K_{33} \end{bmatrix}. \quad (3.16)$$

The new matrices, denoted by MD, CD and KD respectively, have the dimensions $n \times (m-2), n \times (m-2)$:

$$MD = \left[\begin{array}{cc|cc|cc} M_{11} & 0 & M_{12} & 0 & M_{13} & 0 \\ 0 & M_{11} & 0 & M_{12} & 0 & M_{13} \\ \hline M_{21} & 0 & M_{22} & 0 & M_{23} & 0 \\ 0 & M_{21} & 0 & M_{22} & 0 & M_{23} \\ \hline M_{31} & 0 & M_{32} & 0 & M_{33} & 0 \\ 0 & M_{31} & 0 & M_{32} & 0 & M_{33} \end{array}\right], \tag{3.17a}$$

$$CD = \left[\begin{array}{cc|cc|cc} C_{11} & 0 & C_{12} & 0 & C_{13} & 0 \\ 0 & C_{11} & 0 & C_{12} & 0 & C_{13} \\ \hline C_{21} & 0 & C_{22} & 0 & C_{23} & 0 \\ 0 & C_{21} & 0 & C_{22} & 0 & C_{23} \\ \hline C_{31} & 0 & C_{32} & 0 & C_{33} & 0 \\ 0 & C_{31} & 0 & C_{32} & 0 & C_{33} \end{array}\right], \tag{3.17b}$$

$$KD = \left[\begin{array}{cc|cc|cc} K_{11} & 0 & K_{12} & 0 & K_{13} & 0 \\ 0 & K_{11} & 0 & K_{12} & 0 & K_{13} \\ \hline K_{21} & 0 & K_{22} & 0 & K_{23} & 0 \\ 0 & K_{21} & 0 & K_{22} & 0 & K_{23} \\ \hline K_{31} & 0 & K_{32} & 0 & K_{33} & 0 \\ 0 & K_{31} & 0 & K_{32} & 0 & K_{33} \end{array}\right]. \tag{3.17c}$$

The main challenge now is to create a matrix operator able to differentiate automatically the objective function R with respect to p_{ij}. As mentioned in Chapter II, parameters p_{ij} are related to the stiffness matrix K, damping matrix C and mass matrix M. To explain the aforementioned differentiation in a very simple way, let us assume that our p_{ij} parameters are the stiffness coefficients of every element of the structure as described by the matrix K using FEM. If the two elements with stiffness' K1 and K2 describe element #1 and element #2,

$$K = K1_g + K2_g = \begin{bmatrix} K1_{11} & K1_{12} & 0 \\ K1_{21} & (K1_{22} + K2_{11}) & K2_{12} \\ 0 & K2_{21} & K2_{22} \end{bmatrix}, \tag{3.18}$$

where $K1_g$ and $K2_g$ are the stiffness matrices written using all DOF:

$$K1_g = \begin{bmatrix} K1_{11} & K1_{12} & 0 \\ K1_{21} & K1_{22} & 0 \\ 0 & 0 & 0 \end{bmatrix} \qquad K2_g = \begin{bmatrix} 0 & 0 & 0 \\ 0 & K2_{11} & K2_{12} \\ 0 & K2_{21} & K2_{22} \end{bmatrix}. \tag{3.19}$$

Each matrix can be described as the multiplication of a scalar representing coefficient responsible for the stiffness changes, and a matrix of coefficients which are not affected by the stiffness changes but represents the properties of a particular type of the element:

$$K1_g = p_1 \overbrace{\begin{bmatrix} k1_{11} & k1_{12} & 0 \\ k1_{21} & k1_{22} & 0 \\ 0 & 0 & 0 \end{bmatrix}}^{k_1} \qquad K2_g = p_2 \overbrace{\begin{bmatrix} 0 & 0 & 0 \\ 0 & k2_{11} & k2_{12} \\ 0 & k2_{21} & k2_{22} \end{bmatrix}}^{k_2}. \tag{3.20}$$

By producing a vector of stiffness coefficients P and a matrix of element coefficients k as follows:

$$P^T = \begin{bmatrix} p_1 & p_2 \end{bmatrix} \qquad k = \begin{bmatrix} k_1 \vdots k_2 \end{bmatrix}, \tag{3.21}$$

differentiating is very simple:

$$\frac{\partial KD}{\partial p_i} = kd_i, \tag{3.22}$$

where kd_i matrix is assembled from k_i matrix in the same way as KD matrix from K matrix. One more matrix operator is needed if the vibrating system is to be identified by accelerations or displacements measured not at all DOF. Matrix B chooses only those DOF from all DOF of the finite element model which correspond to the measured data of the vibrating structure. In the example it is assumed that accelerations are measured only at n = 1 and n = 3:

$$B=\left[\begin{array}{cc|cc|cc} 1 & 0 & 0 & 0 & 0 & 0 \\ 0 & 1 & 0 & 0 & 0 & 0 \\ \hline 0 & 0 & 0 & 0 & 1 & 0 \\ 0 & 0 & 0 & 0 & 0 & 1 \end{array}\right]. \tag{3.23}$$

As one can see, the above presented matrix operators are very easy to establish, and they may be modified automatically for a vibrating system with any DOF and using different types of elements. The differentiation necessary for assembling a gradient vector G and Hessian matrix H can be done in a very simple fashion and will be presented in the next section.

3.1.2 Numerical Solution for System Identification

As stated in Chapter II, the identification procedure is utilised as a base for identifying the stiffness of each element of a structure from measured accelerations. Using previously described matrix operators, the objective functions R can be defined as follows:

$$R=\frac{1}{2}\left[BD_2u-a^*\right]^T\left[BD_2u-a^*\right]+\left[\tilde{D}u\right]^T\left[\lambda\right], \tag{3.24}$$

where

$$\tilde{D}\equiv\left[MD\,D_2+CD\,D_1+KD\,D_0\right]. \tag{3.25}$$

To proceed with Newton-Raphson method, it is necessary to provide the solution vector X, gradient vector G and Hessian matrix H as follows:

$$X^T = \left[u \;\vdots\; \lambda \;\vdots\; p \right], \tag{3.26}$$

$$G^T = \left[\frac{\partial R}{\partial u_{ij}} \;\vdots\; \frac{\partial R}{\partial \lambda_{ij}} \;\vdots\; \frac{\partial R}{\partial p_i} \right], \tag{3.27}$$

$$H = \left[\begin{array}{c|c|c} H_{11} & H_{12} & H_{13} \\ \hline H_{12}^T & 0 & H_{23} \\ \hline H_{13}^T & H_{23}^T & 0 \end{array} \right], \tag{3.28}$$

where $$H_{11} = \frac{\partial^2 R}{\partial u_{ij}^2}, \quad H_{12} = \frac{\partial^2 R}{\partial u_{ij} \partial \lambda_{ij}}, \quad H_{13} = \frac{\partial^2 R}{\partial u_{ij} \partial p_i}, \quad H_{23} = \frac{\partial^2 R}{\partial \lambda_{ij} \partial p_i}.$$

Using previously described matrix operators, we can write above derivatives as follows:

$$\frac{\partial R}{\partial u_{ij}} = D_2^T B^T \left[B D_2 u - a^* \right] + \left[\tilde{D} \right]^T \left[\lambda \right], \tag{3.29}$$

$$\frac{\partial R}{\partial \lambda_{ij}} = \left[\tilde{D} u \right]^T, \tag{3.30}$$

$$\frac{\partial R}{\partial p_i} = \left[\left[kd_1, \ldots, kd_e \right] D_0 u \right]^T \lambda, \tag{3.31}$$

$$\frac{\partial^2 R}{\partial u_{ij}^2} = D_2^T B^T B D_2, \tag{3.32}$$

$$\frac{\partial^2 R}{\partial u_{ij} \partial \lambda_{ij}} = \left[\tilde{D} \right]^T, \tag{3.33}$$

$$\frac{\partial^2 R}{\partial u_{ij} \partial p_i} = \left[\left[kd_1 \quad \cdots \quad kd_e \right] \left[D_0 \right] \left[\lambda \right] \right]^T, \tag{3.34}$$

$$\frac{\partial^2 R}{\partial \lambda_{ij} \partial p_i} = \left[\left[kd_1 \quad \cdots \quad kd_e \right] \left[D_0 \right] \left[u \right] \right]^T. \tag{3.35}$$

Now, when the identification procedure is simplified to the basic matrix and vector operations, the parameters can be identified. In our case they are the stiffness properties of a vibrating structure. Since the Newton - Raphson method is used, it is very important to provide sufficiently good initial guesses. These initial values, given to the computing system, are entries to the first solution vector X. It includes displacements for all DOF - u, vector of Lagrangian multipliers - λ, and vector of stiffness coefficients - P. To obtain vector P is the easiest problem since the original stiffness properties of the vibrating system can be used. The vector of displacements u can be obtained in different ways. Probably the most efficient way is to obtain it from accelerometers through a double-integrating electronic circuit. Although with less accuracy than acceleration, but it still is a very close guess for the identification procedure.

Element Stiffness from System Identification		Affected by Crack	Affected by Corrosion
period #1	period #2		
$EI_1 = EI_{org}$	$EI_2 = EI_{org}$	No	No
$EI_1 < EI_{org}$	$EI_2 = EI_{org}$	Yes	No
$EI_1 = EI_{org}$	$EI_2 < EI_{org}$	Yes	No
$EI_1 < EI_{org}$	$EI_2 < EI_{org}$ $EI_1 = EI_2$	No	Yes
$EI_1 < EI_{org}$	$EI_2 < EI_{org}$ $EI_1 < EI_2$	Yes	Yes
$EI_1 < EI_{org}$	$EI_2 < EI_{org}$ $EI_1 > EI_2$	Yes	Yes

Table 3.1 Key to determine cracked and corroded members from System Identification output data

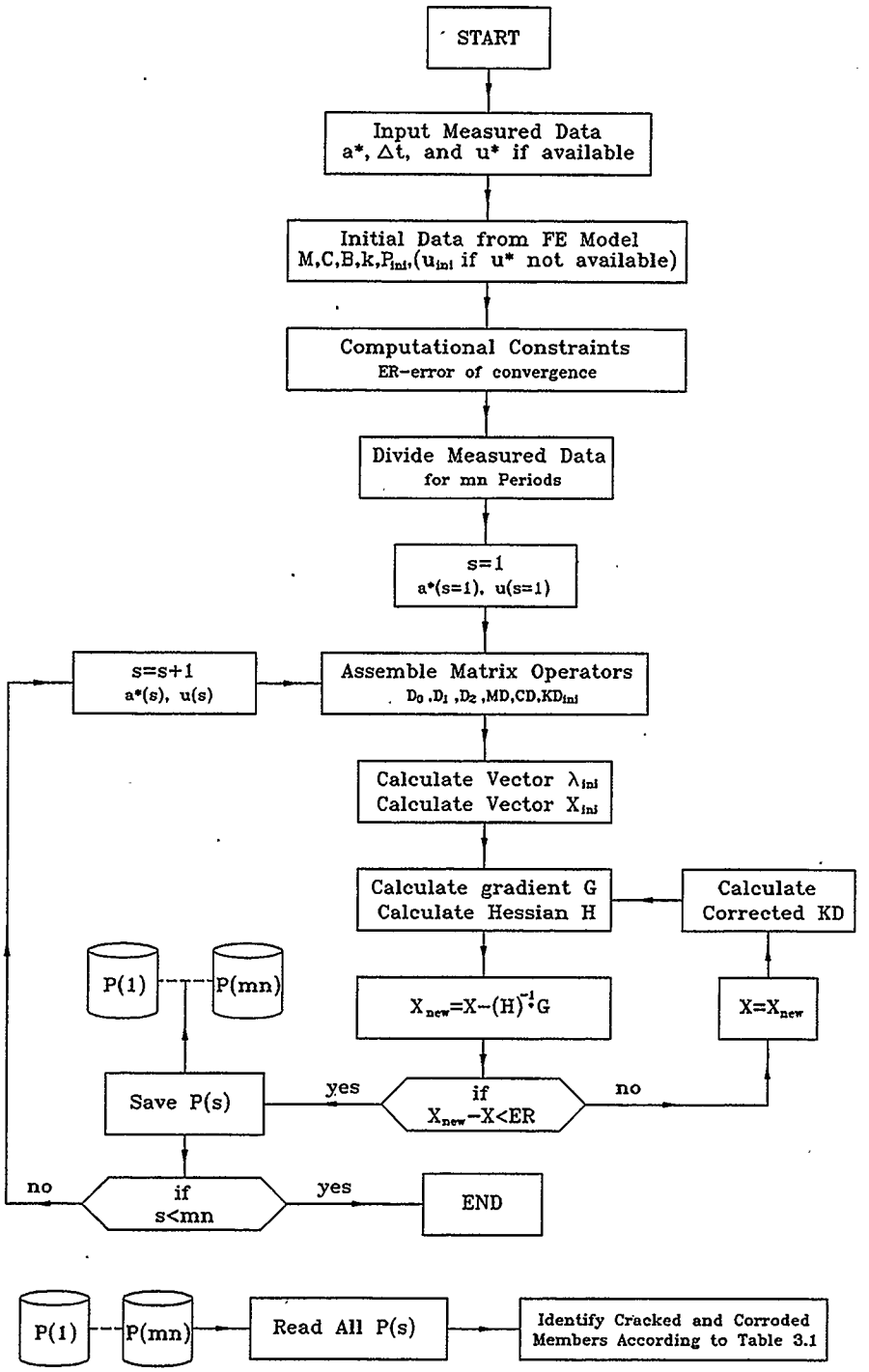

Figure 3.2 Flow chart of System Identification

It might be also a wild guess, with all values randomly taken. However, if the displacement selected is not close enough, the method can fail to converge. Initial values of Lagrangian multipliers can be calculated by rearranging equation (2.13a):

$$\lambda_{init} = \left[\tilde{D}\tilde{D}^{T}\right]^{-1} D_2^{T}\left(D_0 a^{*} - D_2 u_{init}\right). \tag{3.36}$$

To be able to recognise the occurrence of cracks in vibrating structure, the measuring data must be taken from the time period when the deformation of the structure is in the same mode for each element (par. 2.2). It requires the analysis of the displacement of each member of the structure to properly establish the time periods. It is necessary to choose at least two time periods, but for a complicated structure many more may be necessary. Once having the stiffness of a member defined from different time periods, it is possible to find if the crack or corrosion changed the stiffness properties of an element. If in both periods the stiffness is the same, it automatically rejects the possibilities of cracks occurrence. If the found stiffness is smaller than the original, then corrosion has taken place. If in the two periods the stiffness is different, we have a crack. The simplified algorithm for the analysis of the solution is presented in Table 3.1. Figure 3.2 presents the flow chart of the identification procedure.

3.2 Data Generation Techniques

To evaluate any theoretical problem, comparison of experimental data with theoretical analysis is the most valuable procedure. Unfortunately, since the author had no opportunity to proceed with experiments to prove the validity of the method, computer simulation of the vibrating system with known properties provided the data for System Identification. Simulating the real behaviour of the vibrating structure in a 'controlled environment' most of the time provides enough information to asses the theoretical approach. The author believes, that the performed 'computer experiment' is able to demonstrate in a very clear way that the method is working in a very efficient manner.

To obtain the data for System Identification of the vibrating structure, a non-linear multidegree-of-freedom system must be solved. There are many methods available, but because of personal preference and overall effectiveness of the Wilson-θ method, it will be utilised to provide input data.

The basic assumption of the Wilson-θ method is that the acceleration varies linearly over the time interval from t to $t + \theta\Delta t$ where $\theta \geq 1.0$. The value of the factor θ is determined to obtain optimum stability of the numerical process and accuracy of the solution. It has been shown by Wilson [45], that, for $\theta \geq 1.38$, the method becomes unconditionally stable. The equation expressing the incremental equilibrium conditions for a multidegree-of-freedom system can be derived as the matrix equivalent of the incremental equation of the motion for the single degree-of-freedom system. Thus taking the difference between dynamic

equilibrium conditions defined at time t_i and $t_i + \tau$, where $\tau = \theta\Delta t$, we obtain the incremental equations:

$$M\hat{\Delta}\ddot{y}_i + C(\dot{y})\hat{\Delta}\dot{y}_i + K(y)\hat{\Delta}y_i = \hat{\Delta}F_i, \tag{3.49}$$

in which the circumflex over Δ indicates that the increments are associated with the extended time step $\tau = \theta\Delta t$. Thus:

$$\hat{\Delta}y_i = y(t_i + \tau) - y(t_i), \tag{3.50}$$

$$\hat{\Delta}\dot{y}_i = \dot{y}(t_i + \tau) - \dot{y}(t_i), \tag{3.51}$$

$$\hat{\Delta}\ddot{y}_i = \ddot{y}(t_i + \tau) - \ddot{y}(t_i), \tag{3.52}$$

and

$$\hat{\Delta}F_i = F(t_i + \tau) - F(t_i). \tag{3.53}$$

It is assumed that the stiffness matrices and damping are obtained for each time step as the initial values of the tangent to the corresponding curves as shown in Figure 3.4 rather than the slope of the secant line which requires iteration. Hence, the stiffness coefficient is defined as:

$$k_{ij} = \frac{dF_{si}}{dy_j}, \tag{3.54}$$

and the damping coefficient as:

$$c_{ij} = \frac{dF_{Di}}{d\dot{y}_j}, \tag{3.55}$$

in which F_{si} and F_{Di} are, respectively, the elastic and damping forces at nodal coordinate i; y_j and $\dot{y}_j$ are, respectively, the displacement and velocity at nodal coordinate j.

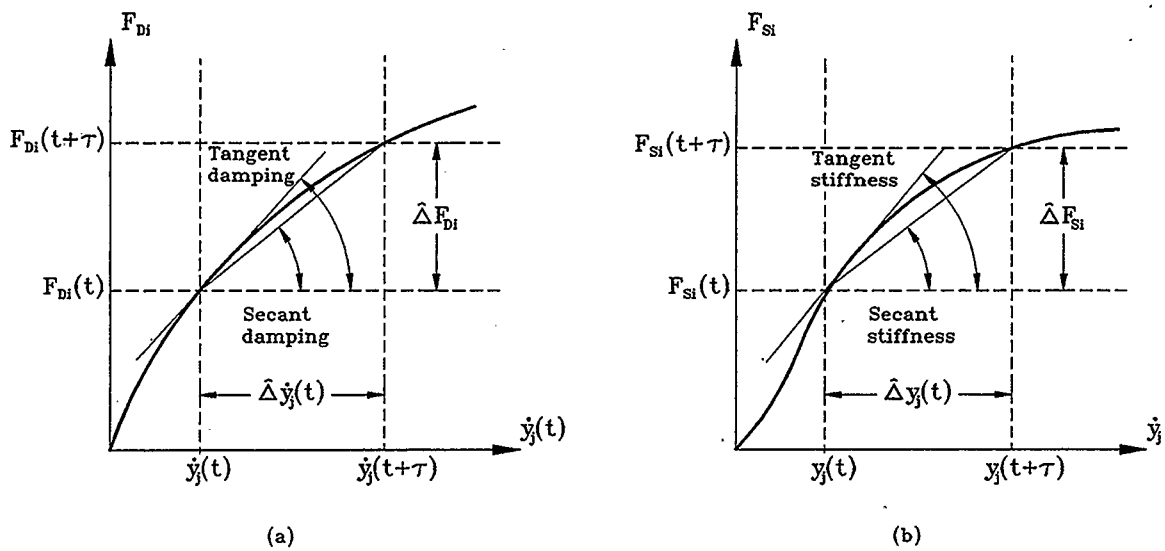

Figure 3.3 Definition of influence coefficients (a) - nonlinear viscous damping c_{ij}

(b) - nonlinear stiffness k_{ij}

As mentioned earlier, the Wilson-θ method is based on the assumption that the acceleration may be represented by a linear function during the time step $\tau = \theta\Delta t$ as shown in Figure 3.5.

The linear expression for the acceleration during the extended time step can be written as:

$$\ddot{y}(t) = \ddot{y}_i + \frac{\hat{\Delta}\ddot{y}_i}{\tau}(t - t_i), \tag{3.56}$$

in which $\hat{\Delta}\ddot{y}_i$ is given by equation (3.52). Integrating equation (3.56) twice, yields:

$$\dot{y}(t) = \dot{y}_i + \ddot{y}_i(t - t_i) + \frac{\hat{\Delta}\ddot{y}_i}{2\tau}(t - t_i)^2, \tag{3.57}$$

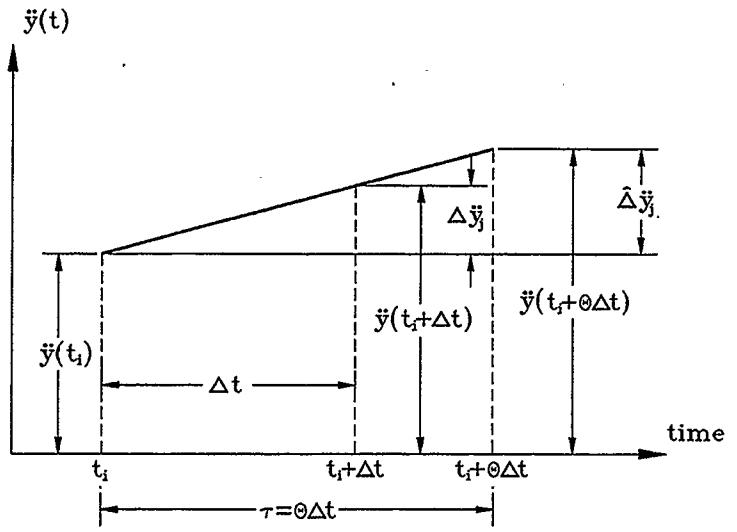

Figure 3.4 Linear acceleration assumption in the extended time interval

and

$$y(t) = y_i + \dot{y}_i(t-t_i) + \frac{1}{2}\ddot{y}_i(t-t_i)^2 + \frac{\hat{\Delta}\ddot{y}_i}{6\tau}(t-t_i)^3. \tag{3.58}$$

Evaluation of equation (3.57) and (3.58) at the end of the extended interval $t = t_i + \tau$, gives:

$$\hat{\Delta}\dot{y}_i = \ddot{y}_i\tau + \frac{1}{2}\hat{\Delta}\ddot{y}_i\tau, \tag{3.59}$$

and

$$\hat{\Delta}y_i = \dot{y}_i\tau + \frac{1}{2}\ddot{y}_i\tau^2 + \frac{1}{6}\hat{\Delta}\ddot{y}_i\tau^2, \tag{3.60}$$

in which $\hat{\Delta}y_i$ and $\hat{\Delta}\dot{y}_i$ are defined by equations (3.50) and (3.51) respectively. Equation (3.60) is solved for the incremental acceleration $\hat{\Delta}\ddot{y}_i$ and substituted in equation (3.59):

$$\hat{\Delta}\ddot{y}_i = \frac{6}{\tau^2}\hat{\Delta}y_i - \frac{6}{\tau}\dot{y}_i - 3\ddot{y}_i, \tag{3.61}$$

and

$$\hat{\Delta}\dot{y}_i = \frac{3}{\tau}\hat{\Delta}y_i - 3\dot{y}_i - \frac{\tau}{2}\ddot{y}_i . \tag{3.62}$$

Finally, substituting equations (3.61) and (3.62) into the incremental equation of motion, equation (3.49), results in an equation for the incremental displacement $\hat{\Delta}y_i$ which may be conveniently written as:

$$\overline{K}_i \hat{\Delta}y_i = \hat{\Delta}\overline{F}_i , \tag{3.63}$$

where

$$\overline{K}_i = K_i + \frac{6}{\tau^2}M + \frac{3}{\tau}C_i , \tag{3.64}$$

and

$$\hat{\Delta}\overline{F}_i = \hat{\Delta}F_i + M\left(\frac{6}{\tau}\dot{y}_i + 3\ddot{y}_i\right) + C_i\left(3\dot{y}_i + \frac{\tau}{2}\ddot{y}_i\right). \tag{3.65}$$

Equation (3.63) may be solved for the incremental displacement $\hat{\Delta}y_i$ by simply solving a system of linear equations. To obtain the incremental acceleration $\hat{\Delta}\ddot{y}_i$ for the extended time interval, the value of $\hat{\Delta}y_i$ obtained from the solution of equation (3.63) is substituted into equation (3.61). The incremental acceleration $\Delta\ddot{y}_i$ for the normal time interval Δt is then obtained by a simple linear interpolation. Hence:

$$\Delta\ddot{y} = \frac{\hat{\Delta}\ddot{y}}{\theta}. \tag{3.66}$$

To calculate the incremental velocity $\Delta\dot{y}_i$ and incremental displacement Δy_i corresponding to the normal interval Δt, equations (3.59) and (3.60) are used with the extended time interval parameter τ substituted for Δt, which gives:

$$\Delta\dot{y}_i = \ddot{y}_i \Delta t + \frac{1}{2}\Delta\ddot{y}_i \Delta t, \tag{3.67}$$

and

$$\Delta y_i = \dot{y}_i \Delta t + \frac{1}{2}\ddot{y}_i \Delta t^2 + \frac{1}{6}\Delta\ddot{y}_i \Delta t^2. \tag{3.68}$$

Finally, the displacement y_{i+1} and velocity $\dot{y}_{i+1}$ at the end of the normal time interval are calculated by:

$$y_{i+1} = y_i + \Delta y_i, \tag{3.69}$$

and

$$\dot{y}_{i+1} = \dot{y}_i + \Delta\dot{y}_i. \tag{3.70}$$

The initial acceleration for the next step is calculated from the condition of dynamic equilibrium at the time $t + \Delta t$; thus:

$$\ddot{y}_{i+1} = [M]^{-1}\left[F_{i+1} - C_{i+1}\dot{y}_{i+1} - K_{i+1}y_{i+1}\right], \tag{3.71}$$

in which the products $C_{i+1}\dot{y}_{i+1}$ and $K_{i+1}y_{i+1}$ represent, respectively, the damping force and stiffness force vectors evaluated at the end of the time step $t_{i+1} = t_i + \Delta t$. Once the displacement, velocity and acceleration vectors have been determined at the time $t_{i+1} = t_i + \Delta t$, the outlined procedure is repeated to calculate these quantities at the next time step $t_{i+2} = t_i + \Delta t$ and the process is continued to any desired time.

The algorithm for the integration process of a linear system by the Wilson-θ method is presented below:

Initialisation

(1) Assemble the system stiffness matrix K, mass matrix M, and damping matrix C.

(2) Set initial values for displacement y_0, velocity $\dot{y}_0$, and forces F_0.

(3) Calculate initial accelerations $\ddot{y}_0$ from

$$M\ddot{y}_0 = F_0 - C\dot{y}_0 - Ky_0. \tag{3.72}$$

(4) Select a time step Δt, the θ (usually taken as 1.4) and calculate the constants τ, a_1, a_2, a_3, and a_4 from the relations

$$\tau = \theta\Delta t \qquad a_1 = \frac{3}{\tau} \qquad a_2 = \frac{6}{\tau} \qquad a_3 = \frac{\tau}{2} \qquad a_4 = \frac{6}{\tau^2}. \tag{3.73}$$

(5) Form the effective stiffness matrix $\overline{K}$, namely

$$\overline{K} = K + a_4 M + a_1 C. \tag{3.74}$$

For Each Time Step

(1) By linear interpolation, calculate the incremental load $\hat{\Delta}F_i$ for the time interval t_i to $t_i + \tau$, from the relation

$$\hat{\Delta}F_i = F_{i+1} + (F_{i+2} - F_{i+1})(\theta - 1) - F_i. \tag{3.75}$$

(2) Calculate the effective incremental load $\hat{\Delta}\overline{F}_i$ for the time interval t_i to $t_i + \tau$, from the relation

$$\hat{\Delta}\overline{F}_i = \hat{\Delta}F_i + (a_2 M + 3C)\dot{y}_i + (3M + a_3 C)\ddot{y}_i. \tag{3.76}$$

(3) Solve for the incremental displacement $\hat{\Delta}y_i$ from

$$\overline{K}\,\hat{\Delta}y_i = \hat{\Delta}\overline{F}_i. \tag{3.77}$$

(4) Calculate the incremental acceleration for the extended time interval τ, from the relation

$$\hat{\Delta}\ddot{y}_i = a_4\hat{\Delta}y_i - a_2\dot{y}_i - 3\ddot{y}_i. \tag{3.78}$$

(5) Calculate the incremental acceleration for the nominal time interval from

$$\Delta\ddot{y} = \frac{\hat{\Delta}\ddot{y}}{\theta}. \tag{3.79}$$

(6) Calculate the incremental velocity $\Delta\dot{y}_i$, and the incremental displacement Δy_i from time t_i to $t_i + \Delta t$ from the relations

$$\begin{aligned}\Delta\dot{y}_i &= \ddot{y}_i\Delta t + \frac{1}{2}\Delta\ddot{y}_i\Delta t\\ \Delta y_i &= \dot{y}_i\Delta t + \frac{1}{2}\ddot{y}_i\Delta t^2 + \frac{1}{6}\Delta\ddot{y}_i\Delta t^2.\end{aligned} \tag{3.80}$$

(7) Calculate the velocity and displacement at time $t_{i+1} = t_i + \Delta t$ using

$$\begin{aligned}y_{i+1} &= y_i + \Delta y_i\\ \dot{y}_{i+1} &= \dot{y}_i + \Delta\dot{y}_i.\end{aligned} \tag{3.81}$$

(8) Calculate the acceleration $\ddot{y}_{i+1}$ at time $t_{i+1} = t_i + \Delta t$ directly from the equilibrium equation of motion namely

$$M\ddot{y}_{i+1} = F_{i+1} - C\dot{y}_{i+1} - Ky_{i+1}. \tag{3.82}$$

End of Wilson-θ Integration Method

During data generation, computation of free response (F = 0) of a structure with cracks, one slight modification of the Wilson-θ method must be made. Since the crack is changing the stiffness of a member of a structure, a small routine to check the geometry of each element is necessary after every time-step of calculation in Wilson-θ routine. If, by analysing displacements at each end of the element, it is observed that the geometry changes in such a way that the crack is open or closed after the last time-step, the effective stiffness matrix $\overline{K}$ must be updated. The updated effective stiffness matrix $\overline{K}$ is assembled with new stiffness coefficients for those elements which are affected by crack closing or opening after the last calculation. In the next time-step with updated stiffness matrix, new accelerations, velocities and displacements are computed based on displacements and velocities from the previous time-step. This procedure guarantees that the continuity conditions are satisfied.

It is also worth mentioning that the size of time step Δt can dramatically affect the accuracy of the calculated results. The best idea is to assume Δt to be:

$$\Delta t \leq \frac{1}{20\,\omega_{max}}, \tag{3.83}$$

which assures that the acceleration is changing less than 1% of its value between the steps and that the produced data is very accurate.

CHAPTER IV
Numerical Results and Analysis

4.1 Beam structure

The loss of bending stiffness due to transverse cracks and corrosion has been examined using a ten-element beam model, fixed at both ends. Figure 4.1 illustrates the model of a beam, shape of a beam in two different geometric configurations, and a table of stiffness coefficients for every element of a beam. As mentioned in Chapter II, the structure was analysed in two different time periods. This step is very important, since in every independent time period, every element of a ten-element beam must have the same curvature, positive or negative. In this case, the structure was excited into the first mode, and it was necessary to select only two corresponding time periods. In the case of a more complex modal shape of the vibrating beam, it will be necessary to analyse more time periods. Seven elements of the ten-element beam have a smaller cross-sectional area than

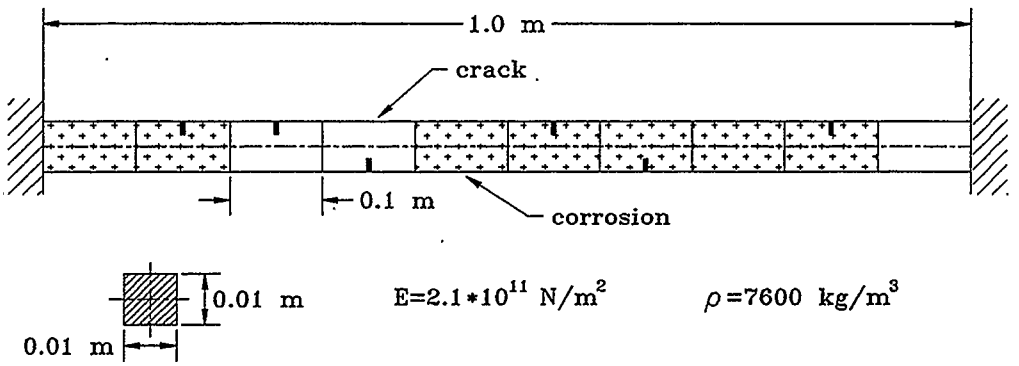

First mode of vibration, configuration # 1

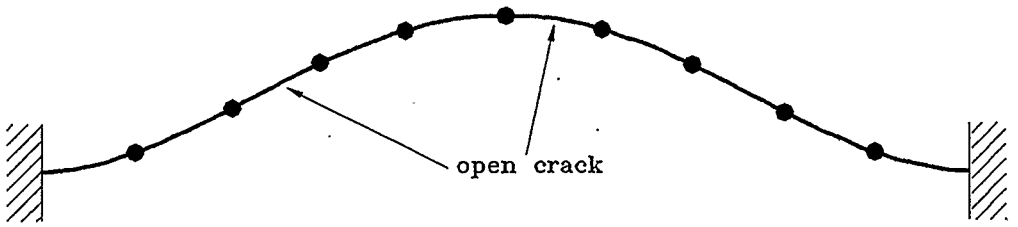

First mode of vibration, configuration # 2

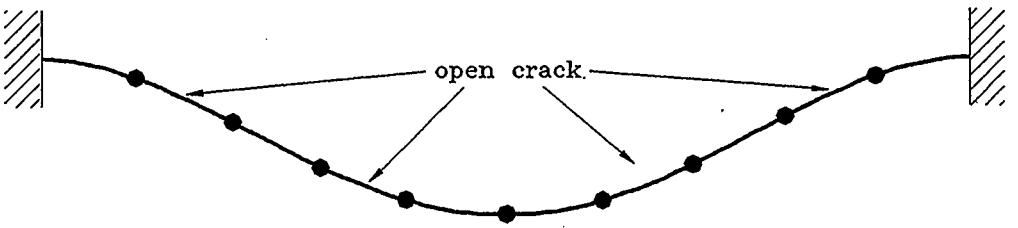

	Element No.	1	2	3	4	5	6	7	8	9	10
Stiffness	Original	1.000	1.000	1.000	1.000	1.000	1.000	1.000	1.000	1.000	1.000
	Corroded element	0.900	0.960			0.970	0.980	0.960	0.940	0.870	
	Cracked element		0.950	0.980	0.900		0.949	0.920		0.970	
	Crack+corrosion		0.912				0.930	0.883		0.844	

Figure 4.1 Vibrating beam, different geometric configurations and stiffness coefficient table

designed, due to corrosion. The loss of cross-sectional areas varies between 0.5% and 3.5% of original values which can be translated to 2% to 13% loss of flexural stiffness. Six elements, some of them already affected by corrosion, have cracks: two on the lower surface, four on the upper surface. The magnitude of stiffness changes varies between 2 and 7%, which can be represented as cracks of a depth from 10% to 30 % of height of a beam element (Figure 2.2).

The stiffness coefficient for an element affected by corrosion and the crack is simply calculated as multiplication of those two values. This is the correct procedure since the stiffness coefficient for a beam with a transverse crack was calculated in comparison to a beam without a crack. Data for system identification were generated using the Wilson-θ method. A stiffness matrix was assembled in every step of this iterative procedure, to make sure that the data mimic the real behavior of the structure. In every time-step, curvature of each element was checked, and the proper values of stiffness coefficients were assigned. After that, the global stiffness matrix was assembled for the next step. The sample data generated in this way are presented in Figure 4.2. These data are very smooth, since there is no error of measurement included in this calculation. Two time periods were established. For evaluation of the identification procedure the first configuration is considered. Also, at the beginning of the evaluating part of this analysis, all degrees of freedom were included in the analysis. Acceleration is our measured quantity, but since displacement is automatically computed in the case of real measurement, displacement can be implemented as initial value for the theoretical model in objective function. Stiffness coefficients are normalised by

definition since they are assigned as new values of the stiffness with respect to original values.

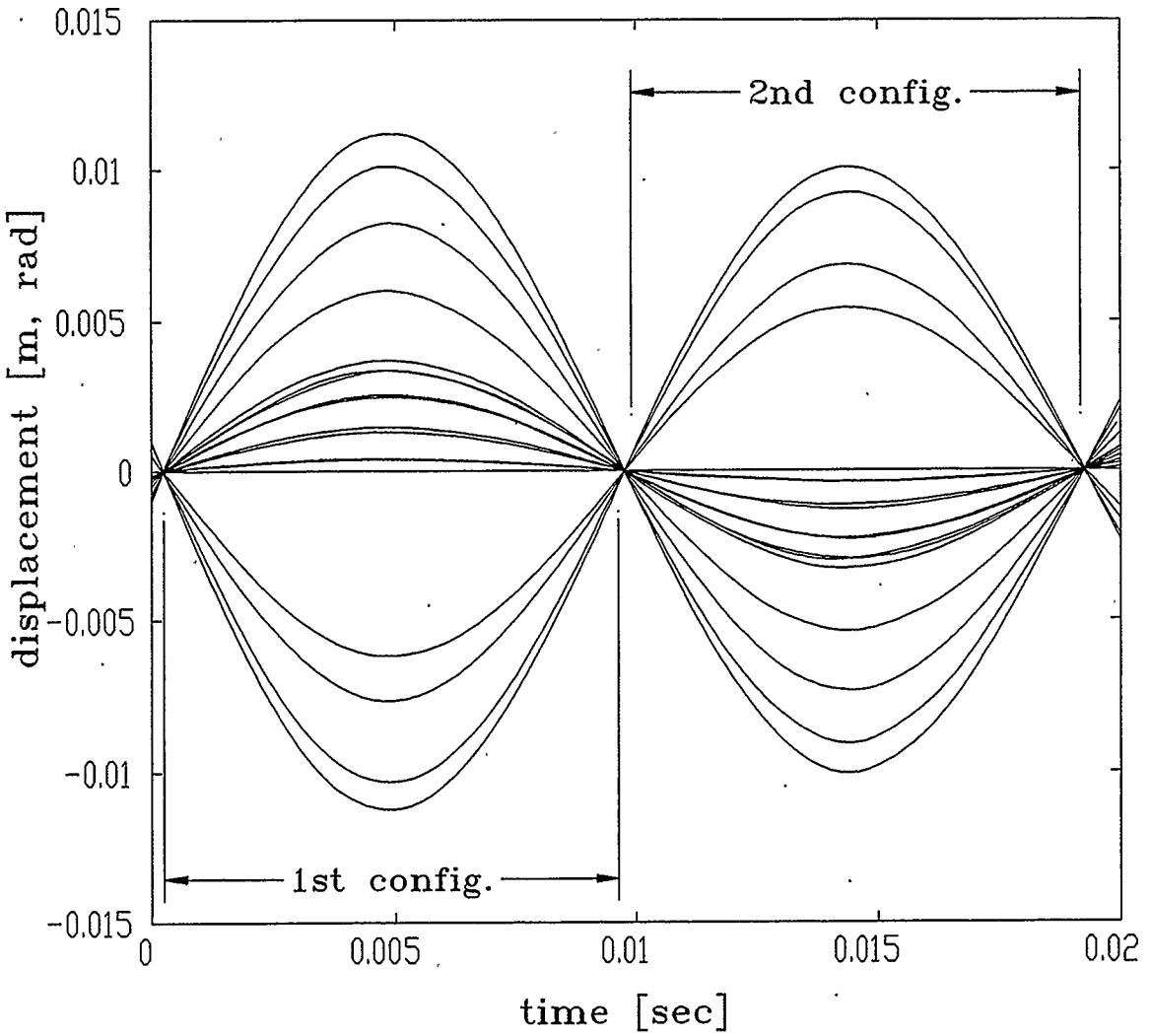

Figure 4.2 Damped vibration of ten-element beam in first mode of vibration

In Figure 4.3 the convergence history is presented for two cases, one with the initial values of stiffness coefficients equal to 2, second with initial values of stiffness coefficients equal to 50. As can be seen, the system is converging unconditionally in two steps with the error less than 0.5%. An extensive analysis was performed to find the dependency of the method on the number of time-steps necessary, and the value of the time-step with respect to the natural period of vibration. As shown in Figure 4.3, those two parameters can vary in the wide range, and still, the system is converging and achieving error less than 0.5 %.

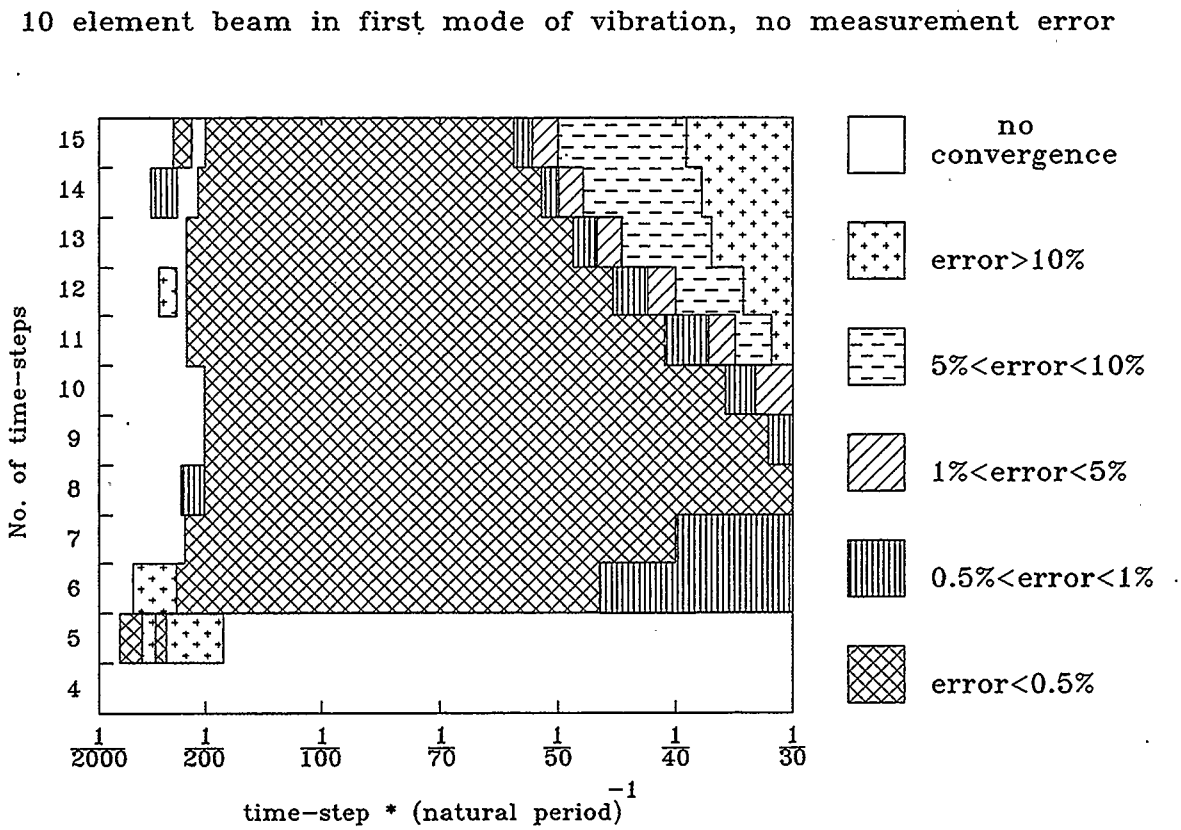

Figure 4.3 Error versus time-step size and number of time steps

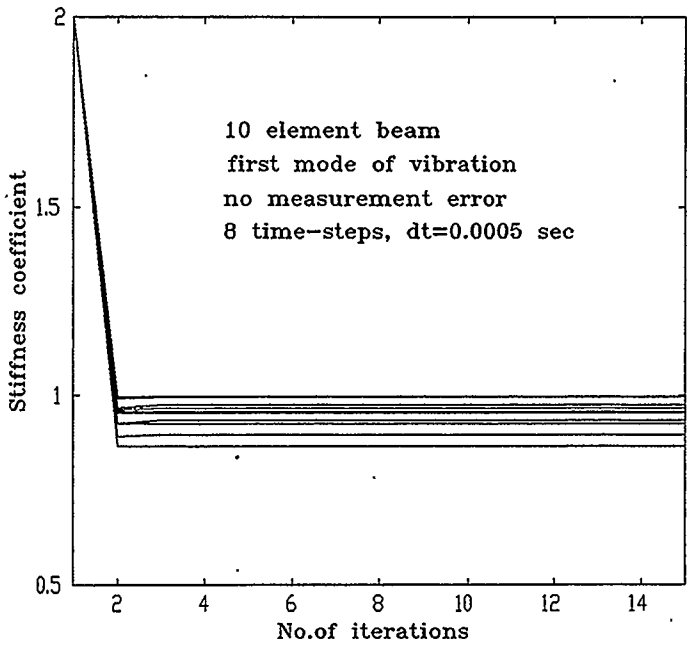

Element No.	Original Stiffness	Identified Stiffness
1	0.900	0.898
2	0.960	0.959
3	0.980	0.975
4	1.000	0.997
5	0.970	0.968
6	0.930	0.928
7	0.960	0.958
8	0.940	0.935
9	0.870	0.869
10	1.000	0.998

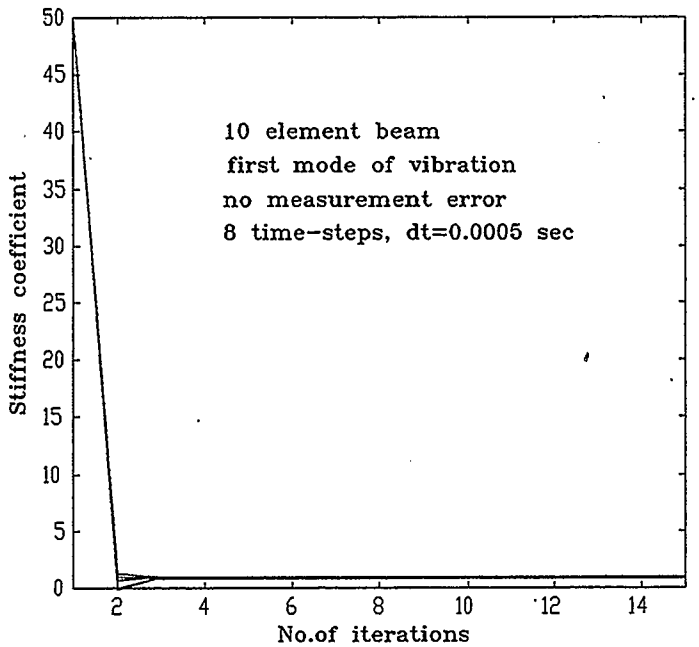

Element No.	Original Stiffness	Identified Stiffness
1	0.900	0.898
2	0.960	0.959
3	0.980	0.975
4	1.000	0.997
5	0.970	0.968
6	0.930	0.928
7	0.960	0.958
8	0.940	0.935
9	0.870	0.869
10	1.000	0.998

Figure 4.4 Convergence history for data without measurement error, two different values of initial stiffness coefficients - '2' and '50'

As we know, in real life the measurement error must be taken into account. If accelerometers are used as sensors, the expected error of measurement can be within ±5 to ±10% of the measured value. This error must be implemented in the evaluation of the identification procedure, since the effectiveness of the method can change dramatically with uncertainty of the solution (error in data can lead to a local minimum of the solution in the Newton-Raphson method). To model the system with measurement error, data without error was used. Next, a vector of normally distributed random numbers was generated, with mean '0' and variance of the desired error. Implementation of error into the data was done by simply multiplying each entry from the vector of the generated data with the corresponding entry from the error vector. Different error vectors were generated for the acceleration and displacement data. The displacement data with a randomly distributed error of ±2.0% is presented in Figure 4.5. For different values of the maximum error a new error vector was generated. Analysis of the influence of the measurement error on the accuracy of convergence of system identification, revealed that data smoothing increased the accuracy of convergence. By using simple polynomial fitting the data was filtered smooth enough, so that the raw differentiating method used in the system identification procedure (central difference method), was able to deal with a measurement error, as large as ±1.5% as could be seen in Figure 4.6 and Figure 4.7. Errors of magnitude ±2.0% made the system identification method unstable (Figure 4.7). Some modification of the Newton-Raphson method leads to better results. Since the oscillation of solutions implies that a full Newton-Raphson step is overshooting the minimum of the function, the strategy used was simple. First, the full

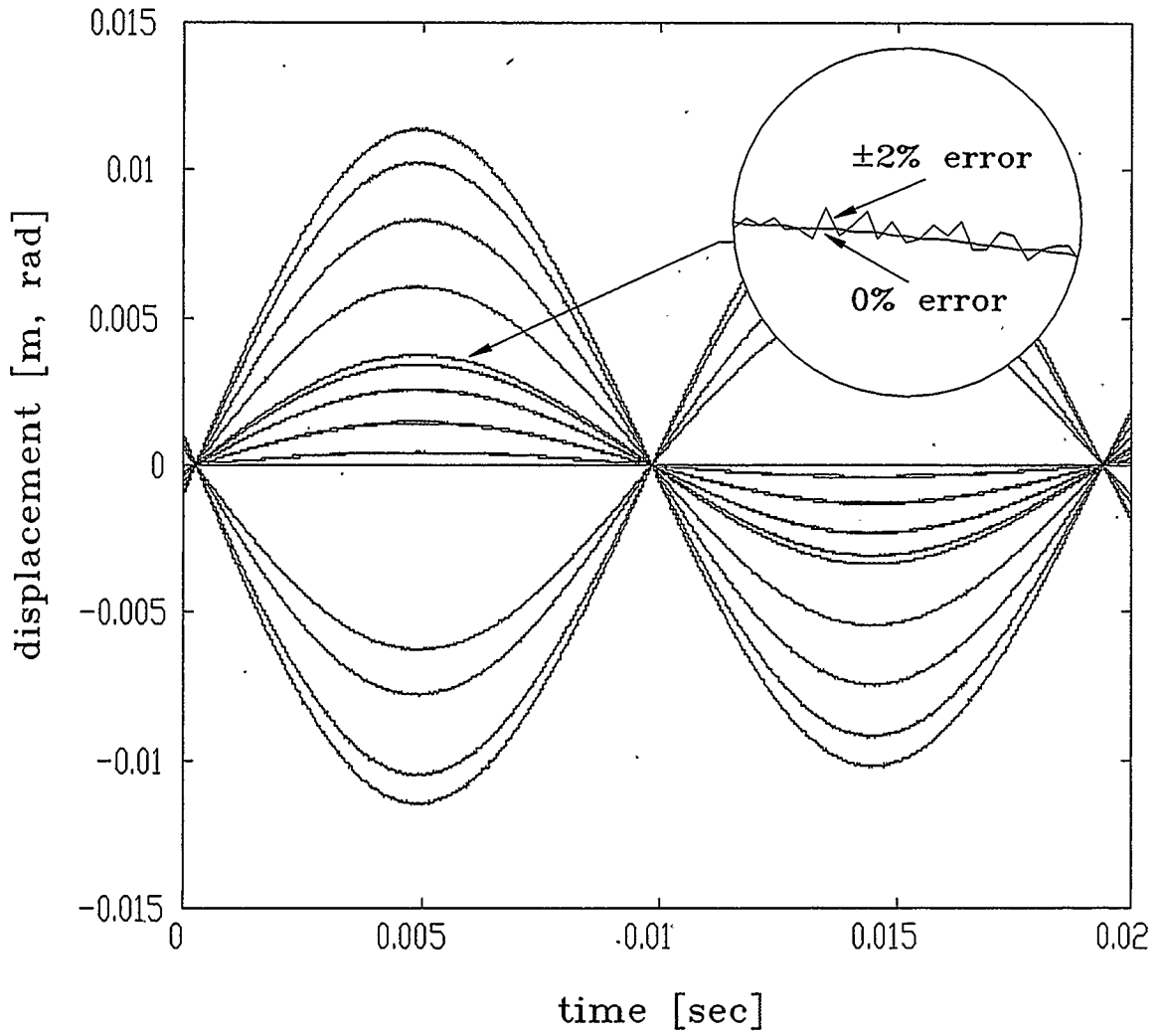

Figure 4.5 Damped vibration of ten element-beam in first mode of vibration, displacement data with ±2.0% error of measurement

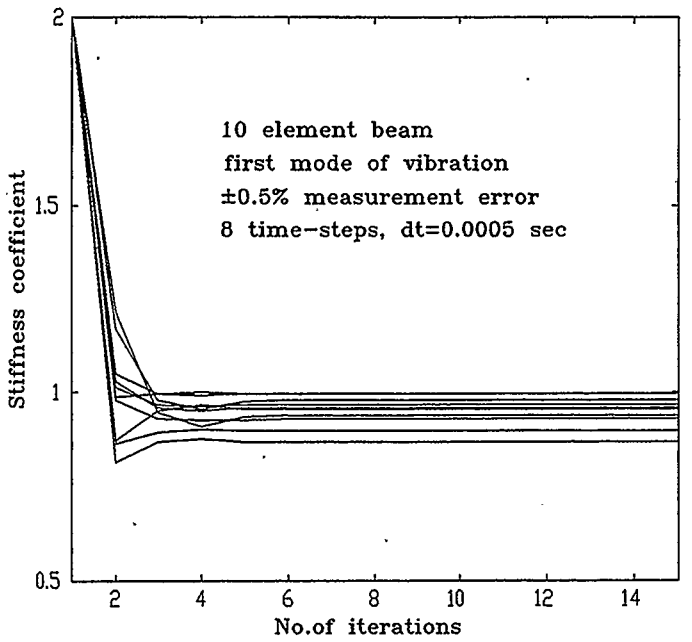

Element No.	Original Stiffness	Identified Stiffness
1	0.900	0.897
2	0.960	0.957
3	0.980	0.980
4	1.000	0.999
5	0.970	0.969
6	0.930	0.929
7	0.960	0.959
8	0.940	0.938
9	0.870	0.869
10	1.000	0.998

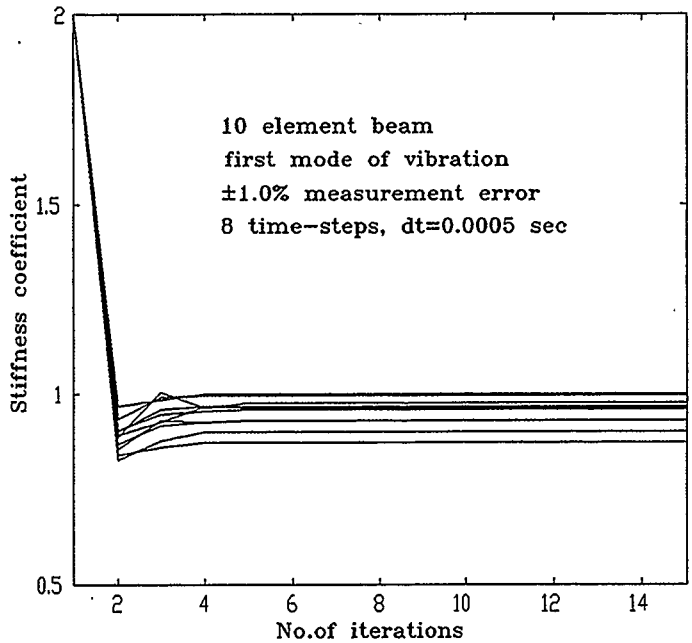

Element No.	Original Stiffness	Identified Stiffness
1	0.900	0.901
2	0.960	0.962
3	0.980	0.975
4	1.000	0.999
5	0.970	0.970
6	0.930	0.930
7	0.960	0.959
8	0.940	0.931
9	0.870	0.875
10	1.000	1.002

Figure 4.6 Convergence history for data with measurement error ±0.5% and ±1.0%

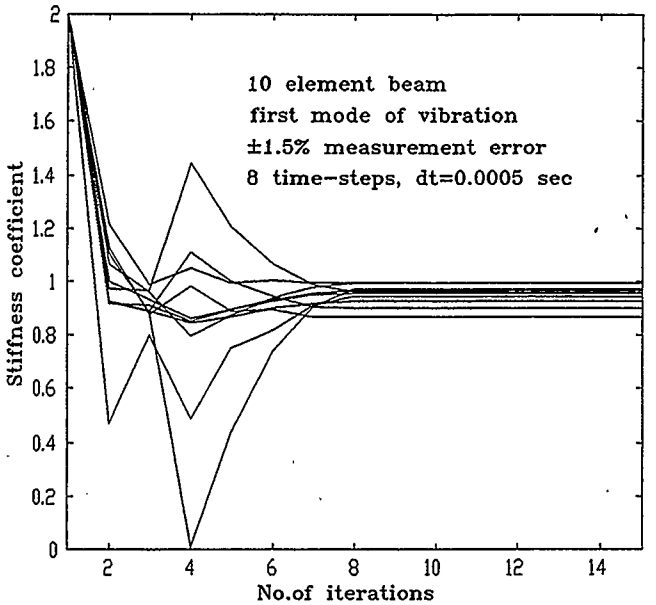

Element No.	Original Stiffness	Identified Stiffness
1	0.900	0.899
2	0.960	0.960
3	0.980	0.975
4	1.000	0.997
5	0.970	0.968
6	0.930	0.928
7	0.960	0.958
8	0.940	0.942
9	0.870	0.866
10	1.000	0.996

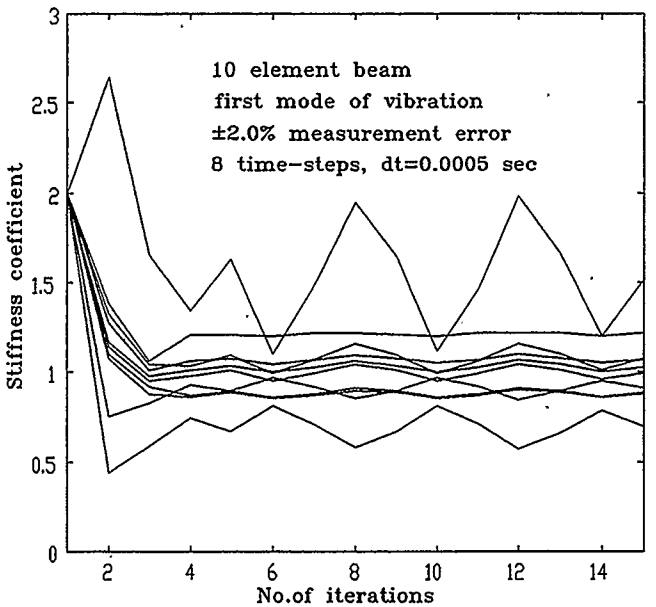

Element No.	Original Stiffness	Identified Stiffness
1	0.900	0.876
2	0.960	0.884
3	0.980	1.215
4	1.000	1.073
5	0.970	1.031
6	0.930	0.998
7	0.960	1.075
8	0.940	1.518
9	0.870	0.700
10	1.000	0.911

Figure 4.7 Convergence history for data with measurement error ±1.5% and ±2.0%

Newton-Raphson step was tried, because once we were close enough to the solution, fast convergence was achieved. However, we checked at each iteration that the proposed step reduces the objective function. If not, we backtracked along the Newton-Raphson direction until we had an acceptable step. Because the Newton-Raphson step is a descent direction for the objective function, finding an acceptable step by backtracking was guaranteed. Also, it is known that the Newton-Raphson method for solving non-linear equations has an unfortunate tendency to wander off into strange results if the initial guess is not sufficiently close to the result. Thus, for the analysis of the data with measurement error, it was wise to take initial data for stiffness of each member as close as possible to the actual one. In our case it was '1', and a modified Newton-Raphson method using line searches and backtracking as described above. Figure 4.8 and Figure 4.9 illustrate the history of convergence using the new approach. Now, the system identification procedure becomes able to handle much larger error of measurement. From the bottom diagram of Figure 4.10 it is evident that convergence for some elements was achieved with high accuracy. For others, even for a few percent error of the data from measurement, the accuracy was not very good. To identify the nature of this behavior we had to calculate the strain energy of each element during its motion. As presented in Figure 4.10, for some elements strain energy changes substantially, for some others very little. When strain energy changes are close to zero, it means that we are approaching a situation when the element is in a state of rigid body motion. In this case, the system cannot identify this particular element properly, and these elements will be identified with large error. As presented in Figure 4.10, if we are not concerned about these elements,

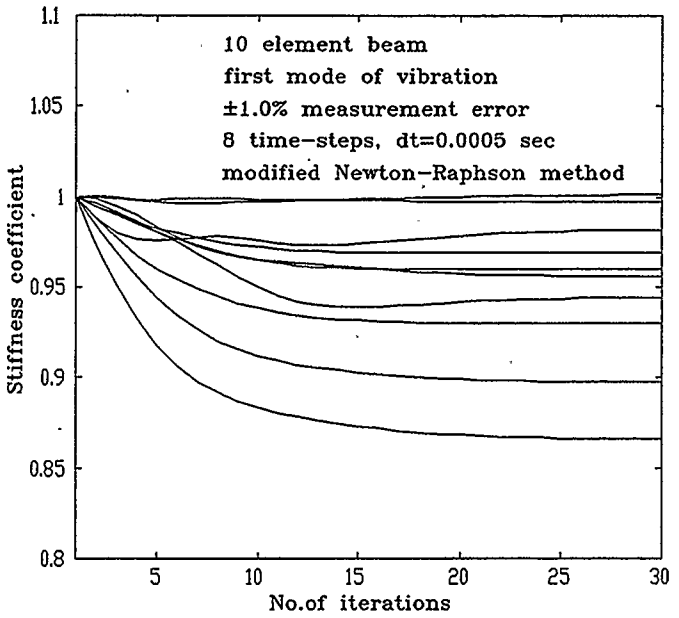

Element No.	Original Stiffness	Identified Stiffness
1	0.900	0.897
2	0.960	0.956
3	0.980	0.982
4	1.000	1.001
5	0.970	0.969
6	0.930	0.929
7	0.960	0.960
8	0.940	0.945
9	0.870	0.866
10	1.000	0.997

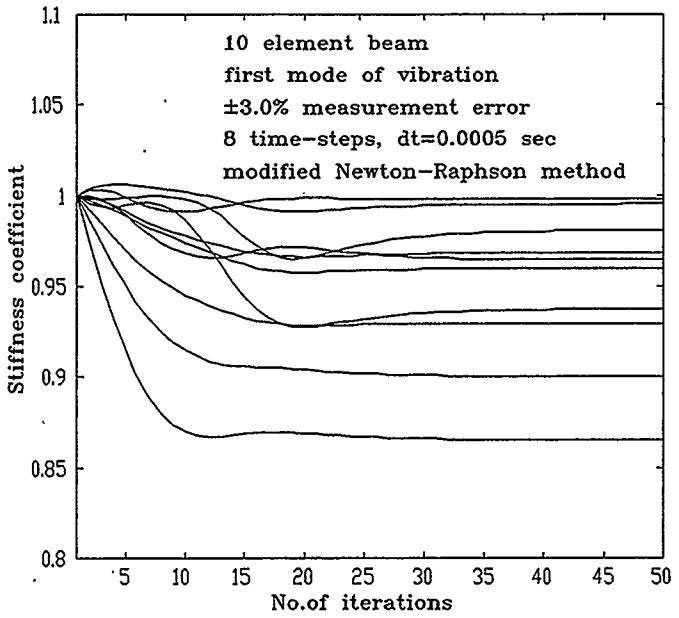

Element No.	Original Stiffness	Identified Stiffness
1	0.900	0.900
2	0.960	0.965
3	0.980	0.981
4	1.000	0.995
5	0.970	0.968
6	0.930	0.929
7	0.960	0.960
8	0.940	0.937
9	0.870	0.865
10	1.000	0.998

Figure 4.8 Convergence history for data with measurement error ±1.0 and ±3.0% for modified Newton-Raphson method

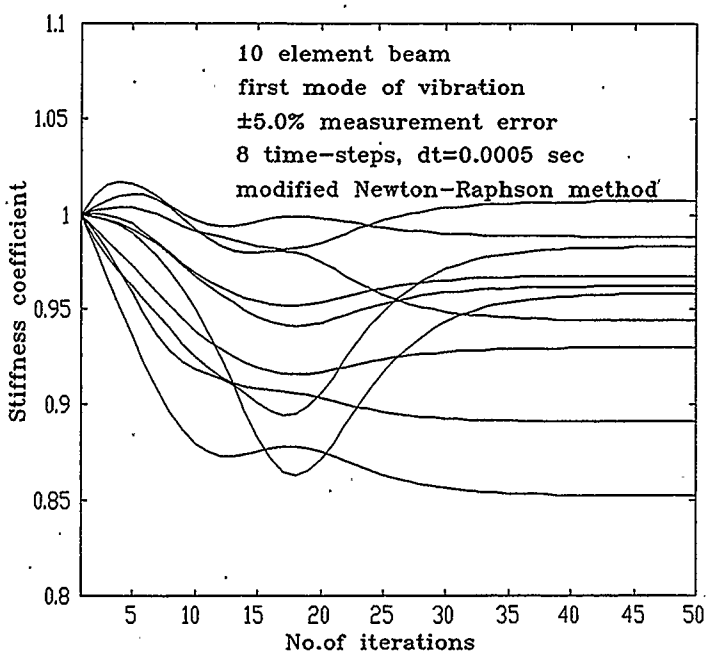

Element No.	Original Stiffness	Identified Stiffness
1	0.900	0.891
2	0.960	0.944
3	0.980	0.983
4	1.000	1.007
5	0.970	0.968
6	0.930	0.929
7	0.960	0.962
8	0.940	0.959
9	0.870	0.852
10	1.000	0.988

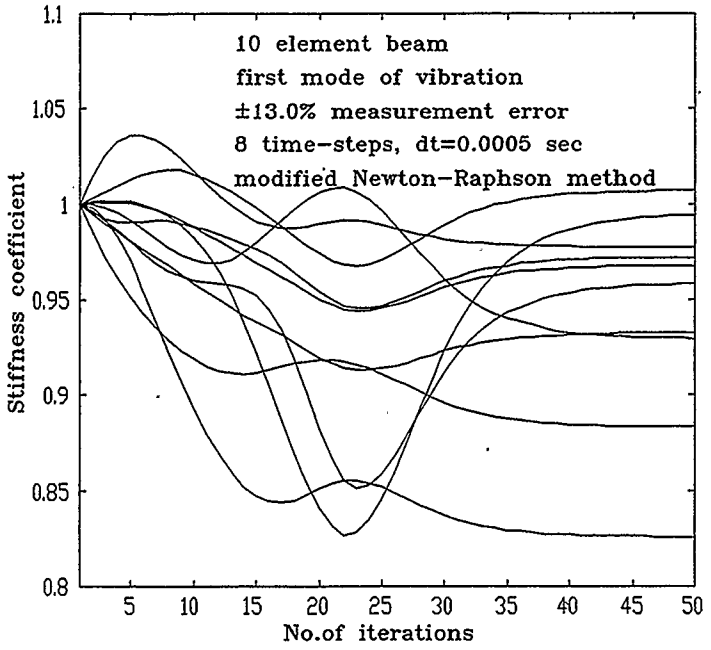

Element No.	Original Stiffness	Identified Stiffness
1	0.900	0.884
2	0.960	0.929
3	0.980	0.994
4	1.000	1.007
5	0.970	0.968
6	0.930	0.934
7	0.960	0.972
8	0.940	0.958
9	0.870	0.826
10	1.000	0.978

Figure 4.9 Convergence history for data with measurement error ±5.0 and ±13.0% for modified Newton-Raphson method

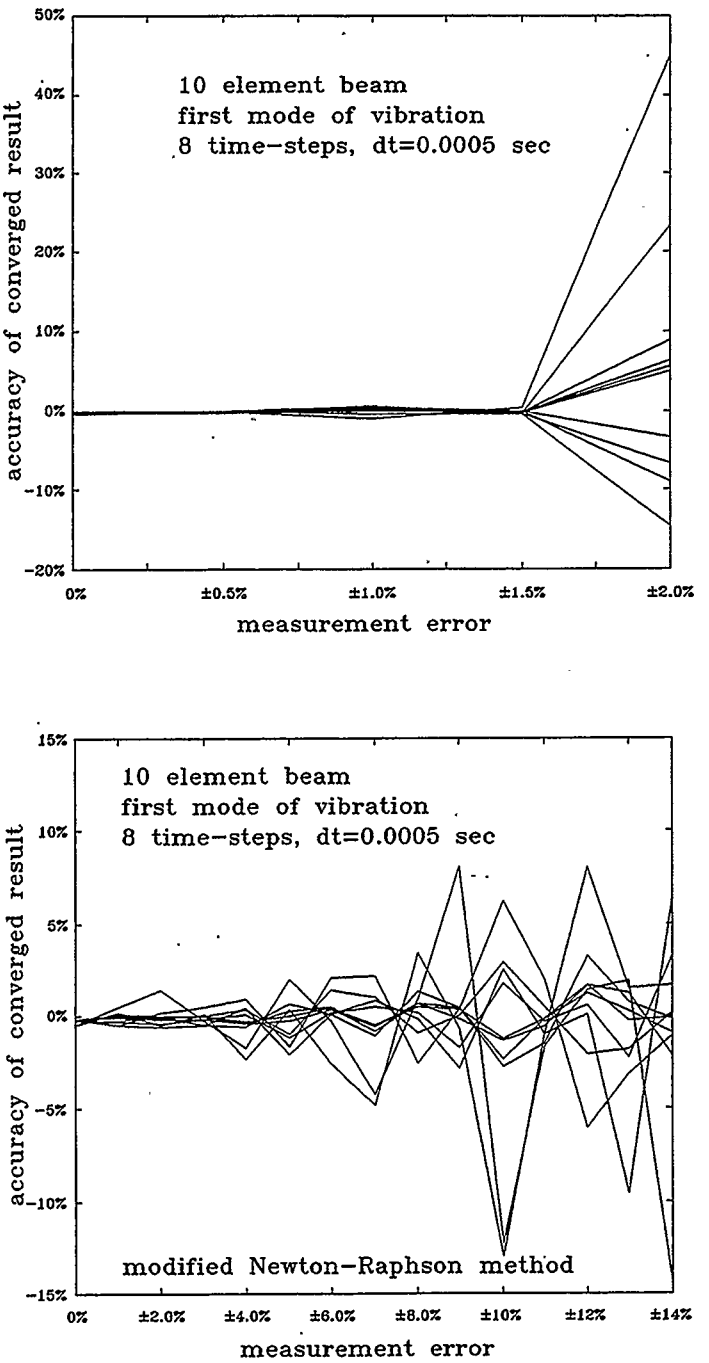

Figure 4.10 Accuracy of convergence for data with measurement errors processed with straight (top) and modified (bottom) Newton-Raphson method

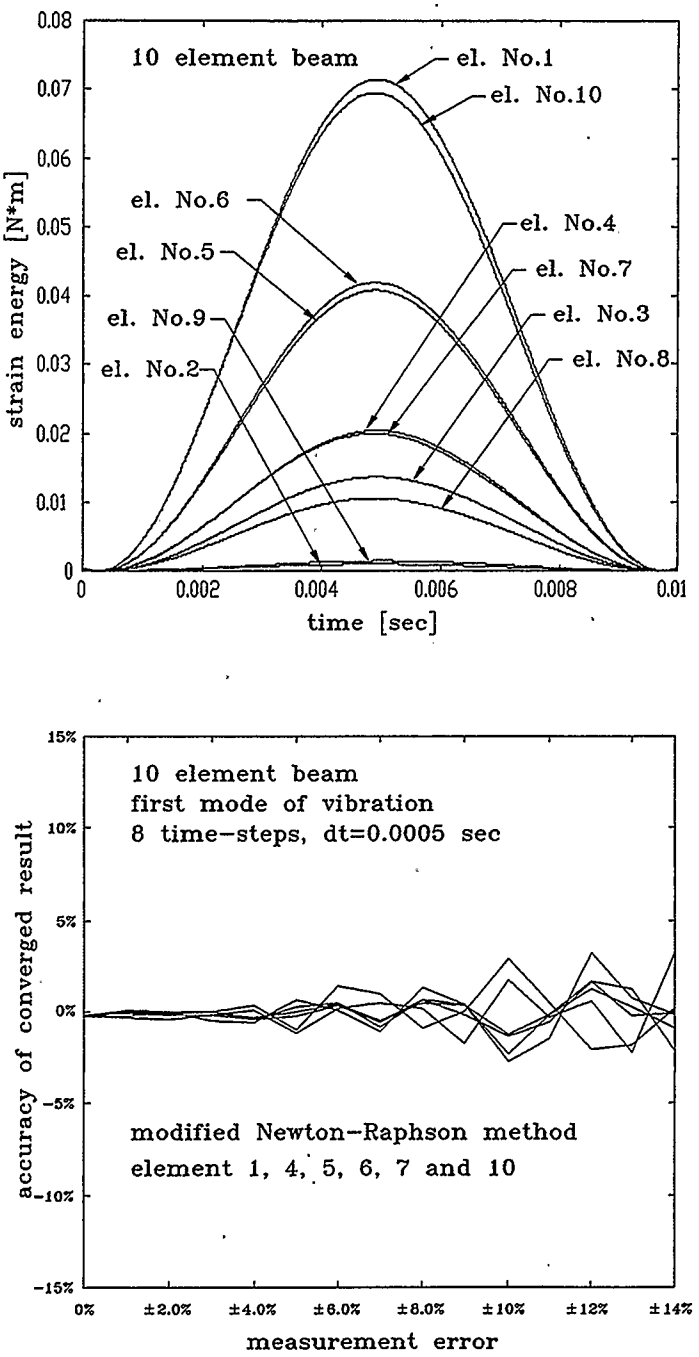

Figure 4.11 Strain energy and accuracy of convergence for elements with high changes in strain energy

the rest are identified with errors of less than 2%, even for ±10% error of measurement.

So far we considered all degrees of freedom in our analysis. But it is difficult to measure angular accelerations. In the case of a ten-element beam it would be desirable to input into the system identification only translational accelerations. Since translational displacements can be obtained automatically from accelerations, it is possible by analyzing locations of elements in space, to roughly calculate the angular displacements. This was done by making a spline curve from the linear displacements in every time-step, and calculating angular displacements obtained using data in the neighborhood of nodal points in order to supply the system identification with the initial data for the displacements as close as possible to exact values. After that, the system was able to correct stiffness coefficients using translational accelerations only. However when the data with greater error was used, the system had a problem with convergence to accurate results. A set of different simulations was performed to check this approach. The system converges with very good accuracy for data without error of measurement as can be seen in Figure 4.12 (top). When data with error of measurement greater than ±0.5% were used, the results were not accurate enough to properly identify changes in the stiffness of the members of the ten-element beam (Figure 4.12-bottom). Also, the number of time-steps increase dramatically, since the Newton-Raphson step was approximately reduced to 1% of the full step. The results of the analysis for the larger error are presented in Figure 4.13.

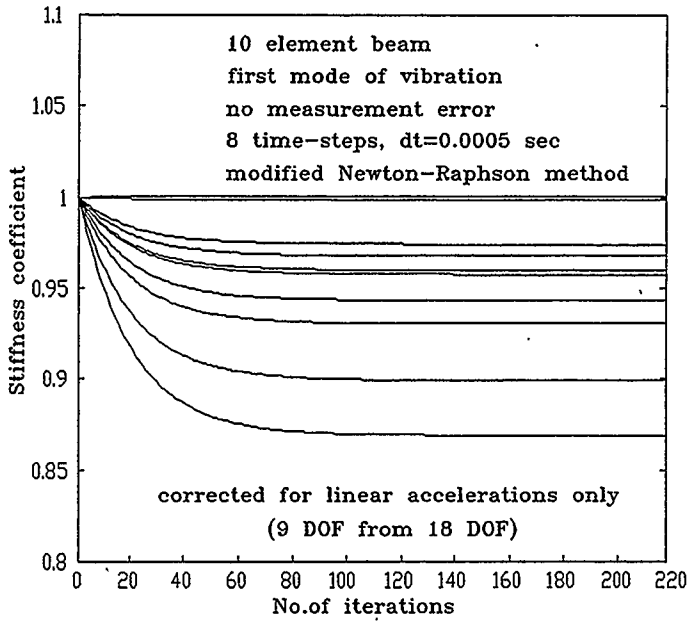

Element No.	Original Stiffness	Identified Stiffness
1	0.900	0.899
2	0.960	0.960
3	0.980	0.974
4	1.000	1.001
5	0.970	0.968
6	0.930	0.931
7	0.960	0.958
8	0.940	0.943
9	0.870	0.869
10	1.000	0.999

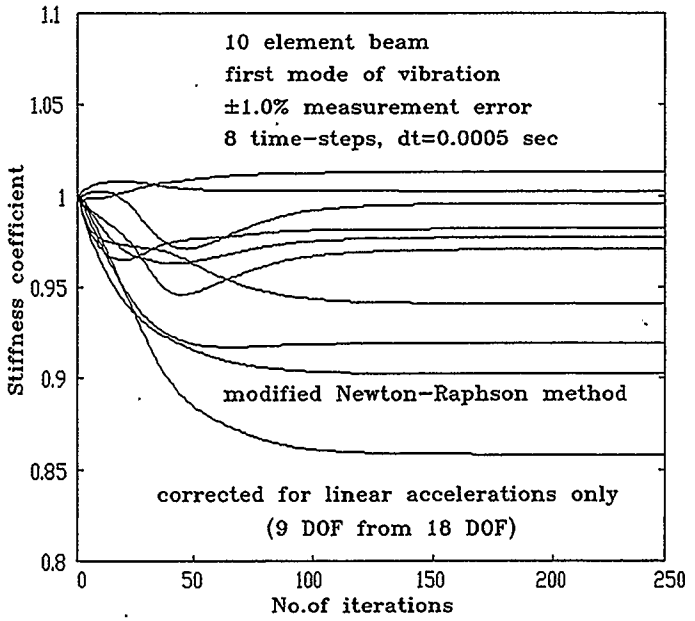

Element No.	Original Stiffness	Identified Stiffness
1	0.900	0.903
2	0.960	0.940
3	0.980	0.996
4	1.000	0.977
5	0.970	1.012
6	0.930	0.919
7	0.960	0.981
8	0.940	0.971
9	0.870	0.858
10	1.000	1.003

Figure 4.12 Convergence history for few DOF, without measurement error (top), with ±1.0% measurement error (bottom)

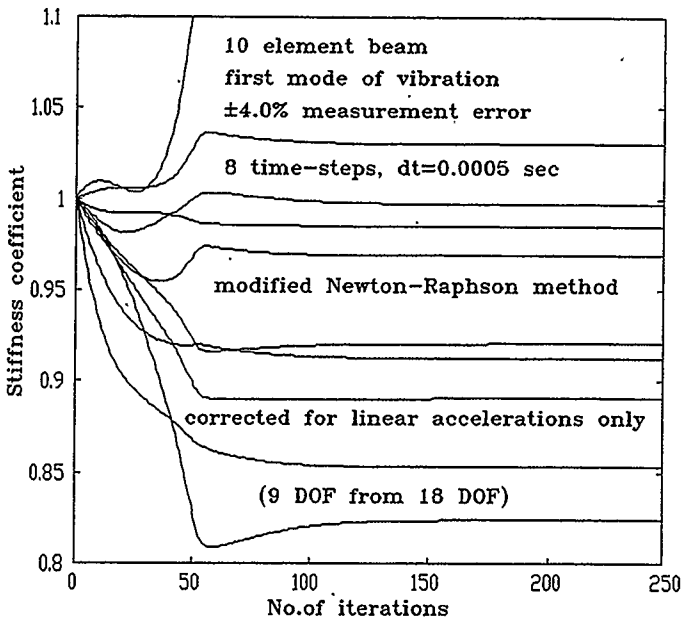

Element No.	Original Stiffness	Identified Stiffness
1	0.900	0.913
2	0.960	0.997
3	0.980	0.824
4	1.000	1.031
5	0.970	0.921
6	0.930	0.969
7	0.960	0.891
8	0.940	1.163
9	0.870	0.853
10	1.000	0.985

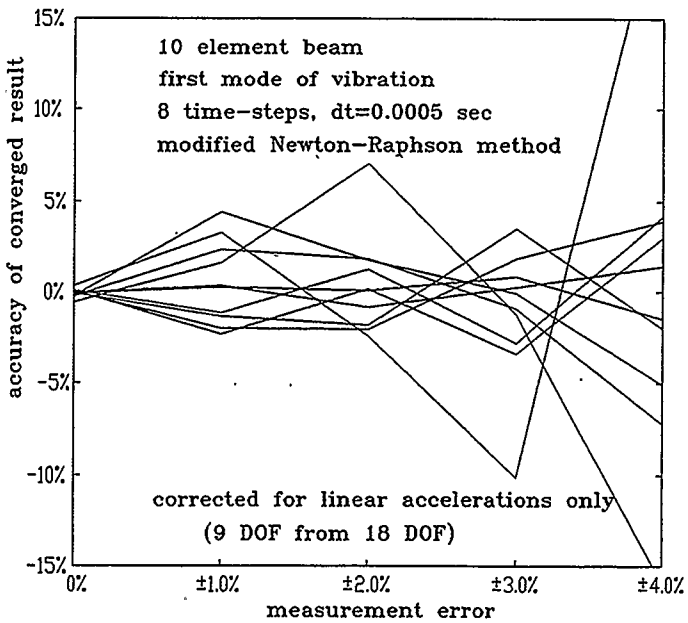

Figure 4.13 Convergence history for few DOF with ±4.0% measurement error (top), accuracy of convergence (bottom)

4.2 Frame structure

The loss of axial and bending stiffness due to transverse cracks and corrosion can be examined using a two dimensional model of a twelve-element frame, as presented in Figure 4.14. The structure was excited in such a way, that every element of the frame was vibrating in the first mode. The distributed loads were applied to the model to simulate the loaded structure. Similarly to the ten-element beam, two different time periods were chosen. Geometry in each of them is presented in Figure 4.15. Nine elements are corroded with 0.5% to 3.5% changes in the cross-sectional area, and six are cracked with magnitude of the flexural stiffness changes between 2% and 7%. When the data was generated using the Wilson-θ method, both the flexural and axial stiffnesses were changed when the configuration of each element was reversed. But in system identification procedures, only changes of the flexural stiffness were looked for, since the axial stiffness is much greater than the flexural stiffness, and the system is less sensitive to those changes. For all degrees of freedom and the data without measurement error, the convergence was very fast, and stiffness coefficients obtained in three iterations were accurate within 0.5% of the real value (Figure 4.16). From two time periods the data were assembled in Table 4.1, and using the key presented in Table 3.1 the causes of the loss of stiffness of each element were deduced. Next, the influence of measurement error on the accuracy of the identification procedure was analysed. As shown on Figure 4.17, for ±5.0% error of measurement, the stiffness coefficients were calculated with error less than 1%, which can be considered as a very

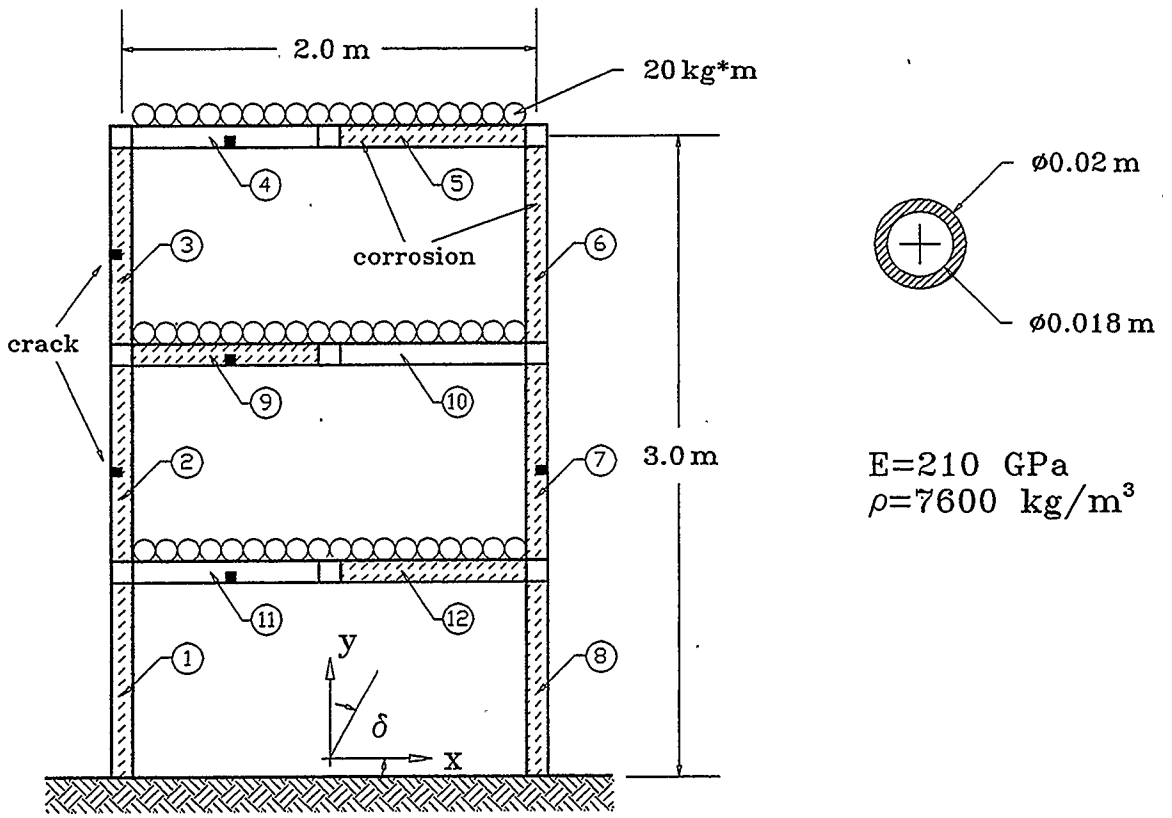

Figure 4.14 Two dimensional model of twelve-element frame

accurate solution. The same frame, identified using only linear accelerations as corrected values, gave good results only with the data without measurement error (Figure 4.18). As in the case of the beam structure analysed earlier, the identification procedure is unable to identify stiffness coefficients with enough precision if measurement error is present. This can be seen in Figure 4.19 for data with ±1.0% measurement error. However, convergence to the results close to the correct ones was reached (Figure 4.18 and 4.19).

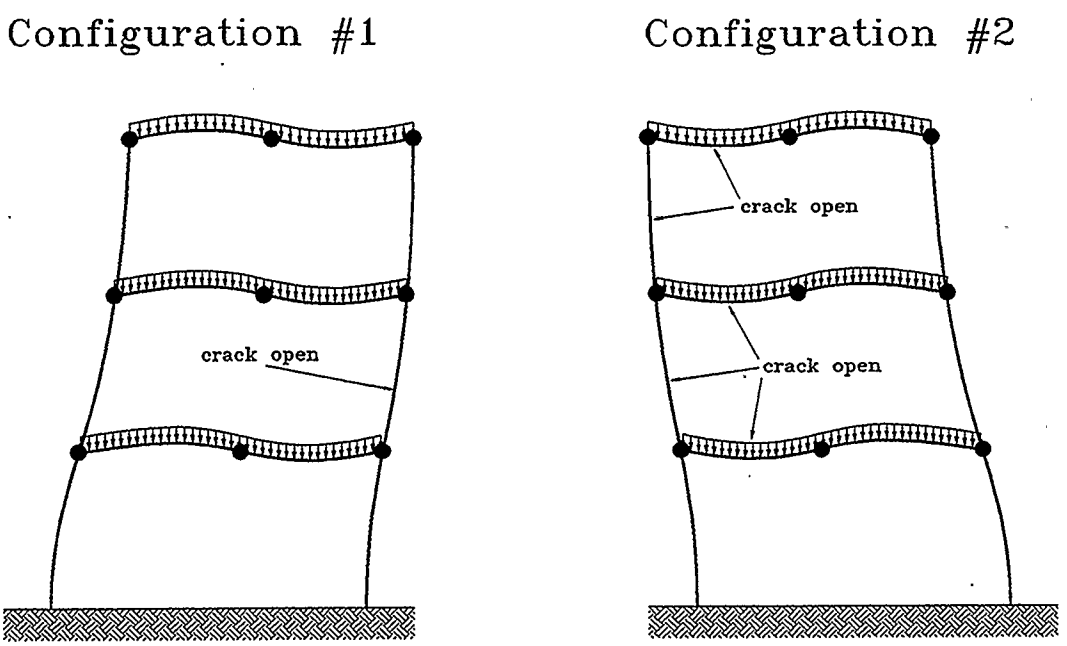

Fig. 4.15 Analysed vibration mode in two different configurations

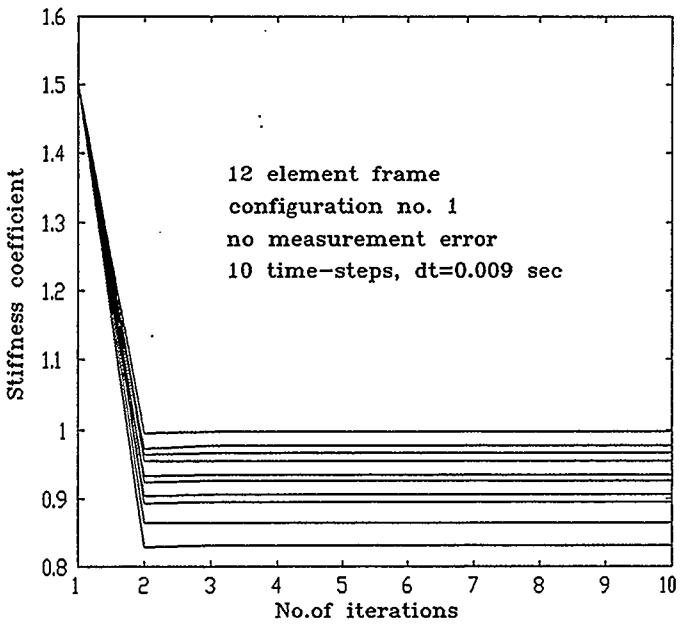

Element No.	Original Stiffness	Identified Stiffness
1	0.900	0.896
2	0.960	0.956
3	0.980	0.976
4	1.000	0.996
5	0.970	0.966
6	0.930	0.926
7	0.835	0.830
8	0.940	0.935
9	0.870	0.865
10	1.000	0.996
11	1.000	0.996
12	0.910	0.905

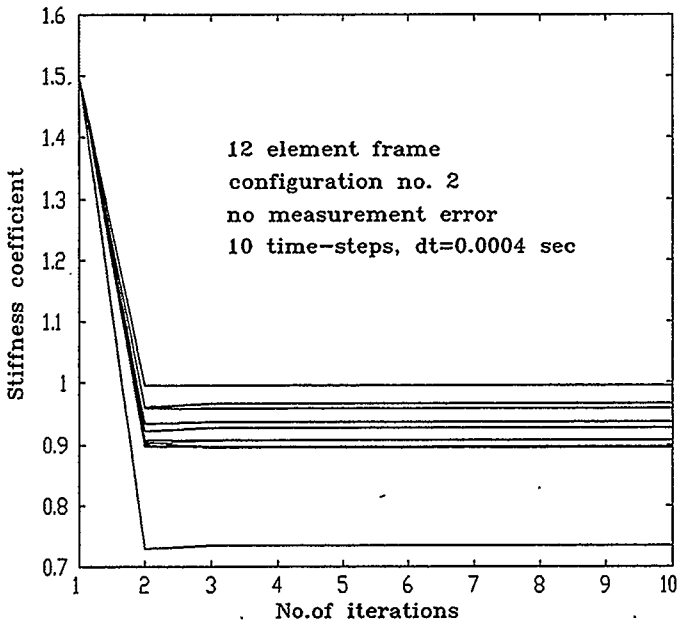

Element No.	Original Stiffness	Identified Stiffness
1	0.900	0.896
2	0.912	0.907
3	0.902	0.896
4	0.900	0.895
5	0.970	0.966
6	0.930	0.926
7	0.960	0.958
8	0.940	0.936
9	0.740	0.735
10	1.000	0.996
11	0.970	0.965
12	0.910	0.906

Figure 4.16 Convergence history for data without measurement error for frame structure

Element Number		#1	#2	#3	#4	#5	#6
Data for Wilson -Theta Method	k_c Due to Corrosion	0.900	0.960	0.980	1.000	0.970	0.930
	k_c Due to Crack	1.000	0.950	0.920	0.900	1.000	1.000
	k_c Due to Crack and Corrosion	0.900	0.912	0.902	0.900	0.970	0.930
k_c Initial Value for System Identification		1.200	1.200	1.200	1.200	1.200	1.200
Configuration #1	Element Crack Mode Open/Closed		Closed	Closed	Closed		
	k_c From System Identification	0.896	0.956	0.976	0.996	0.966	0.926
Configuration #2	Element Crack Mode Open/Closed		Open	Open	Open		
	k_c From System Identification	0.896	0.907	0.896	0.895	0.966	0.926
Loss of Stiffness Due to Corrosion k_c		0.896	0.956	0.976	0.996	0.966	0.926
Loss of Stiffness Due to Crack k_c		1.000	0.949	0.918	0.901	1.000	1.000
Element Number		#7	#8	#9	#10	#11	#12
Data for Wilson -Theta Method	k_c Due to Corrosion	0.960	0.940	0.870	1.000	1.000	0.910
	k_c Due to Crack	0.870	1.000	0.850	1.000	0.970	1.000
	k_c Due to Crack and Corrosion	0.835	0.940	0.740	1.000	0.970	0.910
k_c Initial Value for System Identification		1.200	1.200	1.200	1.200	1.200	1.200
Configuration #1	Element Crack Mode Open/Closed	Open		Closed		Closed	
	k_c From System Identification	0.830	0.935	0.865	0.996	0.996	0.905
Configuration #2	Element Crack Mode Open/Closed	Closed		Open		Open	
	k_c From System Identification	0.958	0.936	0.735	0.996	0.965	0.906
Loss of Stiffness Due to Corrosion k_c		0.958	0.936	0.865	0.996	0.996	0.905
Loss of Stiffness Due to Crack k_c		0.866	1.000	0.850	1.000	0.969	1.000

k_c -> stifness coefficient

Table 4.1 Results of identification procedure for twelve-element frame

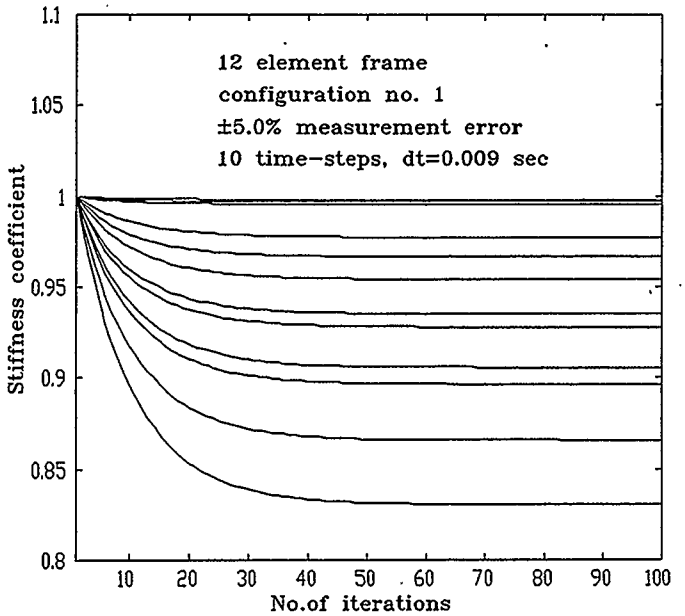

Element No.	Original Stiffness	Identified Stiffness
1	0.900	0.897
2	0.960	0.954
3	0.980	0.978
4	1.000	0.998
5	0.970	0.967
6	0.930	0.928
7	0.835	0.831
8	0.940	0.935
9	0.870	0.866
10	1.000	0.996
11	1.000	0.997
12	0.910	0.906

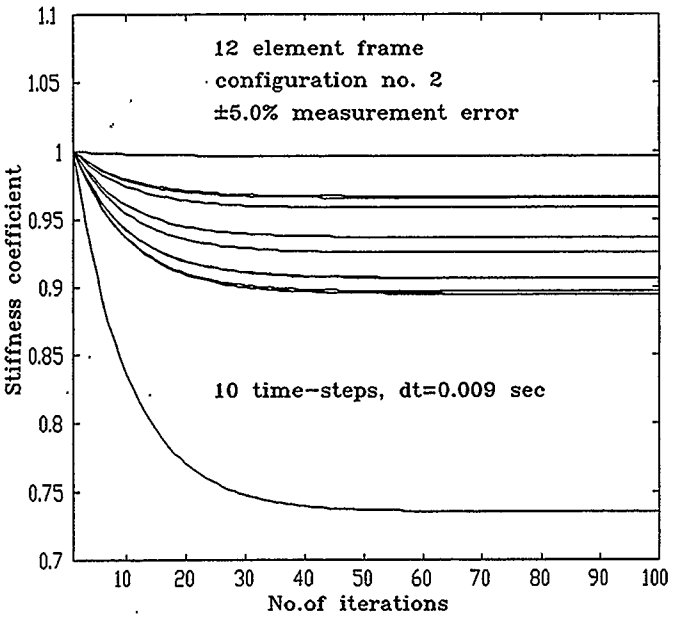

Element No.	Original Stiffness	Identified Stiffness
1	0.900	0.896
2	0.912	0.907
3	0.902	0.895
4	0.900	0.895
5	0.970	0.965
6	0.930	0.925
7	0.960	0.958
8	0.940	0.936
9	0.740	0.736
10	1.000	0.996
11	0.970	0.967
12	0.910	0.907

Figure 4.17 Convergence history for data with ±5.0% measurement error for frame structure

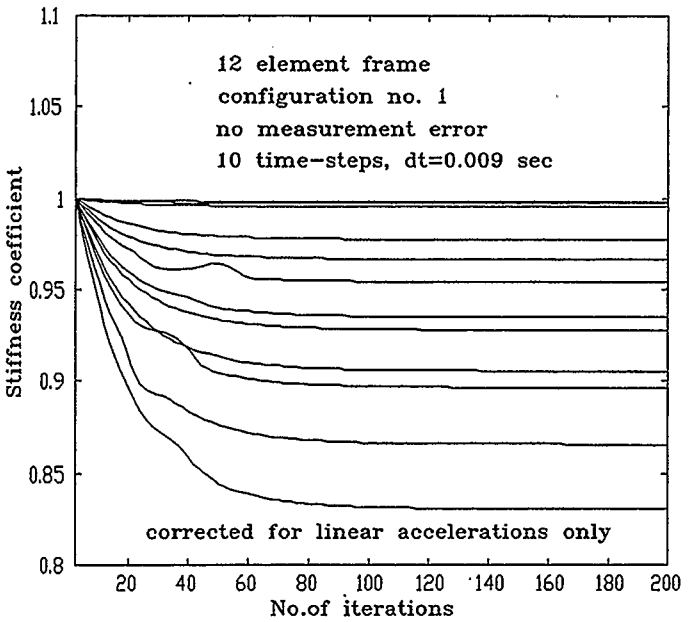

Element No.	Original Stiffness	Identified Stiffness
1	0.900	0.892
2	0.960	0.951
3	0.980	0.979
4	1.000	0.995
5	0.970	0.966
6	0.930	0.929
7	0.835	0.830
8	0.940	0.934
9	0.870	0.863
10	1.000	0.992
11	1.000	0.994
12	0.910	0.903

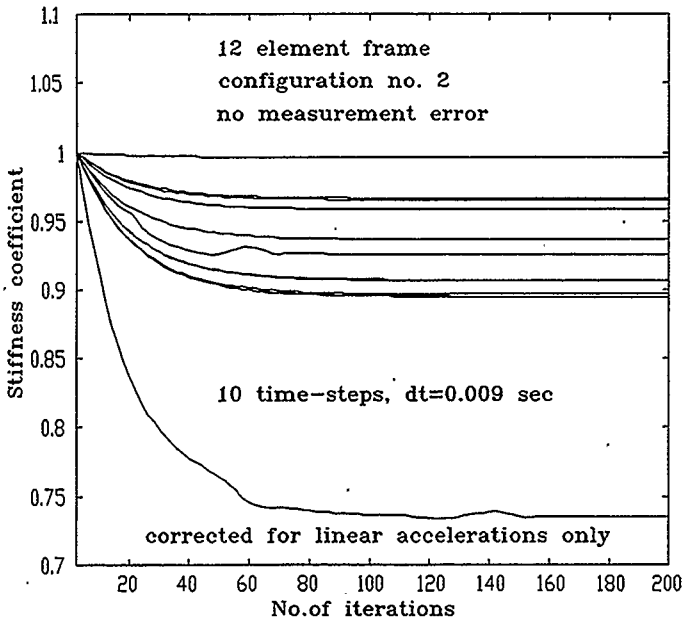

Element No.	Original Stiffness	Identified Stiffness
1	0.900	0.893
2	0.912	0.904
3	0.902	0.892
4	0.900	0.897
5	0.970	0.961
6	0.930	0.925
7	0.960	0.961
8	0.940	0.933
9	0.740	0.735
10	1.000	0.995
11	0.970	0.967
12	0.910	0.908

Figure 4.18 Convergence history for data without measurement error for frame structure using only linear accelerations

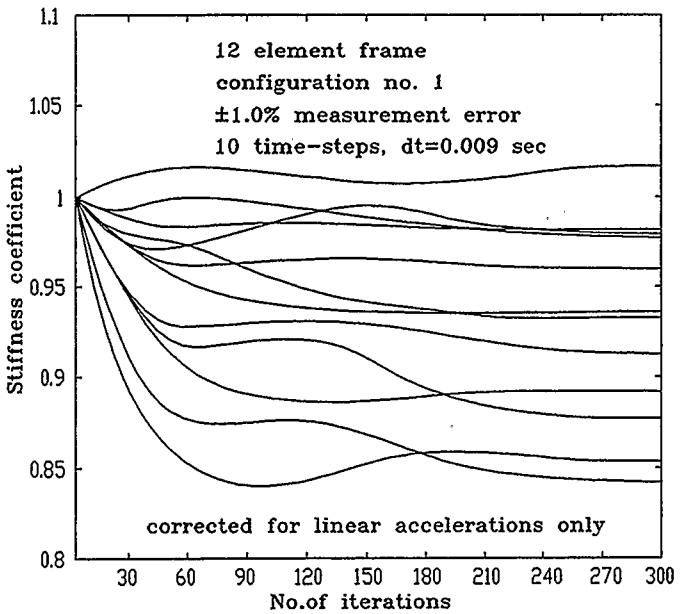

Element No.	Original Stiffness	Identified Stiffness
1	0.900	0.872
2	0.960	0.947
3	0.980	0.962
4	1.000	0.992
5	0.970	0.979
6	0.930	0.919
7	0.835	0.853
8	0.940	0.941
9	0.870	0.841
10	1.000	1.021
11	1.000	0.983
12	0.910	0.894

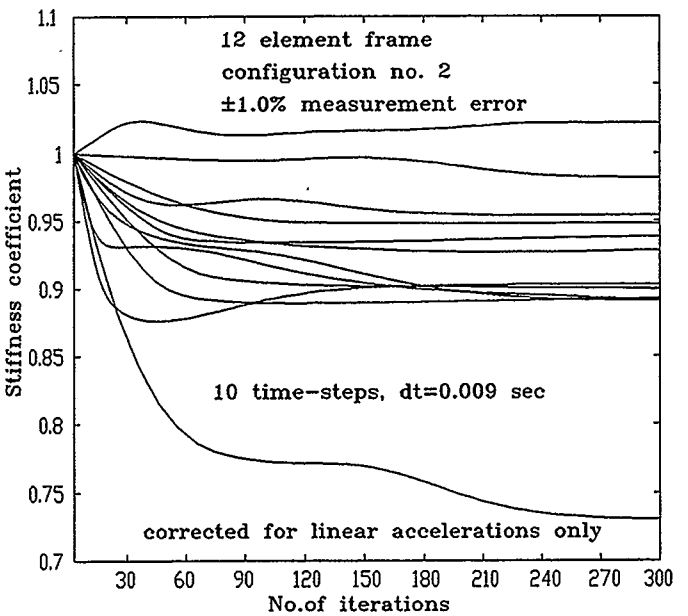

Element No.	Original Stiffness	Identified Stiffness
1	0.900	0.887
2	0.912	0.901
3	0.902	0.889
4	0.900	0.894
5	0.970	0.953
6	0.930	0.942
7	0.960	0.949
8	0.940	0.925
9	0.740	0.726
10	1.000	1.020
11	0.970	0.982
12	0.910	0.899

Figure 4.19 Convergence history for data with ±1.0% measurement error for frame structure using only linear accelerations

4.3 Truss structure

A third kind of structure analysed using the developed identification method was an eleven-element, two dimensional truss structure. The computer model was built using elements made of the steel pipe, and the structure was loaded with distributed load. This time only corrosion was taken into account, since the loss of the stiffness due to cracks and corrosion are identified in a similar fashion. Loss of the area of each element affected by corrosion, was between 2.5% and 31% of the original cross-section area. The data was generated using the Wilson-θ method in a simpler fashion than for the previous examples. There was no need to update the stiffness matrix after every iteration since there were no cracks in the model of the structure. To avoid problems with the rigid motion of any element, the first four modes were analysed to obtain strain energy changes during motion of the structure. As can be seen in Figures 4.21 and 4.22, in the third mode, all the elements were subjected to strain energy changes, and this mode was chosen to analyse the truss structure. For all degrees of freedom and data without measurement error, convergence was very fast (in two iterations), and very accurate (error less than 0.5% of real value) as shown in Figure 4.23.

The most interesting part of this analysis was how many degrees of freedom can be neglected to achieve decent accuracy of the system identification. It was assumed, to neglect first those DOF for which the changes of acceleration are smallest as compared to the rest of the DOF. As can be seen in Figure 4.24, the following measured data were not included in

system identification: x_4 (1 DOF neglected), x_4 & x_5 (2 DOF neglected), x_4 & x_5 & y_3 (3 DOF neglected), x_4 & x_5 & y_3 & x_2 (4 DOF neglected), x_4 & x_5 & y_3 & x_2 & x_1 (5 DOF neglected), x_4 & x_5 & y_3 & x_2 & x_1 & x_3 (6 DOF neglected) and x_4 & x_5 & y_3 & x_2 & x_1 & x_3 & x_6 (7 DOF neglected). Figures 4.25 and 4.26 demonstrate that the system identification procedure handles computation with a good accuracy even for a very limited number of DOF. It must be mentioned that the Newton-Raphson method for the truss example was modified a little differently, than the previous models. This time the method was able

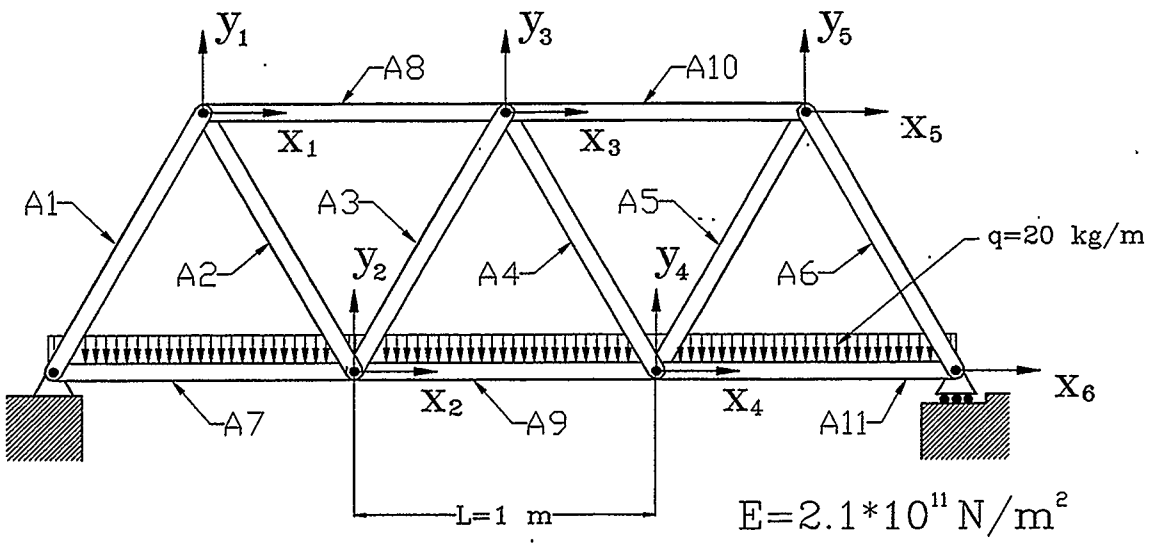

	A1	A2	A3	A4	A5	A6	A7	A8	A9	A10	A11
øD1	36	36	36	36	36	36	36	36	36	36	36
øD2	39.8	39.6	39.4	40.0	39.9	39.7	39.6	38.8	39.9	39.2	39.6
%	94.75	89.53	84.33	100.0	97.37	92.13	89.53	68.90	97.37	79.16	89.53

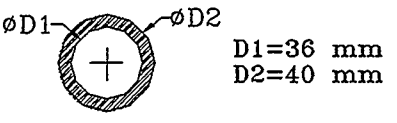

Figure 4.20 Two dimensional model of eleven-element truss structure

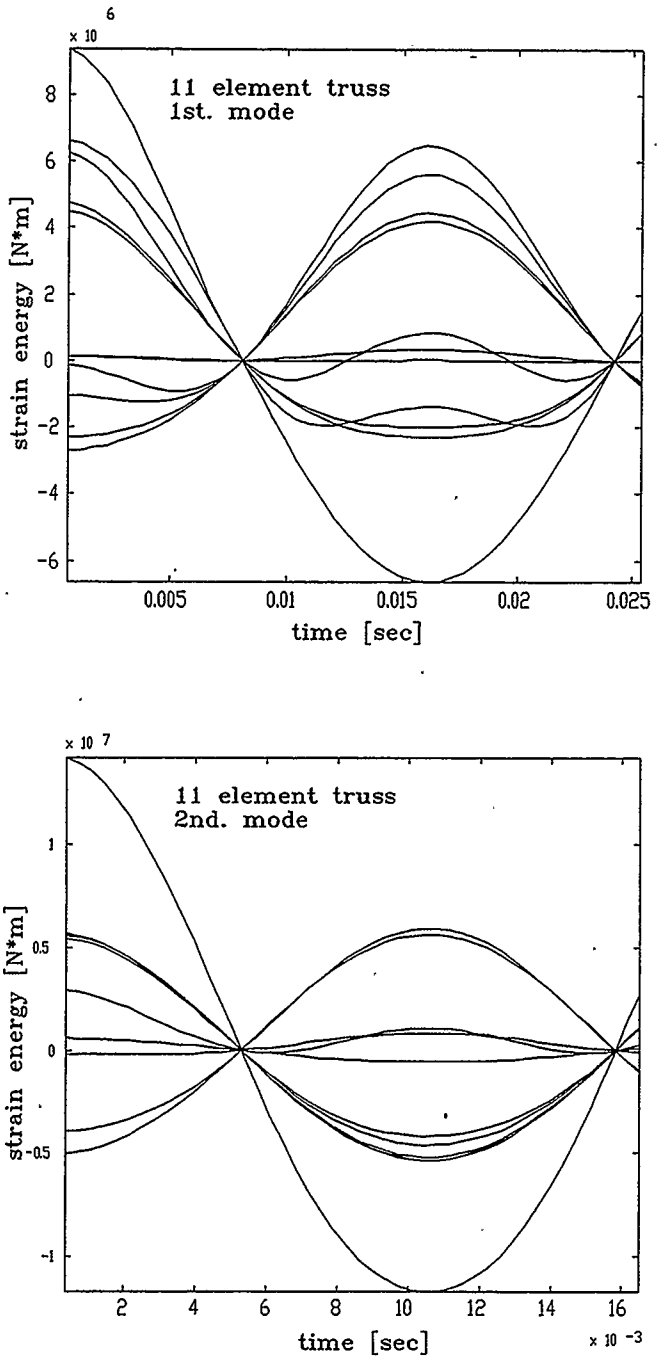

Figure 4.21 Strain energy changes in elements of truss structure for first and second modes of vibration

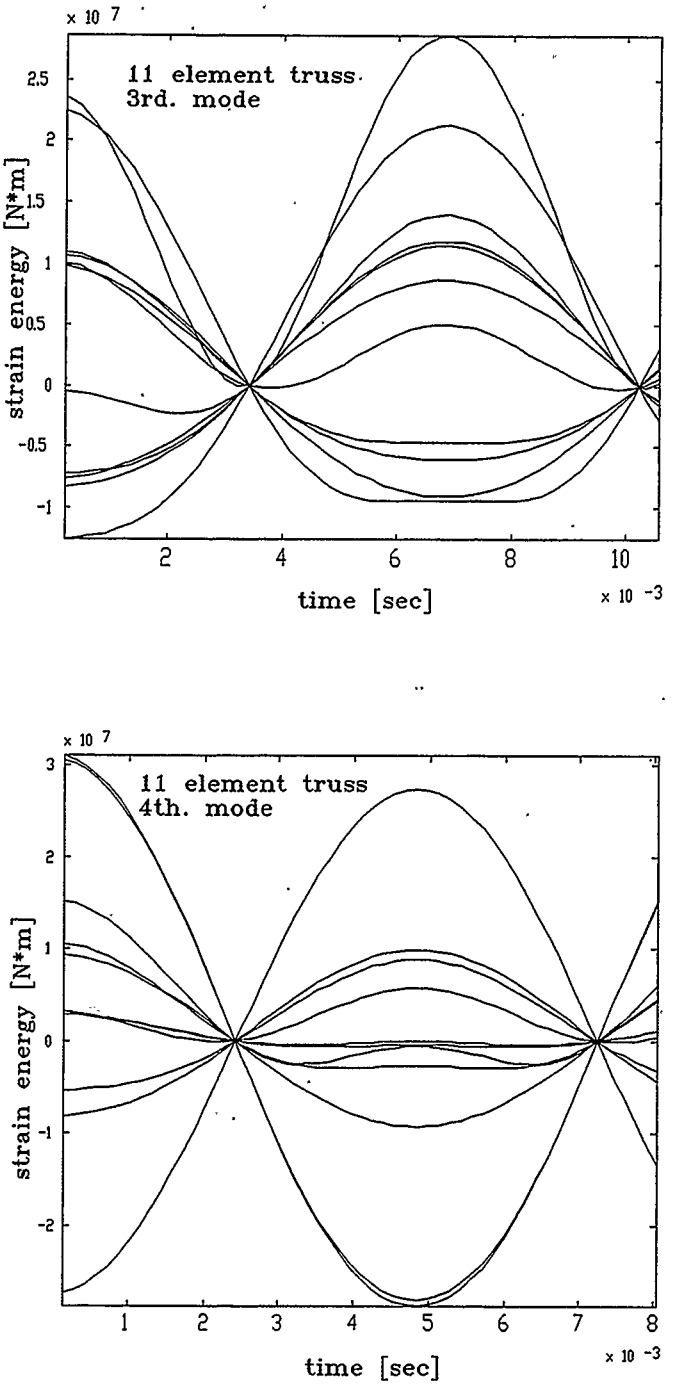

Figure 4.22 Strain energy changes in elements of truss structure for third and fourth modes of vibration

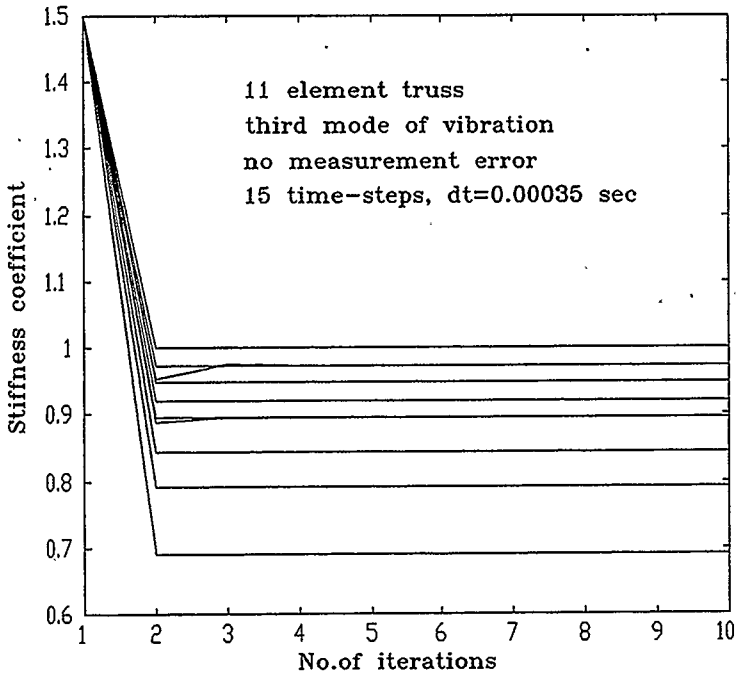

Element No.	Original Stiffness	Identified Stiffness
1	0.948	0.947
2	0.895	0.895
3	0.843	0.843
4	1.000	1.000
5	0.974	0.973
6	0.921	0.921
7	0.895	0.895
8	0.689	0.689
9	0.974	0.973
10	0.792	0.791
11	0.895	0.895

Figure 4.23 Convergence history for data without measurement error, truss structure in third mode of vibration

not only to decrease the step, but also to increase it when the objective function had a smaller value in consecutive steps. The only limitation was the size of the coefficient to correct the Newton-Raphson step. After many runs it was found that the optimal value is between 1 and 0.01. Smaller values of that coefficient always led to interference of roundoff error with the calculation of the next step. This was not a big improvement, since the real number of iterations was usually much higher than presented on the diagrams due to the adjustment procedure within the Newton-Raphson method. It was 20% to 30% faster only for some calculations. The effect of measurement error on the accuracy of the identification

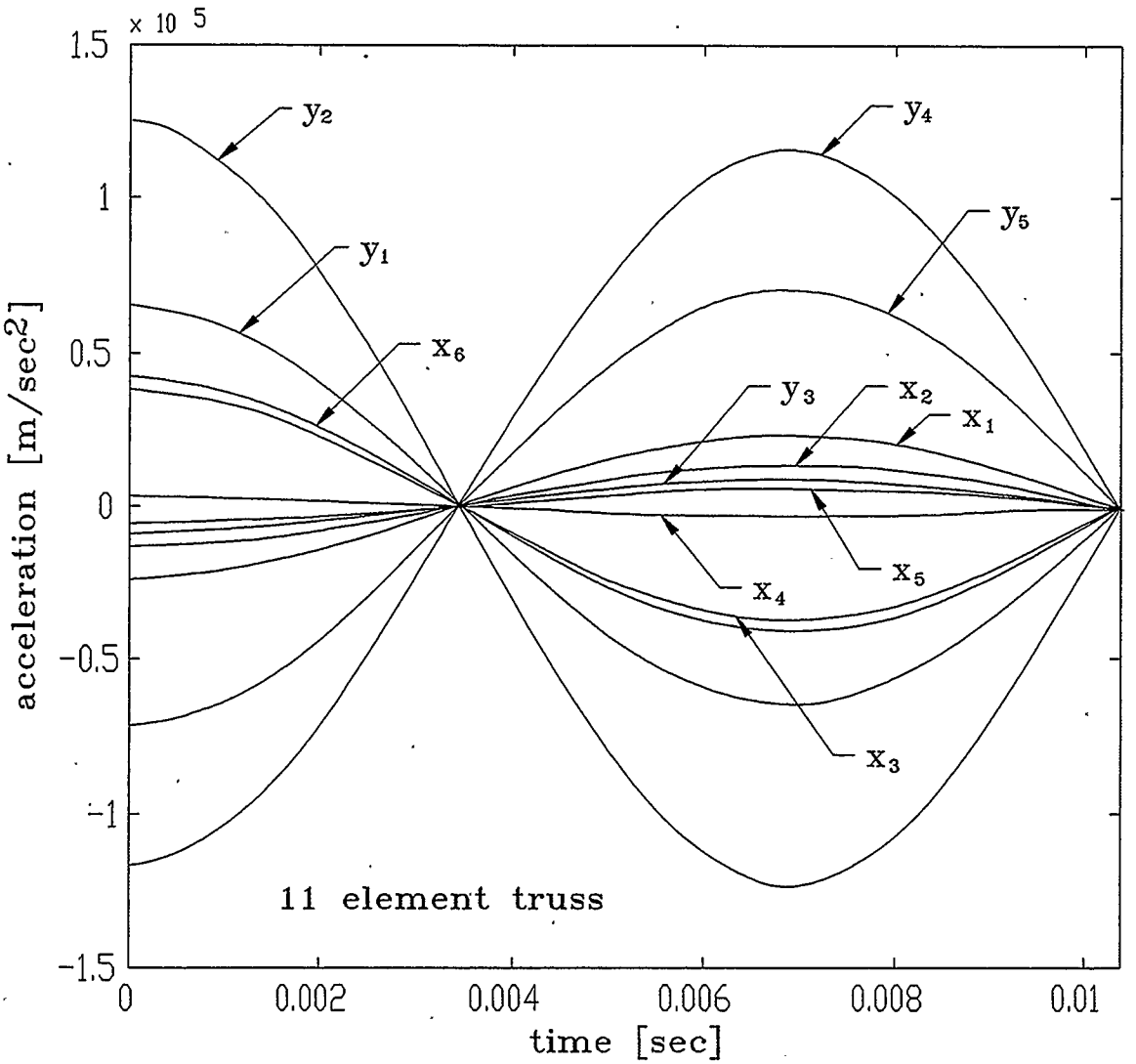

Figure 4.24 Damped vibration of eleven-element truss in third mode of vibration

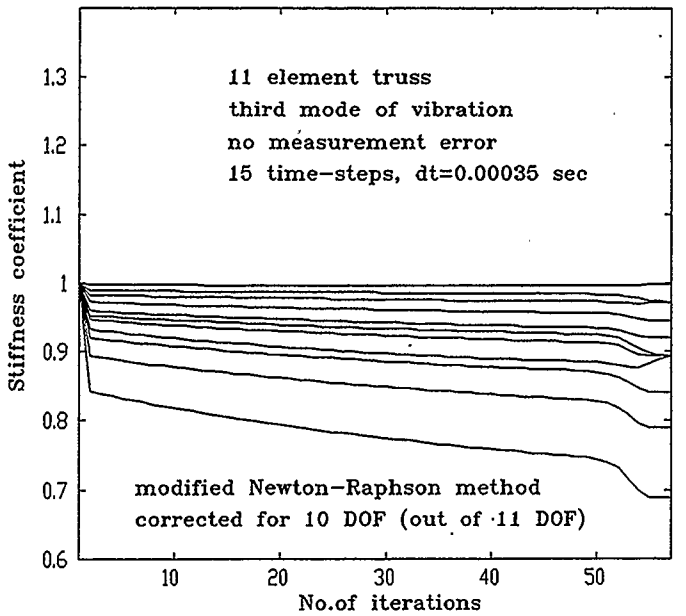

Element No.	Original Stiffness	Identified Stiffness
1	0.948	0.946
2	0.895	0.893
3	0.843	0.842
4	1.000	0.998
5	0.974	0.972
6	0.921	0.920
7	0.895	0.894
8	0.689	0.688
9	0.974	0.972
10	0.792	0.790
11	0.895	0.893

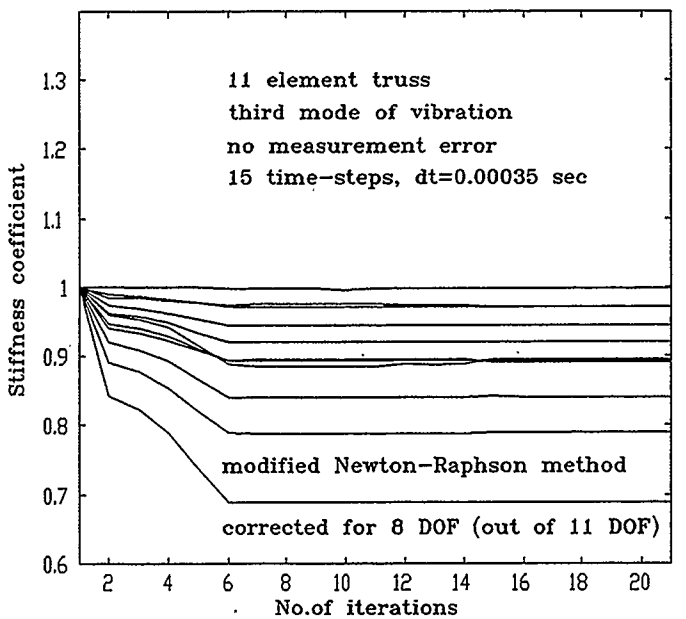

Element No.	Original Stiffness	Identified Stiffness
1	0.948	0.946
2	0.895	0.893
3	0.843	0.841
4	1.000	0.999
5	0.974	0.972
6	0.921	0.920
7	0.895	0.897
8	0.689	0.688
9	0.974	0.972
10	0.792	0.789
11	0.895	0.892

Figure 4.25 Convergence history for data without measurement error, 10 (top) and 8 (bottom) DOF were considered for identification purposes

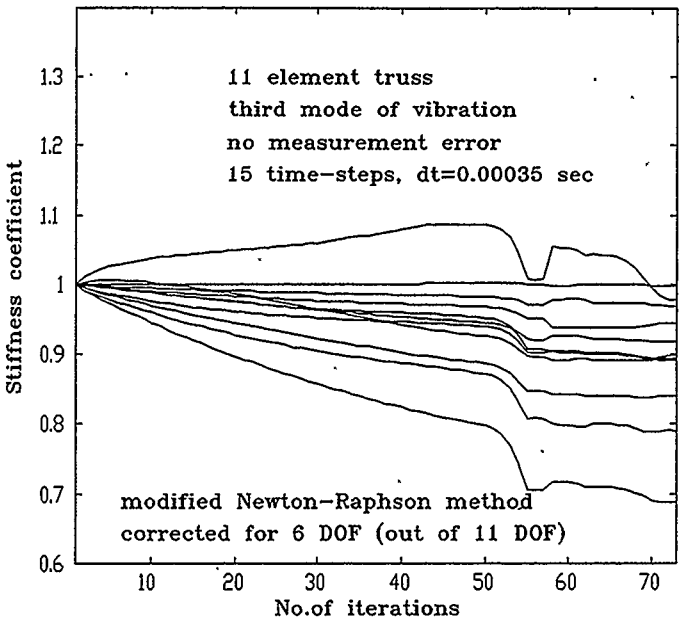

Element No.	Original Stiffness	Identified Stiffness
1	0.948	0.944
2	0.895	0.893
3	0.843	0.842
4	1.000	0.998
5	0.974	0.970
6	0.921	0.919
7	0.895	0.900
8	0.689	0.689
9	0.974	0.979
10	0.792	0.791
11	0.895	0.891

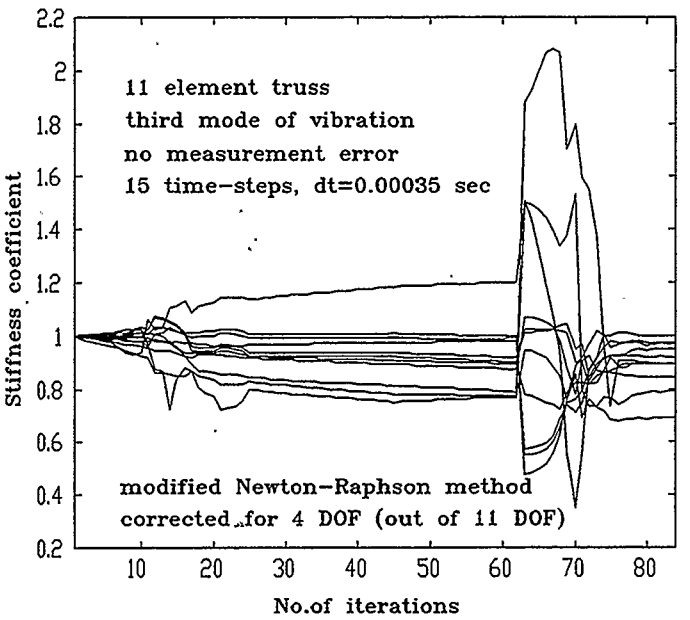

Element No.	Original Stiffness	Identified Stiffness
1	0.948	0.946
2	0.895	0.893
3	0.843	0.842
4	1.000	0.998
5	0.974	0.972
6	0.921	0.920
7	0.895	0.893
8	0.689	0.688
9	0.974	0.972
10	0.792	0.790
11	0.895	0.894

Figure 4.26 Convergence history for data without measurement error, 6 (top) and 4 (bottom) DOF were considered for identification purposes

procedure was analysed as the next step of the analysis. Error of magnitude ±5.0% was assumed since it is very hard to achieve better accuracy in real measurements.

Next, data with error was filtered to minimise error as much as possible. An 8^{th} order polynomial fitting procedure was utilised, which lowers the maximum error down to ±0.3%. This was done using many data points, and only every 50^{th} point was taken as an input data for system identification (time difference between the data point generated by Wilson-θ method was 0.000007 sec). The accuracy of data filtering was significantly improved. If only those data points are available which must be input into system identification, it is unlikely that filtering will give such a small error as the obtained ±0.3%. As is shown in Figure 4.27 (top), for ±5.0% error of measurement and employing all DOF, the stiffness coefficients were calculated with error less than 0.5%. Later the effect of different numbers of neglected degrees of freedom was analysed. The results are presented in Figure 4.27 (bottom) and Figure 4.28. When only one DOF was not included in the system identification procedure, accuracy was within ±0.6%. But if more DOF were neglected, the system was converging to different results, which probably represented the local minima of the objective function.

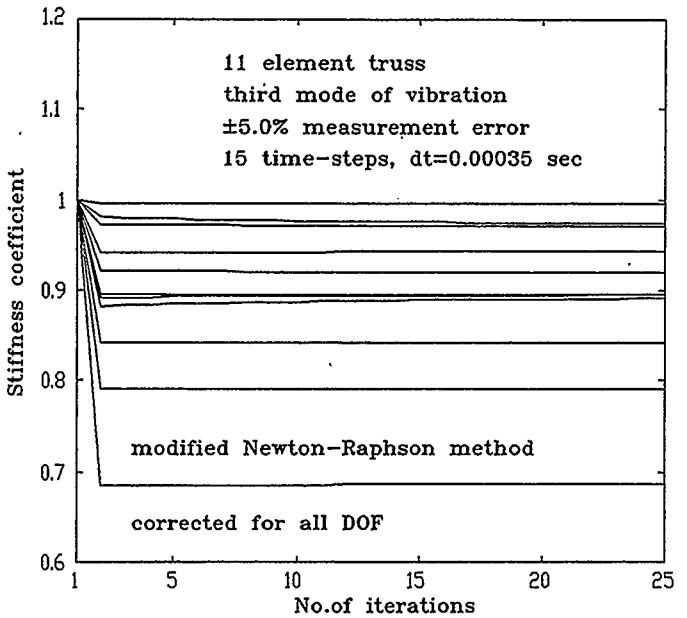

Element No.	Original Stiffness	Identified Stiffness
1	0.948	0.943
2	0.895	0.894
3	0.843	0.842
4	1.000	0.997
5	0.974	0.971
6	0.921	0.920
7	0.895	0.891
8	0.689	0.686
9	0.974	0.974
10	0.792	0.790
11	0.895	0.894

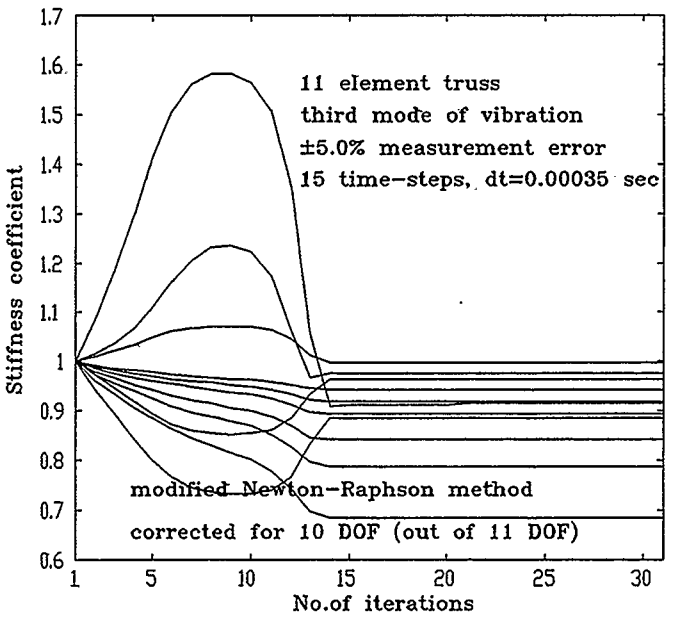

Element No.	Original Stiffness	Identified Stiffness
1	0.948	0.943
2	0.895	0.895
3	0.843	0.842
4	1.000	1.000
5	0.974	0.966
6	0.921	0.920
7	0.895	0.917
8	0.689	0.686
9	0.974	0.977
10	0.792	0.790
11	0.895	0.885

Figure 4.27 Convergence history for data with ±5.0% measurement error, all (top) and 10 (bottom) DOF were considered for identification purposes

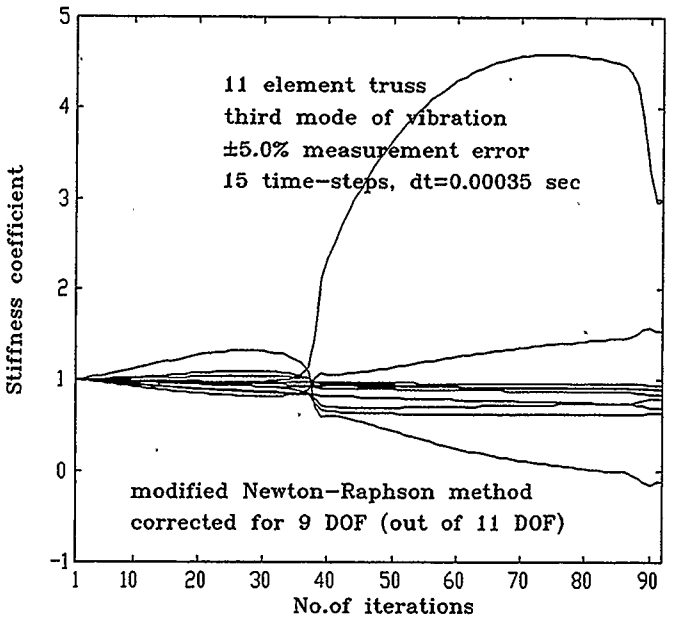

Element No.	Original Stiffness	Identified Stiffness
1	0.948	0.945
2	0.895	0.897
3	0.843	0.841
4	1.000	0.901
5	0.974	0.794
6	0.921	0.648
7	0.895	-0.12
8	0.689	0.688
9	0.974	0.904
10	0.792	2.981
11	0.895	1.539

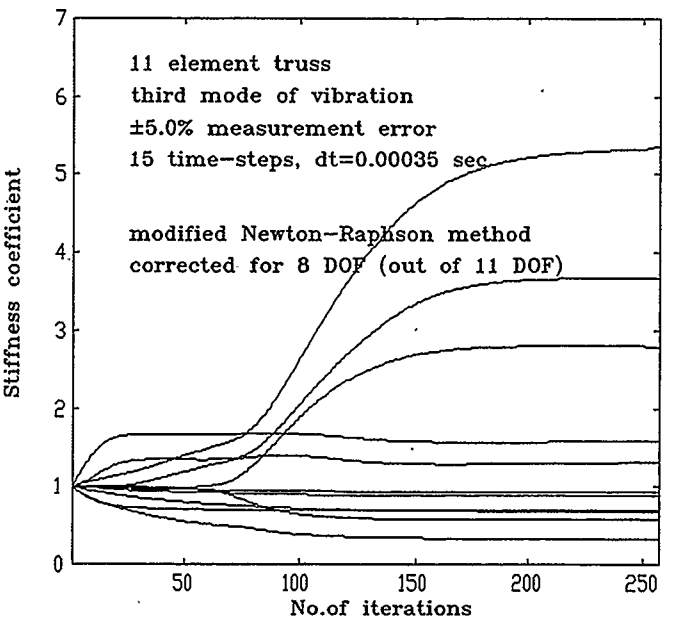

Element No.	Original Stiffness	Identified Stiffness
1	0.948	0.931
2	0.895	0.884
3	0.843	0.572
4	1.000	2.784
5	0.974	3.668
6	0.921	5.359
7	0.895	1.589
8	0.689	0.677
9	0.974	1.319
10	0.792	0.330
11	0.895	0.696

Figure 4.28 Convergence history for data with ±5.0% measurement error, 9 (top) and 8 (bottom) DOF were considered for identification purposes

CHAPTER V
Concluding Remarks and Summary

5.1 Summary and limitations

This thesis presents development and evaluation of an identification method to detect cracks and corroded members in vibrating structures. It is based on the least square technique and minimisation of the global error function. The Finite Element Model of the structure and the equations of motion represent constraints of the objective function. The application of the central difference method to represent accelerations and velocities in terms of displacements in the equation of motion leads to simplification and very efficient notation of the mathematical model. It permits the application of matrix operators to present the objective function as products of matrices and vectors. Also, the first and the second partial derivatives of the objective function are calculated using previously developed matrix operators. This simplifies the assembly of the Gradient vector and the Hessian matrix for the Newton-

Raphson technique reducing it to simple matrix and vector operations. All programming was done on a 486DX/50MHz Personal Computer with 8Mb of RAM. MATLAB 4.2 was used as a programming tool, which simplified the programming task, and allowed further analysis of the technique, rather than straight programming.

Three different structures were analysed. A ten-element beam was the main model to evaluate the behavior of the method with respect to different factors. First, and probably the most important was the analysis of the influence of the length of the time-step and the number of the time-steps on the accuracy of solution. It was surprising that the method worked only if the total analysed time period was less than half of the natural period for a particular mode of vibration. Although, only the analysis for the first mode of a ten-element beam is presented in this thesis, a series of computations were done for the second and third modes. The patterns of the dependency of the solution on the length of the time-step and the number of time-steps was the same as for the first mode. Secondly, the influence of artificially generated measurement error on the accuracy of the solution was investigated. It was proven, that the method handles error in a very good manner as long as all degrees of freedom are included in the measurements. For a limited number of measuring points the method does not work well if errors are present. This limits the use of this procedure to beam and frame structures as long as accuracy of existing sensors will not dramatically improve, or until sensors able to measure angular accelerations are developed. The results from beam analysis were confirmed when a twelve-element frame structure was analysed. The result,

presented only for a few calculations, shows good agreement with those from the analysis of the ten-element beam.

Finally, a truss structure was analysed. It was the most promising analysis for real life application of the method, since the accelerations for all degrees of freedom for this kind of structure can be measured. As expected, the method handled measurement errors in a very good manner, which suggests that the method is applicable for real engineering problems. Although limiting the number of measured degrees of freedom does not usually lead to satisfactory results, we can say that the goal to develop an applicable straight-forward identification method was achieved. It should also be mentioned that during the analysis a slight modification of the Newton-Raphson method was necessary to assure the convergence. A basic line-search and backtracking method was employed, which provided satisfactory results.

In conclusion, following the analysis of these three structures when all DOF are taken into account and the changes in the stiffness of the elements are greater than 2%, it is evident that the developed system identification method is very accurate and efficient.

5.2 Concluding remarks

This thesis contains development and evaluation of an identification method to detect cracks and corroded members in vibrating structures. The least square method was used to minimise the global error functional. The application of the finite element and the central difference methods makes it possible to present the identification process in very simple and elegant mathematical form.

The work presented cannot be treated as a final work in this area. It is rather an initial study which the author believes will lead to experiments and more development to improve the performance of the method, especially for problems with limited numbers of measured DOF. Also, implementation of additional terms in the objective function may lead to overall improvement of the method. Since this thesis is the first work fully presenting the discussed identification procedure, there is definitely much more to come with future research and development of the presented identification method.

REFERENCES

1. Adams, R. D., Cawley, P., "The Location of Defects in Structures from Measurement of Natural Frequencies," *Journal of Strain Analysis*, Vol. 14, pp. 49-57, 1979

2. Baruh, H., Ratan, S., "Damage Detection in Flexible Structures," *Proceedings of the Eighth VPI & SU Symposium on Dynamic and Control of Large Structures* (Blacksburg, VA), edited by L. Meiroritch, pp. 171-179, 1991

3. Christides, S., Barr, A. D. S., "One Dimensional Theory of Cracked Bernoulli-Euler Beams," *International Journal of Mechanical Sciences*, Vol. 26 (11-12), pp. 639-648, 1984

4. Cuiping, L., Smith, S. W., "Hybrid Approach for Damage Detection in Flexible Structures," *Journal of Guidance, Control and Dynamics*, Vol. 18, pp. 419-425, 1995

5. Flanigan, C., "Correction of Finite Element Models Using Mode Shape Design Sensitivity," *Proceedings of the Ninth International Modal Analysis Conference, Society for Experimental Mechanics*, Bethel, CT, pp. 84-88, 1991

6. Goodwin, C. G., Payne, R. A., "Dynamic System Identification, Experiments, Design and Data Analysis," *Academic Press*, New York, 1977

7. Hajela, P., Soeiro, F. J., "Structural Damage Detection Based on Static and Modal Analysis," *AIAA Journal*, Vol. 28, No. 1, pp. 1110-1115, 1990

8. Hasan, W. M., "Crack Detection from the variation of the Eigenfrequencies of a Beam on Elastic Foundation, "*Engineering Fracture Mechanics*, Vol. 52(3), pp. 409-421, 1995

9. Hendricks, S. L., Hayes, S. M., Junkins, J. L., "Structural Parameter Identification for Flexible Spacecraft," *Proceedings of the AIAA 22nd Aerospace Science Meeting* (Reno, NV), AIAA, New York, 1984

10. Hetenyi, M., "Deflection of Beams of Varying Cross Section," *Journal of Applied Mechanics, Trans. ASME*, Vol. 59, pp. A49-A52, 1937

11. Ibrahim, S. R., Mikulcik, E. C., "A method for the Direct Identification of Vibration Parameters from the Free Response," *The Shock and Vibration Bulletin*, Vol. 47 (4), pp. 183-198, 1977

12. Jelonnek, B., Kammeyer, K. -D., "Improved Methods for the Blind System Identification Using Higher order Statistics," *IEEE Transactions on Signal Processing*, Vol. 40, pp. 2947-2960, 1992

13. Juang, J.-N., "An Overview of Recent Advances in System Identification," *A Collection of Technical Papers: 34th AIAA/ASME/ASCE/AHS/ASC Structures, Structural Dynamic, and Materials Conference* (La Jolla, CA), pp. 3342-3352, 1993

14. Kabe, A. M., "Stiffness Matrix Adjustment Using Mode Data," *AIAA Journal*, Vol. 23, No. 9, pp. 1431-1436, 1985

15. Kashangaki, T. A. L., "Ground Vibration Tests of High Fidelity Truss for Verification of On Orbit Damage Location Techniques," *NASA TM 107626*, May 1992

16. Kirmser, P. G., "The Effect of Discontinuities on the Natural Frequency of Beams," *Proceedings of the ASTM*, Vol. 44, pp. 897, 1944

17. Lin, R. M., "Analytical Model Improvement Using Modified IEM," *Proceedings of the International Conference on Structural Dynamics Modeling, National Agency for Finite Element Methods and Standards*, Glasgow, Scotland, UK, pp. 181-194, 1993

18. Lindholm, B. E., West, R. L., "System Identification of Finite Element Modeling Parameters Using Experimental Spatial Dynamic Modeling," *First International Conference on Vibration Measurements by Laser Techniques* (Ancona, Italy), pp. 450-462, 1994

19. Lukasiewicz, S. A., Stanuszek, M. and Czyz, J. A., "Filtering of the Experimental or FEM Data in Plane Stress and Strain Fields," *Numerical Methods in Engineering, Proceedings of the First European Conference on Numerical Methods in Engineering*, Brussels, Belgium, 1992

20. Lukasiewicz, S. A., "Matrix Filter for Correcting Experimental Data," *Communications in Numerical Methods in Engineering*, Vol. 9, pp. 797-803, 1993

21. Lukasiewicz, S. A. and Stanuszek, M., "Constrained, Weighted, Least Square Technique for Correcting Experimental Data," *Proceedings of the Conference 'Computational Methods and Experimental Mechanics VI'*, Elsevier Applied Science, 1993

22. Lukasiewicz, S. A. and Babaei, R., "Identification of Dynamic System by Means of Matrix Filter," *Experimental Mechanics*, (in press), 1993

23. Lukasiewicz, S. A. and Babaei, R., "On Identification of Dynamic Systems," Computational Methods and Experimental Measurements VII, *Computational Mechanics Publications*, Southampton, Boston Editors G. M. Carlomagno, C. A. Brebia, 1995

24. Lukasiewicz, S. A. and Babaei, R., "Effects of Dependent Variables and Instrumental Errors in Filtering of the Experimental Data," *Communications in Numerical Methods in Engineering*, Vol. 12, 1996

25. Lukasiewicz, S. A., Palka, K. "Detection of Cracks and Corroded Members in Frame Structures from Dynamic Response," *32nd Annual Technical Meeting of the Society of Engineering Science Conference* , New Orleans, Louisiana, 1995

26. Lukasiewicz, S. A., Stanuszek, M., Palka, K., "Matrix Filtering for Smooth Distributions," *Computational Mechanics and Experimental Measurements Conferenc,e* Capri, Italy, 1995

27. Lukasiewicz, S. A., Palka, K., "On Identification of Frames from Dynamic Responses," *International Conference on Lightweight Structures in Civil Engineering* , Warsaw, Poland, 1995

28. McGowan, P. E., Smith, S. W., Javeed, M., "Experiments for Locating Damaged Members in a Truss Structure," *Proceedings of the Second USAF/NASA Workshop on System Identification and Health Monitoring of Precision Space Structures*, Vol. 2, Pasadena, Ca, pp. 571-615, March 1990

29. Morassi, A., "Crack-Induced Changes in Eigenparameters of Beam Structures," *Journal of Engineering Mechanics*, ASCE, Vol. 119, pp. 1798-1803, 1993

30. Ostachowicz, W. M., Krawczuk, M., "Analysis of the Effect of Cracks on the Natural Frequencies of a Cantilever Beam," *Journal of Sound and Vibration*, Vol. 150 (2), pp. 191-201, 1991

31. Pabst, U., Hagedorn, P., "On the Identification of Localized Losses of Stiffness in Structures," *Structural Dynamics of Large Scale and Complex Systems - ASME 1993*, DE-Vol. 59, pp. 99-104, 1993

32. Petroski, H. J., "Simple Static and Dynamic Models for the Cracked Elastic Beam," *International Journal of Fracture*, Vol. 17, pp. R71-R76, 1981

33. Qian, G.-L., Gu, S.-N., Jiang, J.-S., "The Dynamic Behaviour and Crack Detection of a Beam with Crack, "*Journal of Sound and Vibration*, Vol.138(2), pp. 233-243, 1990

34. Ricles, J. M., Kosmatka, J. B., "Damage Detection in Elastic Structures Using Vibratory Residual Forces and Weighted Sensitivity," *AIAA Journal*, Vol. 30, No. 9, pp. 2310-2316, 1992

35. Rizos, P. F., Aspragathos, N., Dimarogonas, A. D., "Identification of Crack Location and Magnitude in Cantilever Beam from the Vibration Modes," *Journal of Sound and Vibration*, Vol. 138(3), pp. 381-388, 1990

36. Segelman, D. J., Woyak, D. B. and Rowlands, R. E., "Smooth Spline-Like Finite Element Differentiation of Full-Field Experimental Data Over Arbitrary Geometry," *Experimental Mechanics*, 19, pp. 429-437, 1979

37. Smith, S. W., Hendricks, S. L., "Damage Detection and Location in Space Trusses," *AIAA SDM Issues of the International Space Station: A Collection of Technical Papers* , Williamsburg, VA, AIAA, Washington DC, pp. 56-63, 1988

38. Smith, S. W., McGowan, P. E., "Locating Damage Members in a Truss Structure Using Modal Data: A Demonstration Experiment," *NASA TM 101595,* April 1989

39. Smith, S. W., Beattie, C. A., "Simultaneous Expansion and Orthogonalization of Measured Modes for Structure Identification," *AIAA Dynamics Specialistic Conference: A Collection of Technical Papers* , Long Beach, Ca), AIAA, Washington DC, pp. 261-270, 1990

40. Smith, S. W., Beattie, C. A., "Optimal Identification Using Inconsistent Modal Data," *Proceeding of the 32nd AIAA/ASME/ASCE/AHS/ASC, Structures, Structural Dynamic, and Materials Conference,* Baltimore, MD, AIAA, Washington, DC, pp. 2319-2324, 1991

41. Smith, S. W., Beattie, C. A., "Secant-Method Adjustment for Structural Models," *AIAA Journal,* Vol. 29, No. 1, pp. 119-126, 1991

42. Sutton, M. A., Turner, J. L., Bruck H. A. and Chae, T. A., "Full Field Representation of Discreetly Sampled Surface Deformation for Displacement and Strain Analysis," *Experimental Mechanics,* pp. 168 179, 1991

43. Thomson, W. T., "Vibration of Slender Bars With Discontinuities in Stiffness," *Journal of Applied Mechanics,* Vol. 16, pp. 203-207, 1949

44. Wilson, E. L., Farhoomand, I., and Bathe, K. J. "Nonlinear dynamic analysis of complex structures," *Int. J. Earthquake Engineering and Structural Dynamics*, Vol. 1, pp. 241-252, 1973

45. Yuen, M. M. F., "A Numerical Study of the Eigenparameters of a Damaged Cantilever," *Journal of Sound and Vibration*, Vol. 103(3), pp. 301-310, 1985

46. Zehn, M., Wahl, F., Schmidt, G., "Verification and Adjustment of Dynamic Structural Finite Element Models by Experimental Model Analysis Data" *Computational Methods and Experimental Measurements VII. Computational Mechanics Publications*, Southampton, Boston, Editors G. M. Carlomagno, C. A. Brebia, 1995